NASA CR 137617
MDC E1139

FINAL REPORT

HIGH PURITY SILICA REFLECTIVE HEAT SHIELD DEVELOPMENT

by

James C. Blome
David N. Drennan
Raymond J. Schmitt

MCDONNELL DOUGLAS ASTRONAUTICS COMPANY - EAST

Saint Louis, Missouri

October 1974

prepared for

NATIONAL AERONAUTICS AND SPACE ADMINISTRATION

NASA AMES RESEARCH CENTER

CONTRACT NAS2-7897

FOREWORD

This final report was prepared by McDonnell Douglas Astronautics Company - East, under NASA Contract NAS 2-7897 and covers work performed during the period November 1973 to September 1974. This work was administered under the direction of NASA Ames Research Center with Philip R. Nachtsheim as the Technical Manager.

The authors wish to acknowledge the efforts of the following personnel who contributed to the successful completion of this program: A. Bay, N. Crump, C. Dillow, W. Dinger, D. Kummer, E. Malakelis, A. Seger, J. Smittkamp, B. Whiteson and R. Wilcox.

ABSTRACT

A hyperpure vitreous silica material was developed for use as a reflective and ablative heat shield for planetary entry. Various purity grades and forms of raw materials were evaluated. Various processing methods were also investigated. Slip casting of high purity grain was selected as the best processing method, resulting in a highly reflective material in the wavelength bands of interest (in the visible and ultraviolet).

The selected material was characterized with respect to optical, mechanical and physical properties using a limited number of specimens.

TABLE OF CONTENTS

TABLE OF CONTENTS (Continued)

LIST OF PAGES

Title Page
i thru iv
1-1
2-1 thru 2-6
3-1 thru 3-10
4-1 thru 4-39
5-1 thru 5-33
6-1 thru 6-4
7-1

2.0 PROGRAM AND PROPERTIES SUMMARY

This section contains a summary of the accomplishments of this program and presents limited data showing some of the properties of hyperpure silica. The properties of commercial high purity fused silica are compared with the properties of hyperpure fused silica developed in this program.

2.1 SUMMARY OF ACCOMPLISHMENTS

Reflectance was a most important property under study in this program. One of the non-routine type of measurements made was reflectance in the vacuum ultraviolet down to 0.15μ. Scattering coefficients (S) and absorption coefficients (K) were also measured. These coefficients express the optical properties and can be used directly in a thermodynamic analysis for sizing a heat shield. The effect of the thin silica melt layer formed during entry was also studied from the standpoint of trapped radiant energy.

It was established early in the program by theory and by testing that high purity silica raw materials were required to obtain highly reflective heat shield materials. Reflectance tests were conducted on silica raw materials in various forms and of various purity levels. Of all the raw materials considered and tested only two types were exceptional in that they were highly reflective compared to other materials, over the wavelength band of interest (from approximately 0.1 to 2.0μ). These two materials were the Dynasil and Suprasil type of silica and silica powders formed by condensation after the thermal decomposition of silicone in air. Both of these raw materials have impurities on the order of 10 parts per million (ppm) total metallic ion content. By taking these high purity raw materials and processing them in a specially prepared clean room, it was possible to formulate and control a finished dry pressed or slip cast product to a level of impurities under 25 ppm.

Figure 2-1 shows three widely different purity levels of finished, fabricated silica materials which were investigated in this program. Note that the materials containing 5,000 and 3711 ppm (Reference 2) impurities are considerably less reflective at wavelengths below about 1.0 microns than the hyperpure material containing only 24 ppm impurities. Also shown on Figure 2-1 is a typical radiative flux distribution associated with a nominal entry into the atmosphere of Jupiter. This radiative heating distribution illustrates the importance of high reflectance at the short wavelengths.

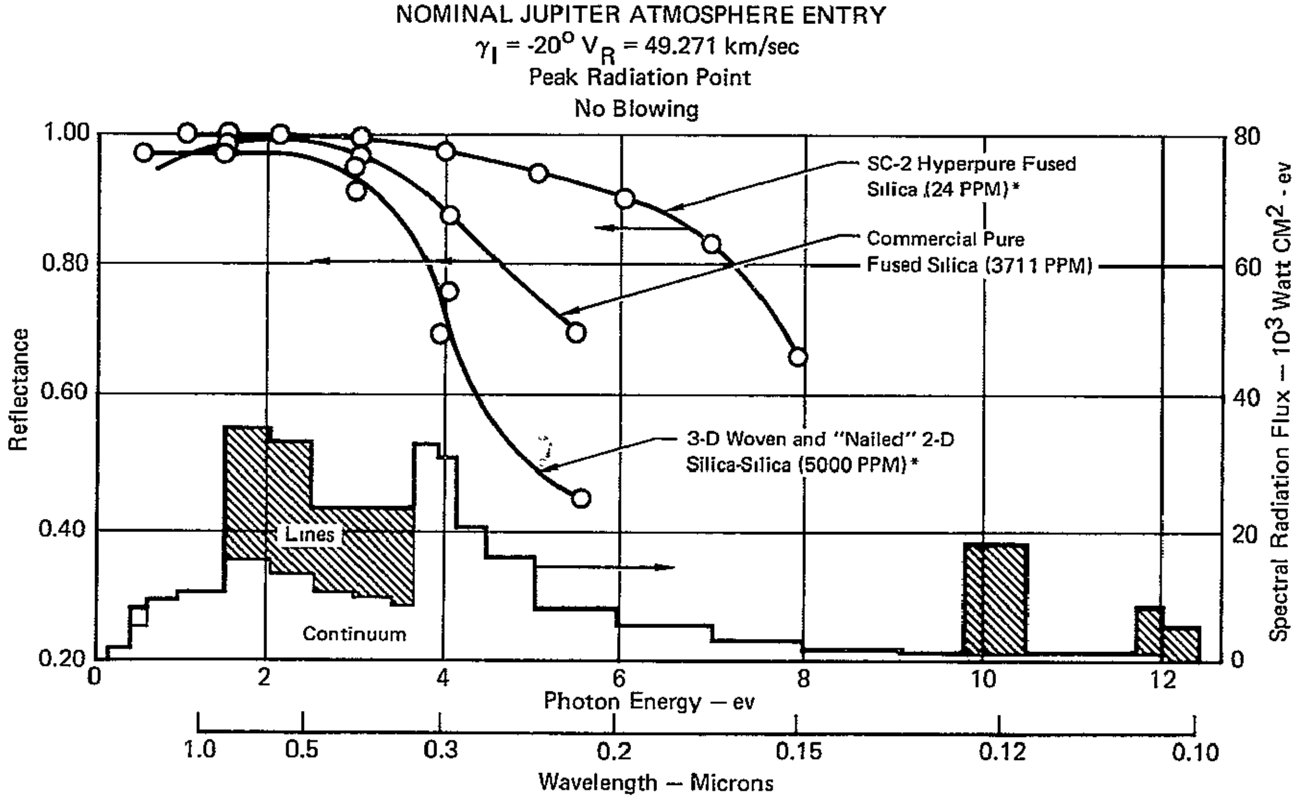
NOMINAL JUPITER ATMOSPHERE ENTRY
$\gamma_I = -20^\circ$ $V_R = 49.271$ km/sec
Peak Radiation Point
No Blowing

*Total metallic ion content estimated from reflectance data

FIGURE 2-1
REFLECTANCE OF SILICA OF VARIOUS PURITY LEVELS AND RADIANT FLUX FOR A JUPITER ENTRY AS A FUNCTION OF SPECTRAL DISTRIBUTION

GP74-4457 51

The impact of purity is shown more vividly in Figure 2-2. This graph was constructed by summing the spectral radiative flux of Figure 2-1 which would be absorbed for each of the three different purity silica materials. For example, at a proton energy level of up to 5.5 electron volts, the heat shield material containing 24 ppm impurities absorbs approximately 3 cumulative percent of the energy, while the less pure material having 5,000 ppm impurities absorbs 28 percent of the incident radiant energy up to 5.5eV.

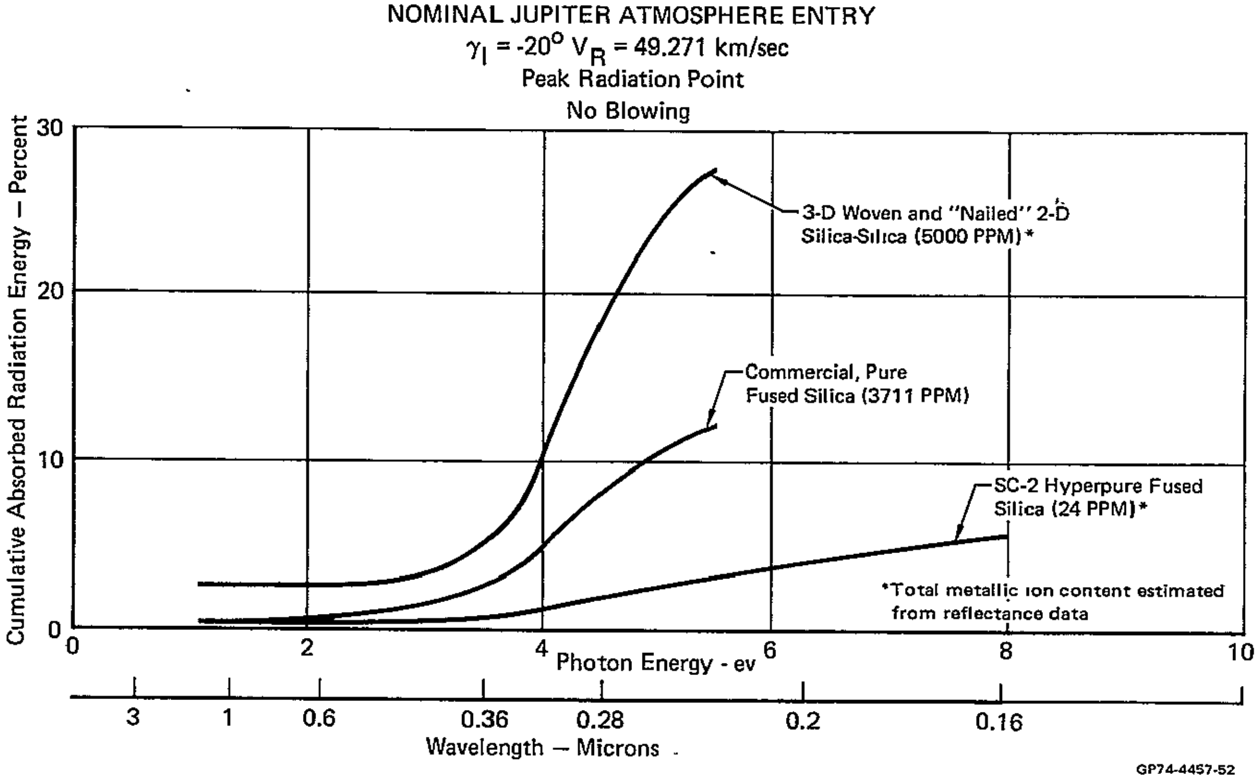

FIGURE 2-2
CUMULATIVE RADIANT ENERGY ABSORBED BY THREE SILICA MATERIALS OF VARYING PURITIES FOR A JUPITER ENTRY

Therefore, it was quite clear that purity was an extremely important consideration for maximizing reflectance and that only very pure materials should be considered in order to achieve the required low absorption coefficient. The other factor that controls the reflectance of silica is the scattering coefficient which should be as high as possible. Scattering coefficient is controlled by the internal structure or morphology of the silica to include void size, number of voids and grain shape. Therefore, the morphology and consequently the reflectance was a function of the silica grain size distribution and the firing temperature.

By refering to the dry pressed material data shown at the left of Figure 2-3, it can be seen that as the processing temperature increases, the density of the material increases rapidly and the reflectance begins to drop. It was found by microscopic examination that the number of scattering sites (voids) in the material decreased as the firing temperature was increased. Referring to the right side of Figure 2-3, it can be seen that the density of the slip cast material has a more gradual increase as the firing temperature is increased. This is due to the fact that the slip formulation contained a larger percentage of large grains (and these are less reactive)than the dry pressed material. For this reason, the reflectance at 0.35μ is always higher for the slip cast material at any given density. The realtionship between maximum reflectance, density and firing temperature is a function of wavelength. For example, the optimum reflectance for the slip cast material at 0.18μ occurs at a firing temperature of 2200°F.

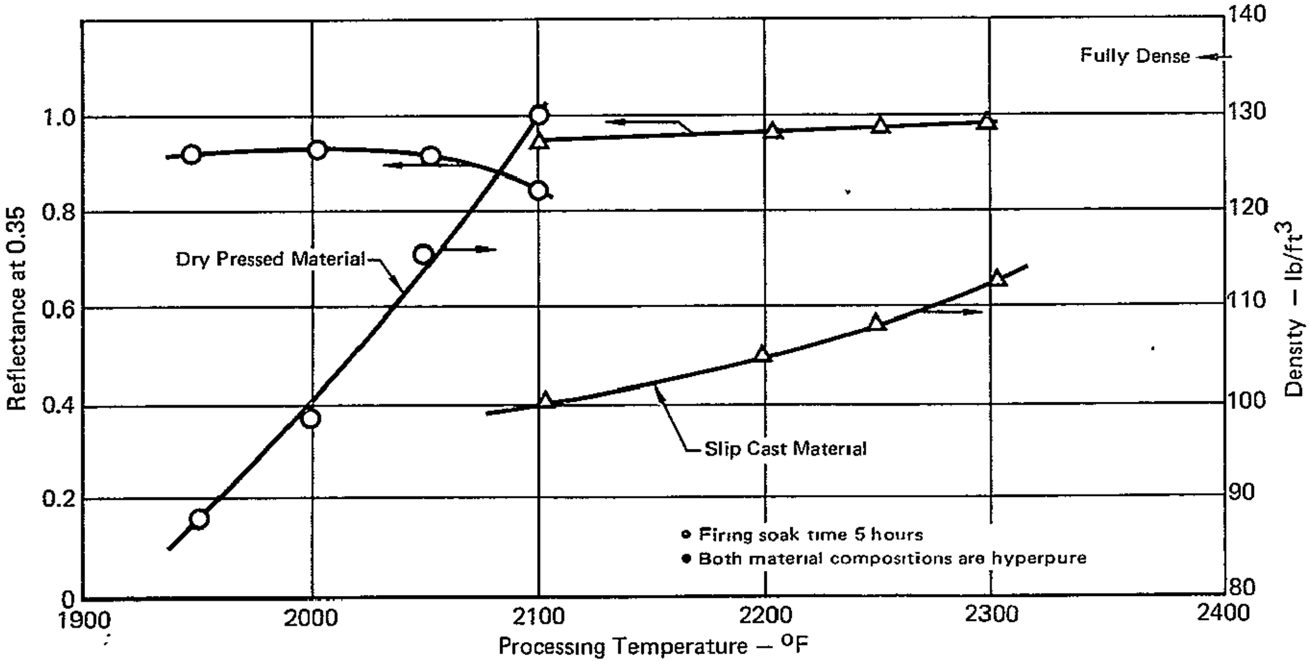

GP74-4457-53

FIGURE 2-3
CHANGES IN REFLECTANCE AND DENSITY OF HYPERPURE FUSED SILICA AS A FUNCTION OF PROCESSING TEMPERATURE

Most high purity fused silica up to the time of this program, were limited in firing temperature to about 2100°F due to devitrification, which is a disruptive phase change from the glassy state to the crystalline state. Devitrification is initiated by the presence of impurities and also by an increase in firing temperature and time. As testing progressed during this program, it became apparent that the hyperpure materials could be processed to higher and higher processing temperatures. Processing temperatures of up to 2400°F were used with no apparent devitrification observed by visual microscopic inspection, strength testing, or by x-ray diffraction. This was found to be a very unusual silica material.

As the processing temperature was increased, the strength and stiffness (as well as the density) were also increased. The property variations with processing temperature are described in the next section (2.2), and these are compared to commercial high purity material.

2.2 PROPERTIES OF HYPERPURE MATERIAL COMPARED TO COMMERCIAL PURITY MATERIAL

Various selected properties of different slip cast fused silica materials are compared in Figure 2-4. The first column in this table shows properties for our hyperpure material fired at 2200°F, which is the tentative processing temperature for optimum reflectivity for this material. The second column shows properties for hyperpure material fired at 2350°F, which is the processing temperature for optimum strength. The third column shows the properties for commercially available slip cast fused silica. Only one processing temperature is shown for this material because, as will be discussed later in this report, the material does not have the processing temperature flexibility of our hyperpure slip cast silica.

As shown in Figure 2-4, several of the properties of the hyperpure material are estimated. These estimates are made based on the corresponding values for the commercial purity material, and on the purity and resistance to devitrification of the hyperpure material. We feel that, considering the properties being estimated, these are valid estimates. The properties of flexural strength, modulus of elasticity and reflectance for which there are substantial differences between the commercial and hyperpure material are all measured values.

	Hyperpure Material Fired at 2200°F	Hyperpure Material Fired at 2350°F	Commercial High Purity (Fired at 2100°F)
Density (lb/ft^3)	108	124	117
Water Absorption (%)	12.0	1.0	4.5
Flexure Strength (psi)	2200	6700	4000 **
Flexure Modulus of Elasticity (psi)	3,500,000	11,500,000	4,500,000 **
Poisson's Ratio	0.15*	0.15*	0.15
Reflectance at 0.15μ (%)	53	16	14
Reflectance at 0.25μ (%)	91	87	71
Reflectance at 0.35μ (%)	98	97	94
Thermal Conductivity at 1000°F (Btu-in)/(Ft^2-hr °F)	3.6*	6.5*	6.0
Specific Heat at 1000°F (Btu)/(Lb-°F)	0.25*	0.25*	0.25
Linear Thermal Expansion Coefficient (in/in/°F, 32-572°F	0.31x10^{-6}*	0.31x10^{-6}*	0.31x10^{-6}

*Estimated Value

**Glasrock Products Data Sheet (Reference 3)

FIGURE 2-4

SELECTED PROPERTIES OF HIGH PURITY SLIP CAST FUSED SILICA HEAT SHIELD MATERIALS

The high fired hyperpure material is 67 percent stronger and has a 155 percent greater flexural modulus of elasticity than the commercial purity material. However, its reflectance is only slightly better. On the other hand, the low fired hyperpure material has a 4 to 278 percent greater reflectance than commercial purity material depending upon wavelength. The greatest improvement in reflectance is associated with the shorter wavelengths which predominate in most outer planet entries. The high fired hyperpure material is less reflective because there are fewer voids and consequently fewer sites for scattering reflectance. Likewise the strength and the elastic modulus of the low fired hyperpure silica is less because of the presence of these same voids.

3.0 RAW MATERIAL CHARACTERIZATION AND SELECTION

This section describes all of the high purity vitreous silica raw materials which were considered for this program. A systematic study was made of all available forms of silica materials and some of these were purchased for evaluation and for possible use in preparing test specimens. The screening of candidate raw materials involved the use of physical inspection, scanning electron microscopy, and optical property measurements. This section also describes the high purity water used for slip preparation and also for coolant in machining of silica specimens.

3.1 RAW MATERIAL AVAILABILITY

Several approaches to the fabrication of a high purity silica reflective heat shield and the types of raw materials required for these approaches were in hand at the start of this program. In order to assure that the highest purity materials which were available were used, one of the first tasks performed on this contract was to make an inquiry in the form of a letter to all the possible vendors of silica materials. A copy of this letter, which was sent to approximately 10 selected firms, is shown in Figure 3-1. Responses were received from about half of the companies.

The basic forms of silica raw materials which were considered included cloths, felts, wools, powders, and transparent optical quality fused silica rod, bar or plate. In the table in Figure 3-2, each material which was evaluated is described.

The silica binders which were evaluated included various colloidal silicas, ethyl silicates, and a silicone resin, from which was prepared a high purity binder powder of uniform particle size. These materials are also described in Figure 3-2.

Figure 3-1. Form Letter Requesting Information on Silica Raw Materials

Gentlemen:

We have just been awarded a contract by NASA-Ames Research Center to study and evaluate the use of high purity vitreous silica as a reflective heat shield. Part of the first phase of this contract is to survey suppliers of silica to determine the purity levels and material forms available.

We are asking you to help us to perform this survey by furnishing us the following information on your vitreous silica products.

Material Properties
  Density
  Fiber Diameter and/or Particle Size and Distributions

Chemical Composition
  Metallic Ion Impurities - Fe, Na, Mg, Al, Li, K, Ca
  Other Impurities - C, Cl.

Configurations Available - Felt, Wool, Cloth, Grain, etc.
  Weaves, Sizes and Shapes

Availability - Lead Time, Quantities, Delivery Schedule

Costs - Minimum Order, 1 lb, 5 lbs, 50 lbs, 100 lbs, 500 lbs.

Reproducibility - Variations to be expected within and between batches and lots.

We are primarily interested in silica containing less than 100 ppm of total impurities and having fiber/particle diameters below 10 microns.

If you do not have all of the information requested above, please send us whatever information you do have on your vitreous silica products.

Very truly yours,

J. C. Blome

J. C. Blome, Program Manager
Dept. E457, Bldg. 106
Level 2, Post E7

Style	Vendor	Thickness Count	Weight oz/yd^2	Fiber Dia / Length	Cost	Lead Time Weeks	Impurities (PPM)							Purity Percent SiO_2
							Li	Na	K	Ca	Mg	Al	Fe	
CLOTHS														
Astroquartz 570 38"W	J.P. Stevens	0.027 in. 38x24	19.5	9μ	$122/ yd^2	1	<1	1-15	1-9	<1	<1	50-150	2-5	99.95
Astroquartz 581	J.P. Stevens	0.011 in. 57x54	8.4	9μ	$58/ yd^2	1	<1	1-15	1-9	<1	<1	50-150	2-5	99.95
Suprasil 570-3" Wide Tape	J.P. Stevens	0.027 in. 38x24	19.5	4-8μ	$4900/ 10 yds	18-24	0.05	0.04	0.001	0.1	0.1	0.1	0.2	<1 PPM Impurities
Refrasil C-100-48 33"W	Hitco	–	–	10μ / 1/64-1/2"	$8/yd^2	1	1	15	40	70	60	100		99.3
Quartz Cloth	Quarts Products J.P. Stevens	0.027 in. 38x24	20	2.2μ / 3 Meters	$2,500/ yd^2	16	3	4	5	10		50	2	99.98-99.99
FIBERS														
Astroquartz Wool 557	J.P. Stevens	–	–	7μ	$75/ lb	1	<1	1-15	1-9	<1	<1	50-150	2-5	99.95
Surprasil Wool	J.P. Stevens	–	–	4.0 to 5.3	$585/ lb	10	0.05	0.04	0.001	0.1	0.1	0.1	0.2	<1 PPM Impurities
Clear Fused Quartz Wool	J.P. Stevens Amersil	–	–	4-8μ	$75/ lb	1	2	1	0.8	3	0.2	15	0.8	99.95
Microquarts Wool 108	Johns-Manville	–	–	1.2-1.4μ	$152/ 25 lb	1	No Info	700-1000	No Info	2200-2500	1000-1600	2400-2800	150	99.1-99.6
Quartz Wool	Quartz Products	–	–	2.2μ / 3 Meters	$95/ lb	6	3	4	4	10		50	2	99.98-99.99
Refrasil F100	Hitco	–	–	10μ / 1/64-1/2"	$25/ 5 lbs	1	1	15	40	70	60	100		99.3
Refrasil-Special High Purity Fibers Made for NASA-Arc	Hitco			1-3μ	$15-20/ lb									99.7

GP74-4457-58

FIGURE 3-2
HIGH PURITY SILICA RAW MATERIALS

Style	Vendor	Cost	Lead Time Weeks	Average Particle Diameter (Microns)	Impurities (PPM)							Purity Percent SiO_2
					Li	Na	K	Ca	Mg	Al	Fe	
Powders												
H40	Philadelphia Quartz Co.	$1.60/lb	1	0.018								98
F20	Philadelphia Quartz Co.	$1.50/lb	1	0.012								98
F22	Philadelphia Quartz Co.	$0.85/lb	1	0.012								98
G30	Philadelphia Quartz Co.	$1.50/lb	1	0.014								98
G32	Philadelphia Quartz Co.	$0.85/lb	1	0.014								98
Submicron Silica	Vitro Labs		1	0.014		300		200	70	400	200	99.73

Style	Vendor	Cost	Lead Time Weeks	Density (Lb/Ft^3)	Impurities (PPM)							Purity Percent SiO_2
					Li	Na	K	Ca	Mg	Al	Fe	
Slip Cast Parts												
Standard	Glasrock Products		2	119				100	90	1000	210	99.6
Hi-Purity	Glasrock Products	$25/lb	4	122	Note. Hi-purity slip cast has been less than 300 PPM alkali metals. Alkali metal impurity level in standard slip cast is not available.			70	60	1000	70	99.7
Foams												
Foam 30	Glasrock Products	$2/lb	2	32				100	90	1000	210	99.6
Foam 50	Glasrock Products	$1/lb	2	52				100	90	1000	210	99.6
Cast Foam 50	Glasrock Products		2	50				70	60	1000	210	99.7
Transparent Plates and Rods												
Type 124	General Electric		2	137								>99.97
Type 125	General Electric											>99.97
1000	Dynasil	$155/lb	2	137	Notes: Ti, Cu, Mn less than one PPM each.	<1	<1	1	1	2	4	99.9987 Typical (13 PPM)

GP74-4457-59

FIGURE 3-2 (Cont)
HIGH PURITY SILICA RAW MATERIALS

Style	Vendor	Cost	Lead Time Weeks	Density (lb/ft^3)	Impurities (PPM)							Purity Percent SiO_2
					Li	Na	K	Ca	Mg	Al	Fe	
Transparent Plates and Rods (Cont)												
Suprasil I	Amersil, Inc.	$471/lb	2	137	Note: Analyses dependent on test method. Performance comparable to dynasil based on transmission in the UV and on reflectance measurements of powders ground from the two materials.							99.9960 to 99.9990 (10 to 40 PPM)
Suprasil II	Amersil, Inc.	$176/lb	2	137								

Style	Vendor	Cost	Lead Time Weeks	Silica Concentration Percent	Impurities (PPM)							Purity Percent SiO_2
					Li	Na	K	Ca	Mg	Al	Fe	
Colloidal Silica Binders												
Syton 200	Monsanto		1	30		4000						
Syton 240	Monsanto		1	40		4000						
Syton 250	Monsanto		1	45		4000						
Ludox-HS-40	Dupont		1	40								
Ludox-HS	Dupont		1	30								
Ludox-LS	Dupont		1	30								
Ludox-SM-30	Dupont		1	30								
Ludox-TM	Dupont		1	49								
Ludox-AS	Dupont		2	30		150					2.2	
Ludox-AM	Dupont		1	30								
Silicate, Silicone and Silane Binders												
Silesteros	Monsanto	$0.55/lb	1	41.0								
Silbond Pure	Stauffer	$0.70/lb	1	28.5								99.0
Silbond Condensed	Stauffer	$0.435/lb	1	28.0								90.0
Silbond 40	Stauffer	$0.55/lb	1	40.0								
Silane	Stauffer		1	22.8								95.0
Silicone 184	Dow Corning	$15/lb	2	Nearly pure SiO_2 when condensed from thermal decomposition of the silicone	Note: 20 PPM alkali metals; 6 to 10 PPM Pt in the original silicone.							

GP74-4457-60

FIGURE 3-2 (Cont)
HIGH PURITY SILICA RAW MATERIALS

3.2 SCREENING AND SELECTION OF RAW MATERIALS

Selected materials shown in Figure 3-2 were purchased for evaluation and possible use in preparing test samples. The methods used for evaluation included physical inspection, scanning electron microscopy, and optical property measurements. Chemical analysis did not prove to be useful for purity evaluation of the generally high purity silica because of the difficulty of the analyses and lead time limitations. Chemical analyses are discussed further in Section 5.2.

Figure 3-3 shows scanning electron micrographs of candidate powder raw materials. The silicone resin pyrolysis product was found to be of a particle size which was nearly optimum for reflectance in the wavelength regions which are of interest. This material was a leading candidate as a binder for high purity silica fibers. Scanning electron micrographs of silica wool are shown in Figure 3-4. The fabrication approach using silicone was eventually discarded due to carbon entrapment as well as other processing problems (see Section 4.0 for more detail).

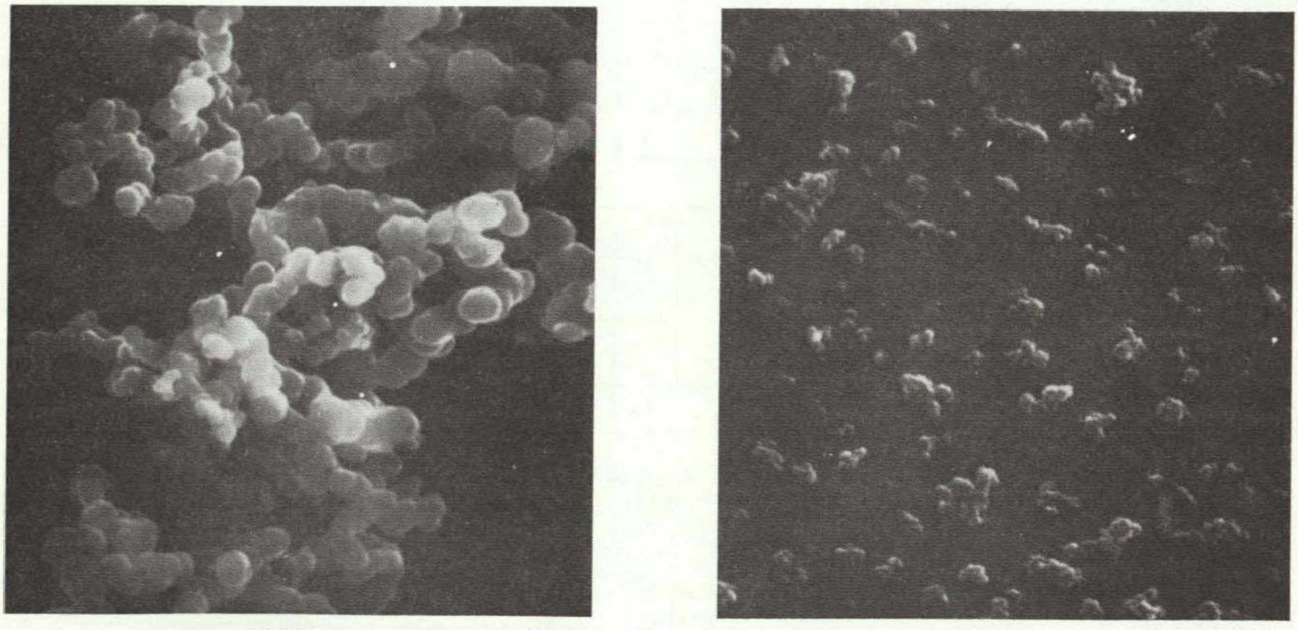

20,000 x
Silicone Resin Pyrolysis Product

20,000 x
Silanox 101

GP74-4457-54

FIGURE 3-3
TWO CANDIDATE, HIGH PURITY SILICA RAW MATERIAL POWDERS

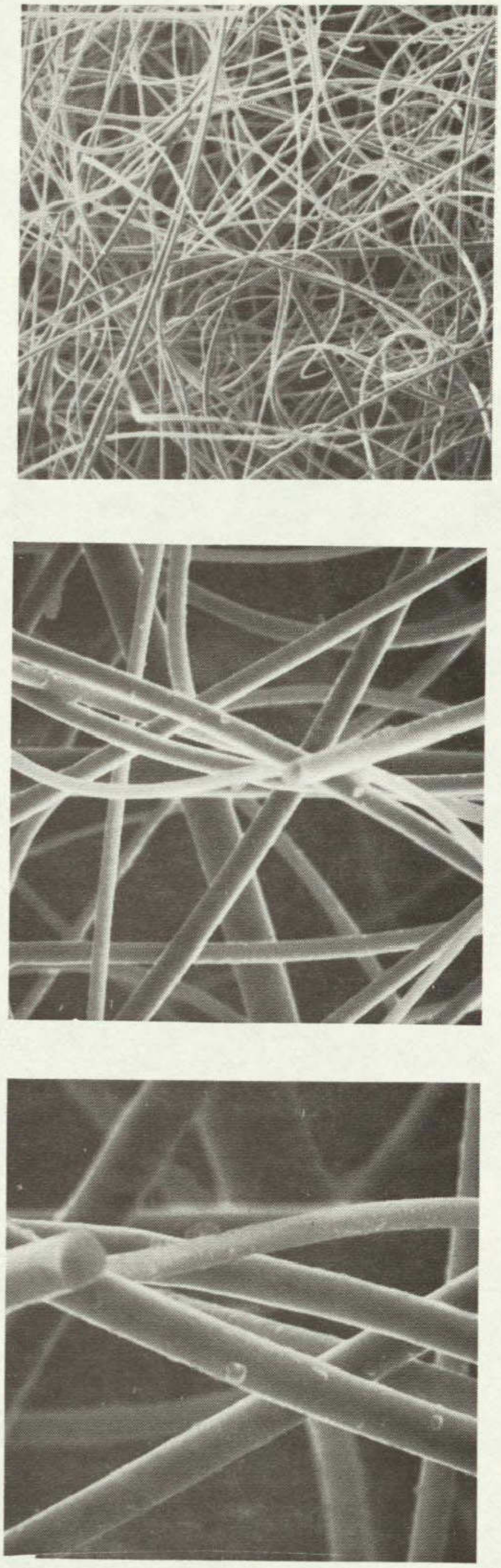

Magnification 100 x

Magnification 500 x

Magnification 1,000 x

FIGURE 3-4
HIGH PURITY ASTROQUARTZ WOOL RAW MATERIAL

GP74-4457-55

Figure 3-5 shows scanning electron micrographs of the selected hyperpure silica raw material at two stages of processing, after crushing and after ball milling. These photographs show the angularity of the particles and the range of particle sizes obtained. This material was used as a raw material in producing dry pressed and slip cast specimens and is the material selected for future work with the slip casting method for producing heat shields.

Magnification 60 x

Magnification 1000 x

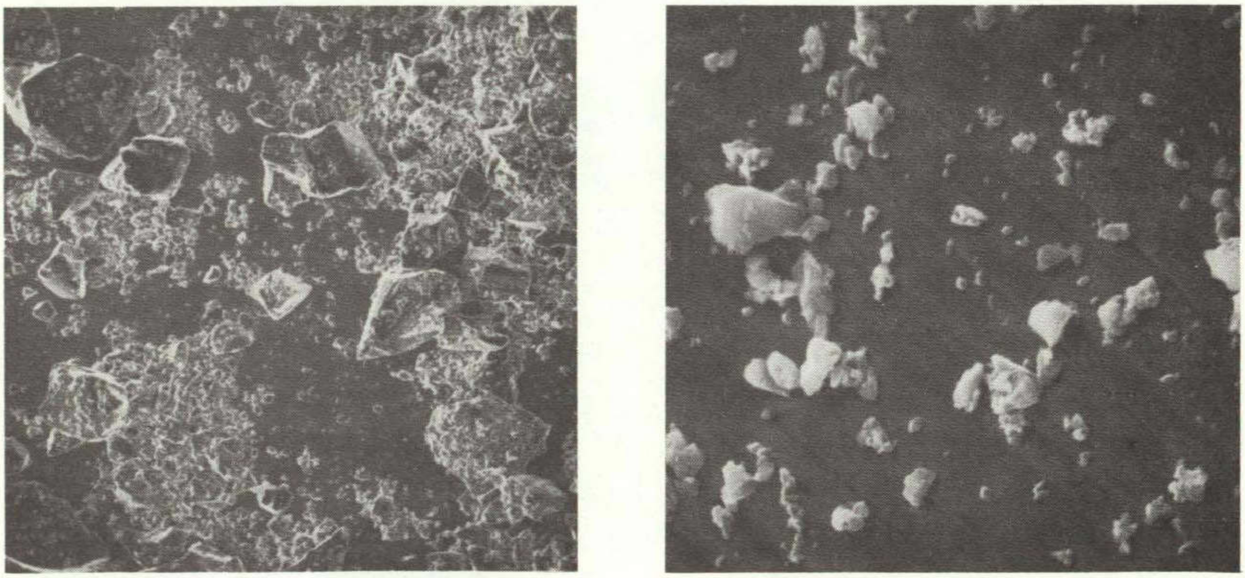

Magnification 60 x
After Crushing

Magnification 3000 x
After Ball Milling

GP72-4457-56

FIGURE 3-5
HYPERPURE SILICA RAW MATERIAL DURING PROCESSING

Reflectivity measurements were used as the primary discriminator in the evaluation of candidate raw materials. A Beckman DK2A spectroreflectometer was the instrument used to measure reflectivity on most of the candidate raw materials. Candidate cloth materials were measured for reflectance by simply stacking a number of cloth layers together with no binder used. Fibrous materials were evaluated by forming a flexible fibrous matt of a given density by a felting method which is described in Section 4.3. Candidate powder materials were measured by placing them in a specially fabricated Plexiglas sample holder which was covered with a glass of known transmittance. Approximately 40 spectral reflectance measurements were made on candidate silica raw materials, and as an example, the reflectance curve for a typical candidate cloth material is shown in Figure 3-6.

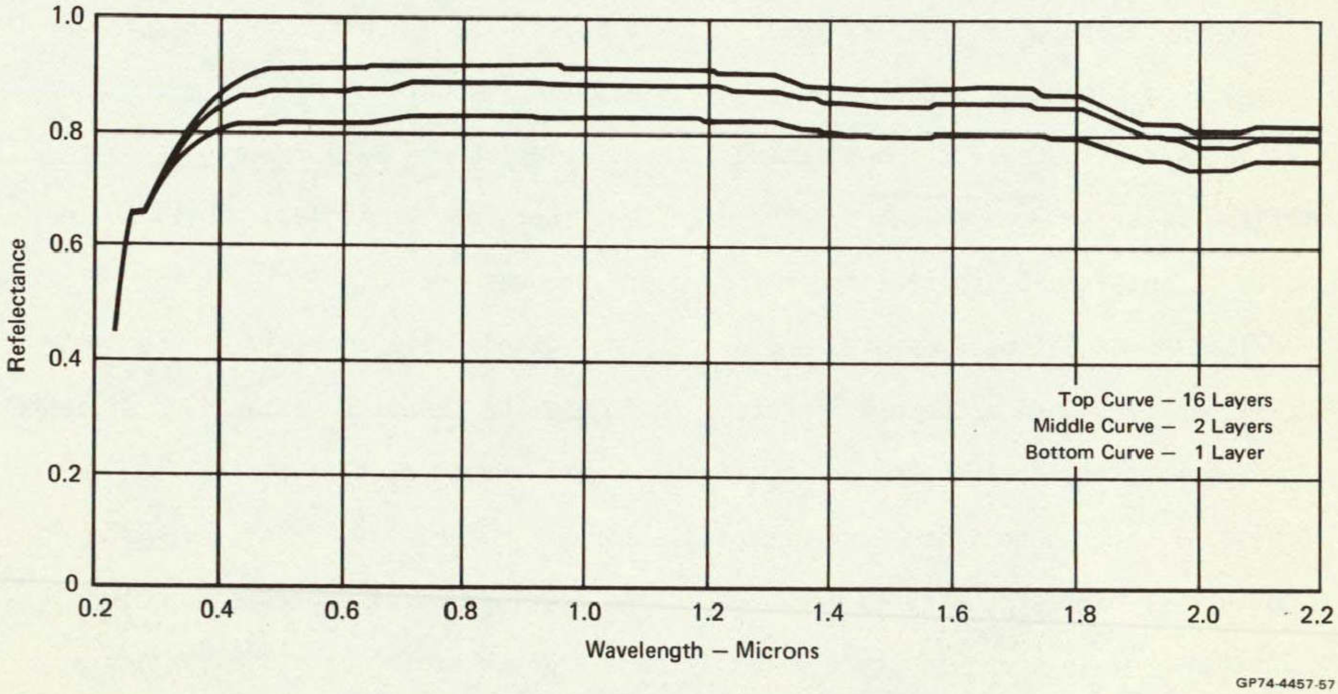

FIGURE 3-6
REFLECTANCE AS A FUNCTION OF WAVELENGTH FOR ASTROQUARTZ CLOTH

In using reflectance data for raw material screening, it was necessary to keep in mind the bulk and surface densities of the samples measured, as well as the morphology of the raw materials as measured. The effect of these factors on reflectance is discussed in Section 5.1.

Water was one of the important raw materials used in this program. The water which was used for the preparation of hyperpure silica slips and for coolant for machining specimens was a special grade of McDonnell Douglas prepared water designated MMS-606. This water was prepared by distilling it through an aluminum or glass still and then passing it through an ion exchange column. The relative metallic ion content of water was determined by measuring the resistivity of the water. The resistivity of a typical sample of MMS-606 water was 0.90 megohm while a similar sample of commercial distilled water measured 0.13 megohm. Only a relative impurity content could be determined, but MMS-606 water was selected for use since it had a higher relative purity.

In summary, the initial selection of materials for experimental evaluation included fibers of two purity levels, colloidal silica binders, silicone binders, two silica cloths, grain and rods. Because of the importance of purity on reflectance, the purest known materials available (Figure 3-2) for a given form of the material were selected. For example, fibers of the highest purity could only be obtained by special order from J. P. Stevens and Co., Inc. As the evaluation techniques improved and processing methods developed, it became clear that purity was so extremely improtant that only the thermally decomposed silicone powders and the grains produced by crushing high purity rods or plates made by chemical vapor deposition were acceptable for raw materials. This limitation on form of highest purity silica, led to the development of processes which could utilize a grain or powder type material namely dry pressing and slip casting.

4.0 FABRICATION TECHNIQUES

This section contains a description of the various approaches which were investigated for the fabrication of a high purity silica reflective heat shield. The processing techniques and the types of raw materials required for each fabrication approach is discussed. Any problems encountered and the relative advantages and disadvantages of each fabrication method is also described. It should be noted that in some cases these fabrication methods were studied in parallel so that there was some overlapping in progress, particularly with regard to the feasibility of the use of various raw materials. Also included in this section is a brief description of the clean room working area which was established especially for the fabrication of hyperpure silica.

4.1 CLEAN ROOM WORK AREA AND PROCESSING EQUIPMENT

A clean working area was constructed especially for this program to minimize contamination during the processing of the silica. The room was constructed from aluminum angles which were covered with a flexible clear plastic material. An air-conditioning unit provides a constant temperature and humidity. A dual air filter blower unit provided a slight positive pressure inside the room while introducing air into the room containing particles no larger than 0.3 microns in diameter. The floor of the clean room was covered with a special ribbed rubber mat which minimizes air-borne contamination by trapping dust particles.

Most of the processing equipment used in this program was located within the clean room work area. A laminar flow bench in the clean room was used to hold specimens between processing steps or after they had been fabricated and were awaiting evaluation. An automatically temperature controlled, air-circulating drying oven and a microwave drying oven were located in the clean room. Plastic lined processing equipment and silica containers were used exclusively to minimize metallic contamination. For example, a Teflon coating was applied to the inside surface of a stainless steel Waring blender cup used to chop silica fibers, and the standard metal chopping blades were replaced with specially fabricated polycarbonate blades.

Also housed in the clean room work area was a high purity silica machining facility. This facility was equipped with high speed diamond tooling cooled with water, which was distilled and further purified by an ion exchange process. This facility was used for coring and final machining or grinding operations. Any rough trimming required before final machining, was performed with a diamond blade cutoff wheel which was also cooled with the high purity water.

Photographs of various views of the clean room work area, including the fused silica machining facility are shown in Figure 4-1.

4.2 LAMINATED CLOTH AND YARN COMPOSITES

The work described in this section on two 6" x 6" laminated cloth billets was performed before work on this contract was started and is included here for completness. The billets were prepared during July 1973 and were delivered to NASA-Ames for evaluation.

The two billets described above are shown in Figure 4-2. They consisted of laminated silica cloth, Astroquartz and Refrasil, and were reinforced with Astroquartz yarn "nails" and bonded with colloidal silica. These samples were fabricated by installing the layers of silica cloth between plywood platens having a hole pattern through which Astroquartz yarn "nails" were manually installed on 3/8" centers, through the thickness. These parts were then vacuum impregnated with Syton colloidal silica binder. The apparatus used for vacuum impregnation of liquid binders is shown in Figure 4-3.

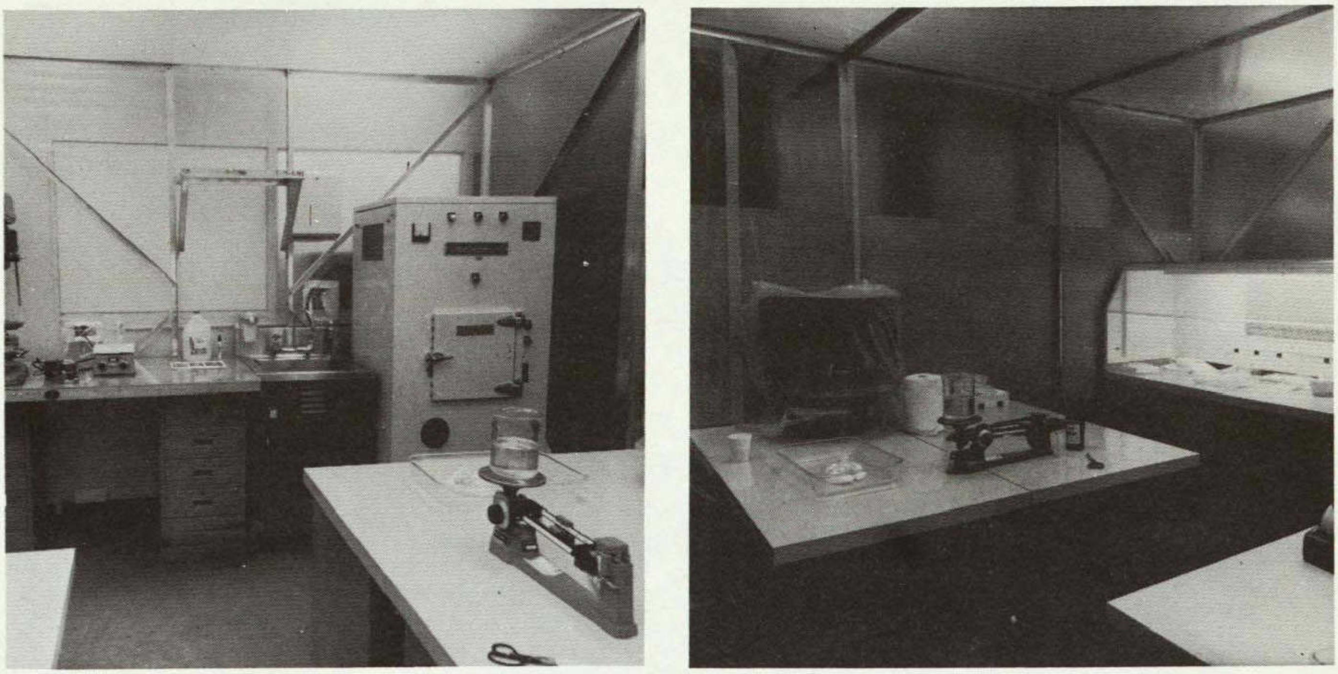

Work Area Showing Microwave Oven, Sink, etc.

Work Area Showing Laminar Flow Bench

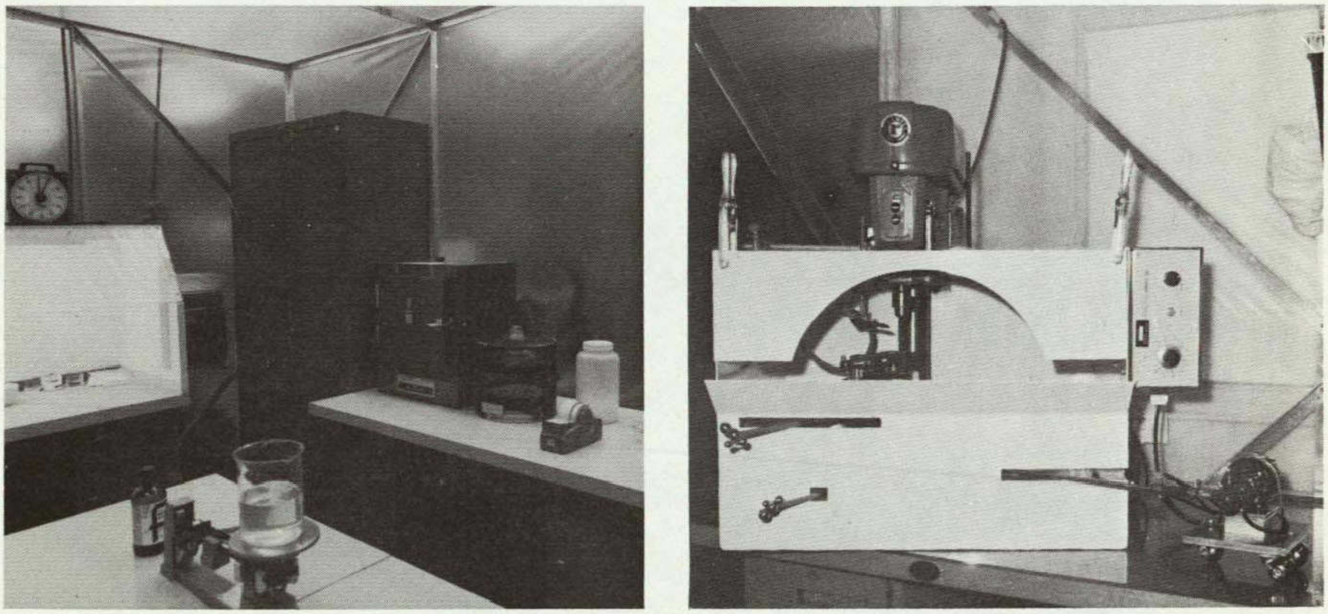

Work Area Showing Oven, Desiccator etc.

Fused Silica Machining Facility with Water Cooled Diamond Tooling

FIGURE 4-1
DEDICATED CLEAN ROOM FOR PROCESSING
HYPERPURE FUSED SILICA

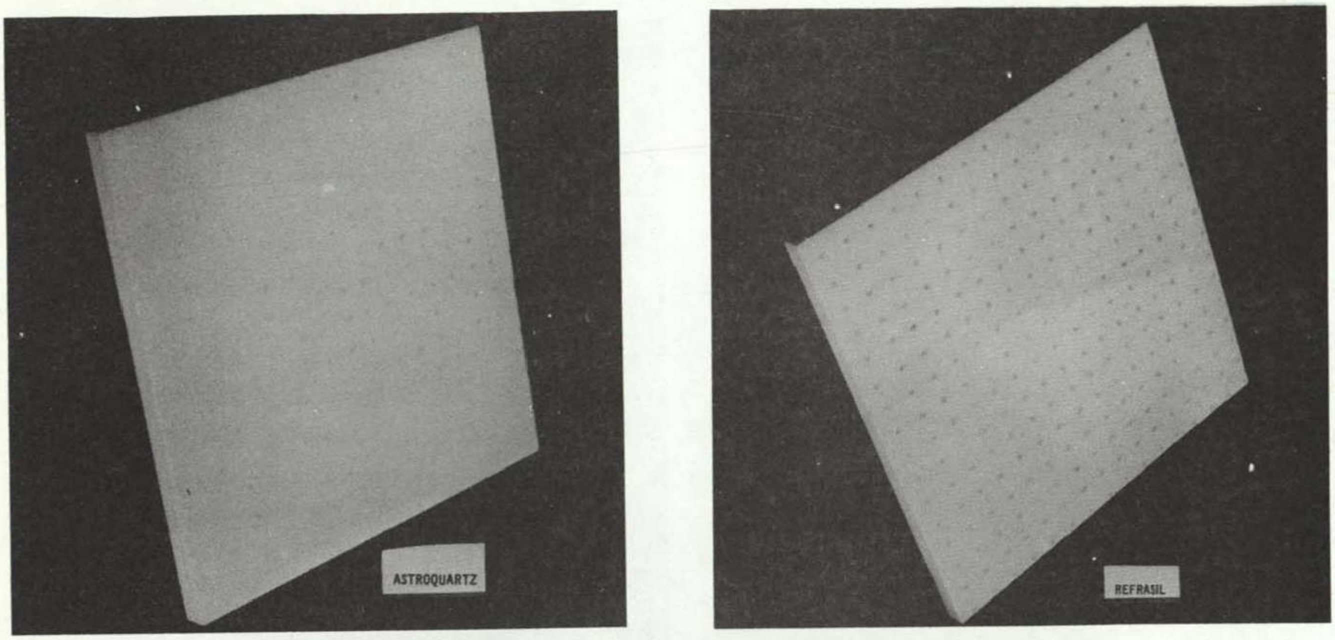

Laminated "Astroquartz" Cloth Reinforced with Silica "Nails" Bonded with Colloidal Silica Binder

Laminated "Refrasil" Cloth Reinforced with Silica "Nails" Bonded with Colloidal Silica Binder

FIGURE 4-2
TYPICAL SILICA-SILICA COMPOSITE MATERIALS

GP74-4457-2

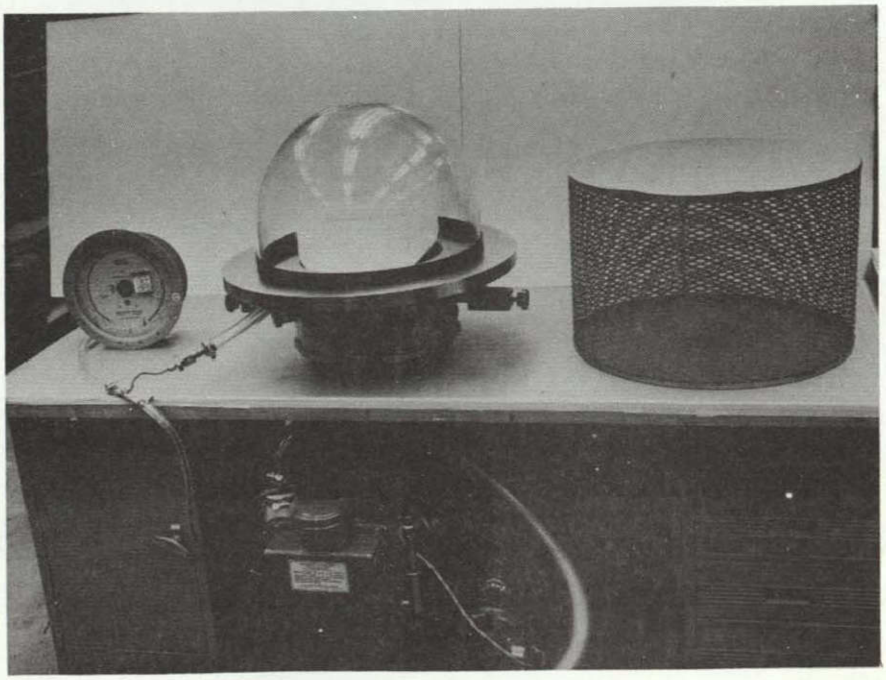

FIGURE 4-3
APPARATUS FOR VACUUM IMPREGNATION
WITH COLLOIDAL SILICA BINDERS

GP74-4457-3

initial impregnation and cure, the laminated sample was removed from the platens and had no tendency to delaminate. Impregnation of the sample was continued to a density of 88 lb/ft^3 at which time it was cut into four parts which were fired at temperatures of 800°F, 1400°F, 1700°F, and 1900°F. The samples fired at 1700°F and 1900°F underwent a 3% and 5% shrinkage in the thickness direction respectively.

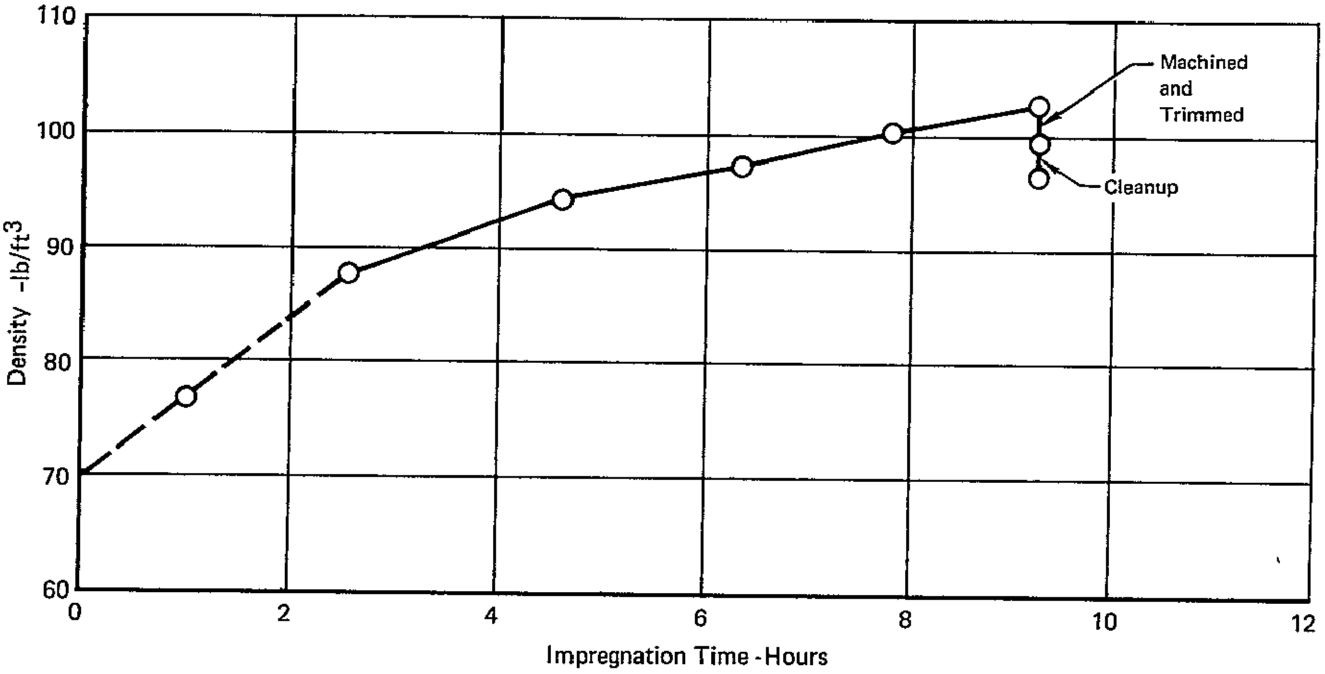

FIGURE 4-5
DENSIFICATION OF REFRASIL-SILICA
BY VACUUM IMPREGNATION

GP74-4457 5

The samples fired at 800°F and 1400°F showed a slight weight loss probably due to the loss of chemically combined water. As shown in Figure 4-6, the reflectance of the sample fired at 1900°F was improved somewhat over the unfired specimen. This shift in reflectance was slightly less for the sample fired at 1700°F and was not observed in the samples fired at 800°F and 1400°F.

After work was started on this contract, we considered using the highly reflective powder produced by the air pyrolysis of Dow Corning 184 silicone resin as a binder for 2-D cloth laminates. As discussed previously (Section 3.1) this particulate material had reflectance values of no lower than 95% of any wavelength between 0.22 and 1.5μ. The proposed method of utilizing this binder in 2-D laminates was to pyrolyze the resin "in place". Accordingly, a sample was prepared by soaking 25 layers of Refrasil cloth with catalyzed resin. These cloth layers were stacked and pressed to 100 psi while heating the sample to 190°F for 3 hours in a hot platen press. This yielded a laminated sample bonded with cured silicone resin, which was uniformly thick and had no apparent disbonds. The resin was then pyrolyzed by heating the part to 1600°F in air at a heating rate of 40°F/hour. The pyrolyzed part had poor interlaminar strength, being delaminated at four places. Also, this binder provided little or no improvement in the reflectance of the Refrasil cloth.

The 2-D laminating approach to fabrication of silica-silica heat shield material was deemphasized primarily due to poor reflectance of the candidate raw materials as discussed previously (Section 3.1).

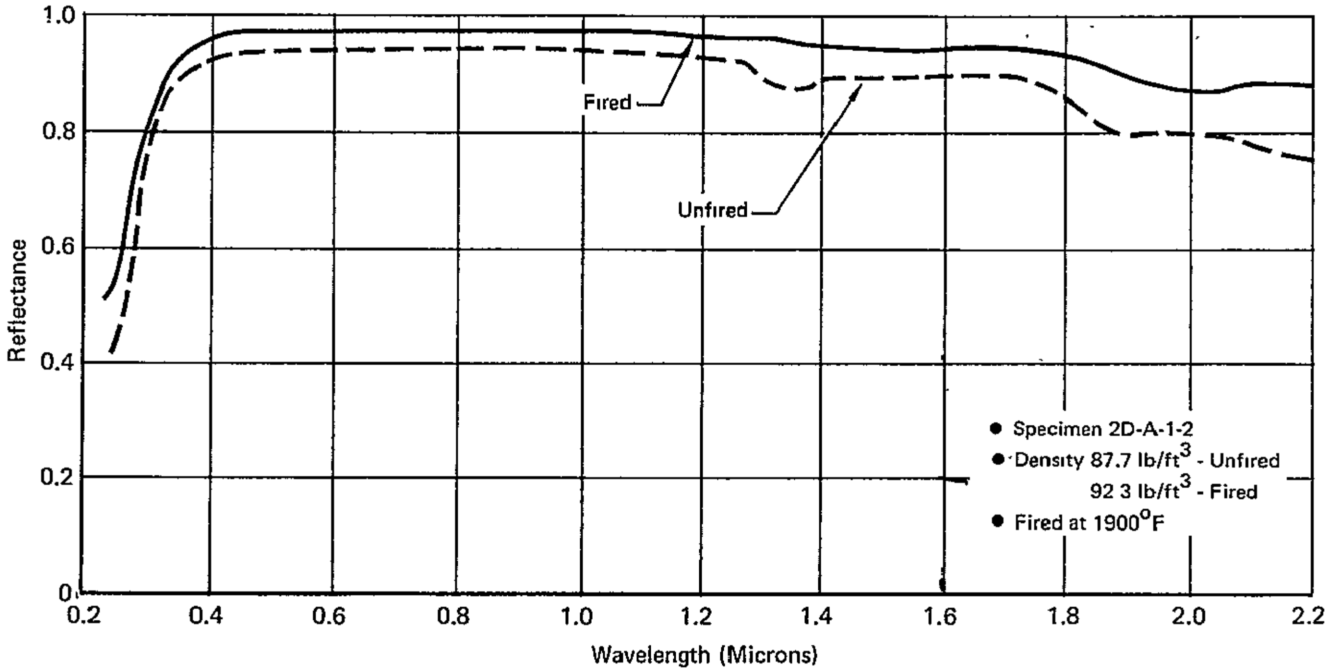

FIGURE 4-6
REFLECTANCE AS A FUNCTION OF WAVELENGTH OF 2-D LAMINATED ASTROQUARTZ CLOTH WITH COLLOIDAL SILICA BINDER

GP74-4457 6

4.3 FELTED FIBROUS MODELS

Silica fibers of various purities and diameters were evaluated for reflectance by forming them into low density flexible fibrous mats of uniform texture. This was done by charging a quantity of bulk fibers and distilled water into a Waring blender, blending for a time to chop and disperse the fibers, to form a low viscosity slurry of chopped fibers and water. The chopped fibers were then vacuum felted on a nonmetallic screen to form the flexible fibrous mat. The felted fibrous structure was then dried and fired at 1550°F to remove all moisture.

Precautions were taken at all times to minimize the introduction of metallic contaminants during the chopping and felting operations. The one-gallon stainless steel Waring blender cup was coated with a commercially available Teflon coating. Also, the steel blender blade was replaced with a specially made polycarbonate blade. A study was made of various non-metallic blade materials as shown in Figure 4-7. The Lexan blade was found to chop the silica fibers efficiently, and the Lexan material proved to be clean burning so that any contaminants introduced by the chopping blades were removed when the samples were fired.

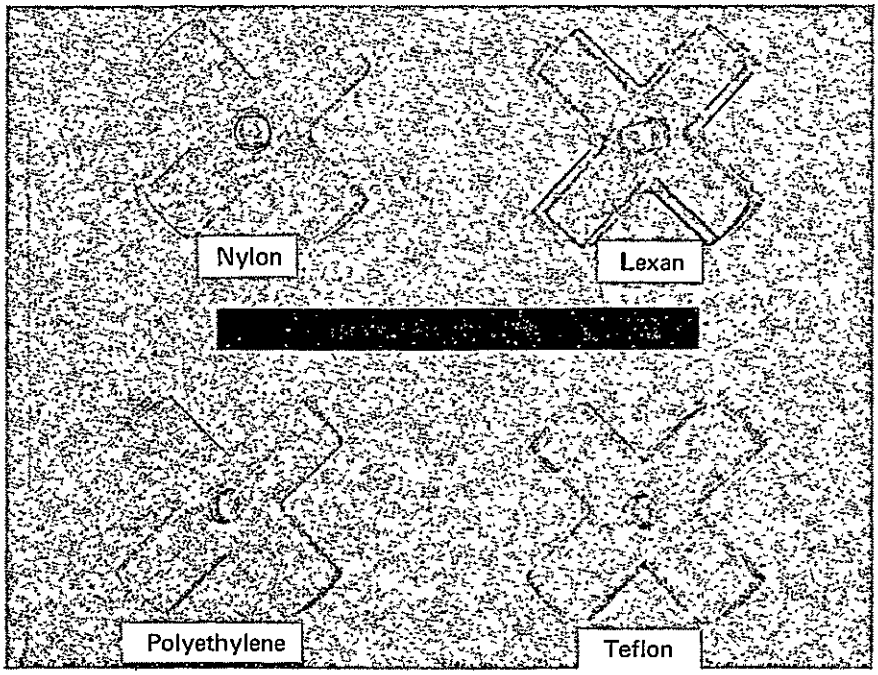

FIGURE 4-7
SPECIALLY FABRICATED NON-METALLIC WARING BLENDER BLADES

GP74-4457-7

The pure fiber silica felts made by the above method had densities ranging from 5 to 8 lbs/ft^3. These models were evaluated from the standpoint of reflectance as a function of wavelength in order to characterize the various fibrous raw materials. This characterization was discussed in Section 3.1.

The felting of fibrous structures was considered as a candidate method of fabricating a reflective heat shield. This fabrication technique would have involved the felting of fibers with colloidal silica or ethyl silicate binder. The felted structure was then to have been pressed to a given density, fired, and then reimpregnated and refired a number of times to achieve a suitable density. An attempt was made to form a sample by this method using Microquartz fibers and a colloidal silica binder. After the initial curing of the pressed sample, it was obvious that the sample was to be very binder rich if densified to a reasonably high density. Processing refinements to correct this problem were not made, and this processing method was abandoned because the available colloidal silicas were determined to contain sufficient impurities to preclude their use as a binder material. Also, the use of ethyl silicate as a binder would involve using an acid hydrolyzing agent which would present processing as well as contamination problems. The felting, pressing, reimpregnating procedure was also deemed unattractive because of the numerous processing steps involved resulting in more chances for foreign contamination to be introduced.

4.4 MOLDED FIBROUS STRUCTURES

Two basic approaches were taken in an attempt to fabricate molded fibrous silica structures having a particulate silica binder. The first approach was to densify a low density flexible fibrous silica mat by molding it under pressure and then reimpregnating it with a colloidal silica binder. The second approach involved the use of the particulate silica pyrolysis product of silicone resin as a binder for high purity silica fibers.

4.4.1 MOLDED AND REIMPREGNATED

The first approach was studied before the start of this contract and prior to the time that colloidal silica binders were virtually out as a binder candidate because of their impurity level. This approach involved the use of low density (∿3.5 lb/ft^3) Microquartz felt which was impregnated with colloidal silica binder and molded under pressure before or during the microwave curing of the binder. The molded parts were then reimpregnated a number of times with colloidal silica in order to increase their density.

A total of four samples were prepared by this method. Figure 4-8 shows the results of the densification process (the initial impregnation being the molding) and the reimpregnation. The molding pressure for each sample is noted on the curve. It should be noted that the molding pressure for samples 1, 2, and 3 was applied during the initial microwave cure of the binder by a dead weight. The molding pressure for sample 4 was applied before the initial microwave cure, the sample being under no pressure during the cure.

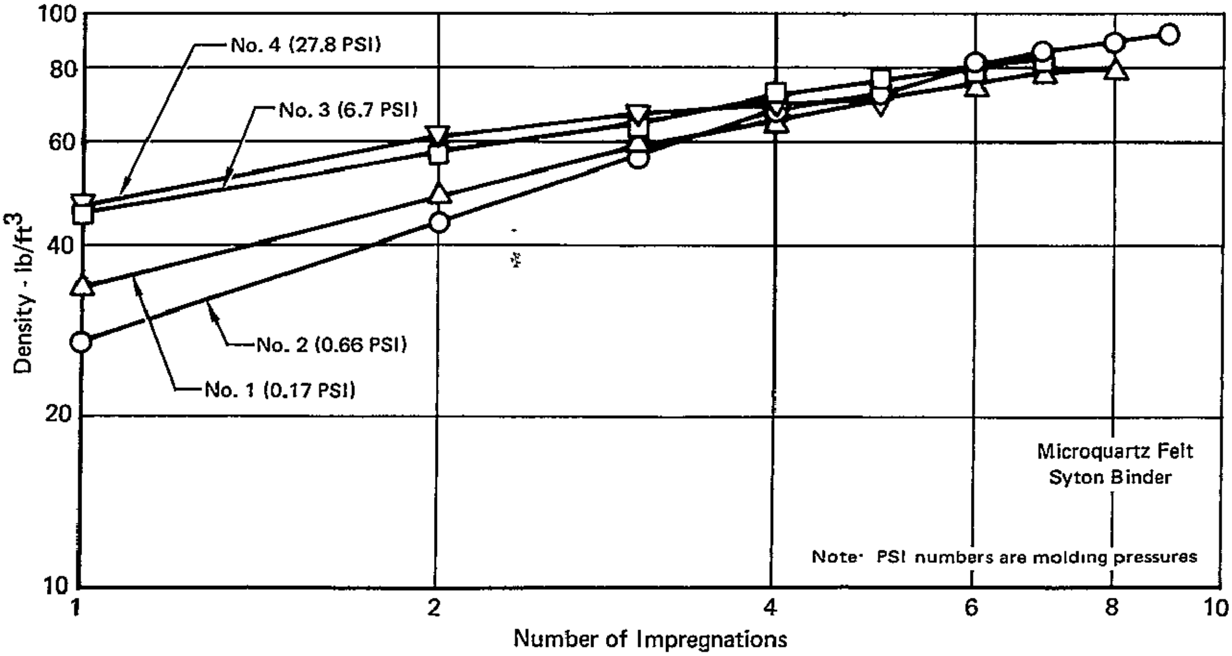

FIGURE 4-8
DENSIFICATION OF MICROQUARTZ
FELT BY IMPREGNATING WITH SYTON COLLOIDAL SILICA

GP74-4457-8

The impregnation process used was either a vacuum impregnation or simply an extended soak in the colloidal silica. The findings showed that after a certain density level is achieved, a vacuum impregnation is most efficient. For sample 1, the fifth impregnation was an overnight soak in full strength binder, while the sixth impregnation was an eighty minute vacuum impregnation at ∿ 20 mm Hg pressure.

Sample 4 was the largest of this series, measuring 6" x 6" x 0.25". After five reimpregnations, the densification of this part was not progressing due to the imperviousness of the outer layer of the sample. At this point the sample was cut into twelve individual samples ∿ 6" x 0.5" x 0.25". These twelve samples were vacuum reimpregnated four additional times, which raised their average density to 84 lb/ft^3. They were then heated in air at 825°F for a period of 16 hours to completely dry them, removing all chemically combined water. This resulted in an average weight loss of 2.5% and an average shrinkage of 0.5% in the X-Y direction and 0.75% in the Z direction.

These twelve samples were then fired at selected temperatures ranging from 900°F to 2300°F in order to characterize shrinkage and density as a function of firing temperature. The resulting data is shown in Figures 4-9 and 4-10. The fired bars exhibited some warpage due to non-uniform shrinkage which was due in turn to non-uniform density.

These twelve fired samples were machined into uniform rectangular samples which were tested for strength using four point flexural loading. The resulting flexure strength and flexure modulus data is shown with respect to processing temperature in Figure 4-11. The scatter of this data reflects the non-uniformities within each sample.

4.4.2 MOLDED WITH SILICONE

The second basic approach toward fabricating molded fibrous structures having a particulate silica binder was adapted in an effort to take advantage of the very

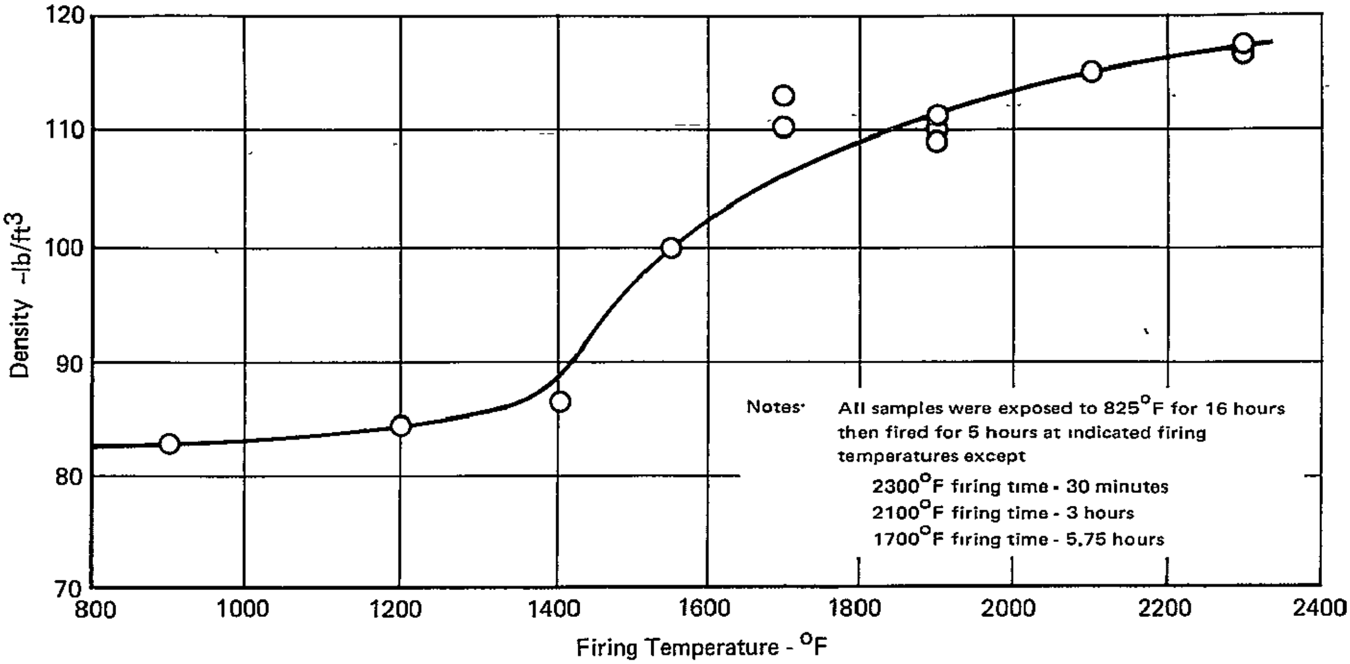

FIGURE 4-9
DENSITY AS A FUNCTION OF FIRING TEMPERATURE
OF MICROQUARTZ FELT IMPREGNATED WITH SYTON COLLOIDAL SILICA

GP74-4457-9

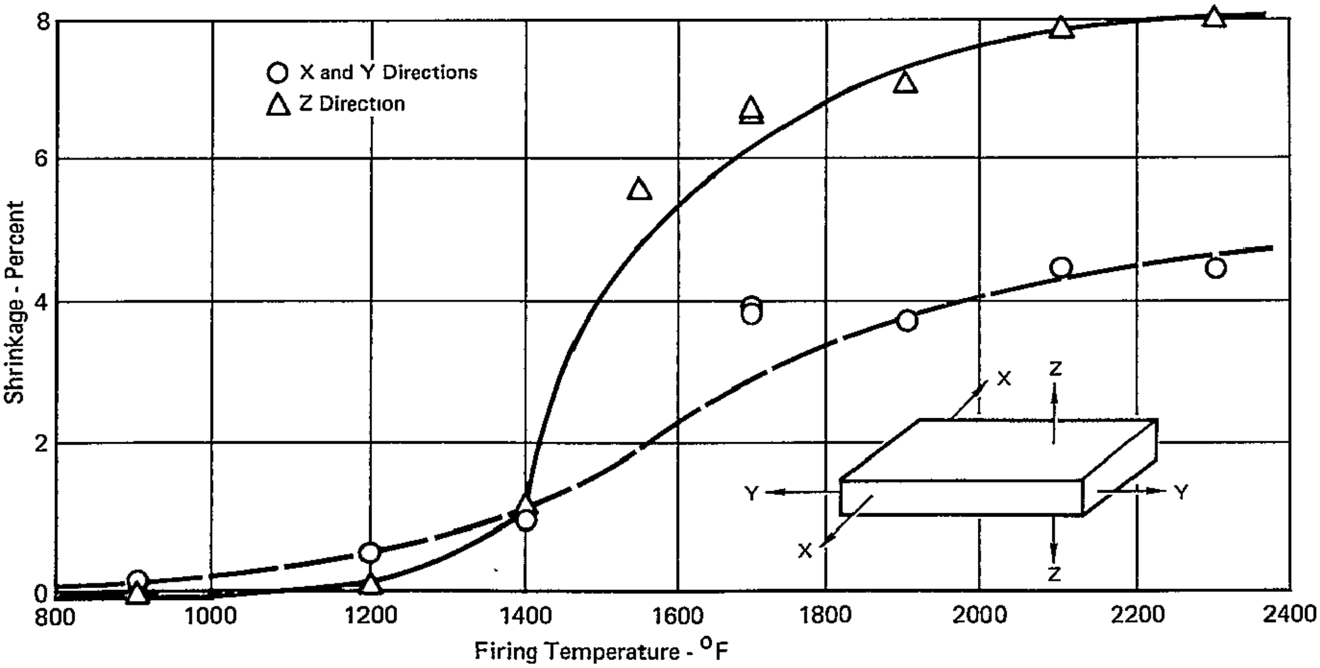

FIGURE 4-10
SHRINKAGE AS A FUNCTION OF FIRING TEMPERATURE OF
MICROQUARTZ FELT IMPREGNATED WITH SYTON COLLOIDAL SILICA

GP74-4457-10

SPECIMEN NUMBER	FIRING TEMPERATURE (°F)	FLEXURAL STRENGTH (PSI)	FLEXURAL MODULUS OF ELASTICITY (PSI)
4-1	1550	1850	1.37×10^6
4-2	1200	3600	1.68×10^6
4-3	1400	3680	2.13×10^6
4-4	1700	1810	0.70×10^6
4-6	1900	1170	0.52×10^6
4-7	2100	4830	2.90×10^6
4-8	1900	1310	0.57×10^6
4-9	2300	1520	0.45×10^6
4-10	900	2595	1.30×10^6
4-12	1900	846	0.70×10^6

FIGURE 4-11
MECHANICAL PROPERTIES OF MICROQUARTZ FELT/SYTON BINDER

high reflectance observed for the silica powder resulting from air pyrolysis of Dow Corning 184 silicone resin. The ultimate goal was to use this as a binder for the very high purity silica fibers.

Several preliminary molded fibrous samples of this type were prepared using Microquartz and 99+% pure Astroquartz fibers. The fibers were mixed with the catalyzed liquid resin, after which the resin was cured by heating the sample to $\sim$190°F for 2 hours or more under pressure. In order to accomplish this, a special mold was fabricated for use with a heated platen press. After molding/curing, the samples were pyrolyzed to convert the silicone resin to particulate silica binder. The typical pyrolysis schedule was a 40°F/hour heating rate from 400°F to 1900°F in air. Normal procedure was to place a slight pressure in the Z direction during pyrolysis by means of a simple dead weight to prevent expansion cracking in the Z direction as the resin was converted to silica.

A summary of the work performed with molded fibrous structures using silicone binder is shown in the table in Figure 4-12.

Samples MF-2, MF-3, and MF-4 showed that the silica fiber could not be well blended with the binder material (DC 184 resin) by manual mixing or kneading of the fibers and resin. The mixture of resin and fibers was relatively dry and there was a tendency for the fibers to agglomerate into clumps which did not become wetted with resin during mixing or during molding. This resulted in a molded and pyrolyzed specimen which was not homogeneous in texture and low in mechanical strength. Therefore these samples also required the use of an amount of resin which yielded a resin rich part.

The resin and fibers for MF-5 and MF-6 were mixed in a mechanical, paddle-type, low-shear mixer. Fibers for MF-5 were prechopped in a high shear Waring blender. The product of mixing the prechopped fibers and resin in the paddle mixer was a seemingly homogeneous dough-like mixture. However, the mixture could not be molded under high pressure because the entire resin-fiber system flowed out of the mold when it was pressurized. Therefore, the material was molded at room temperature and under a pressure which was considered to be sufficient to insure a uniformly thick part. After molding, it was observed that there were still fiber clumps which had not been completely wetted with resin. The mixing procedure for MF-6 was changed in that the fibers were not prechopped. The wool was cut into 4-inch squares and paddle mixed with a smaller amount of resin than for MF-5. The result was a mixture which could be molded under pressure, but the fiber clumping problem was more prevalent.

With samples MF-7 and MF-8, a solvent was introduced into the resin-fiber system to yield a lower viscosity mixture which could be mixed in a high shear Waring blender. After blending, the excess resin and solvent were removed from the fibers by filtration. The fibers were then spread out and held at room

SAMPLE NUMBER	MATERIALS	MIXING PROCEDURE	MOLDING PRESSURE (psi)	AS MOLDED			AS PYROLYZED		DISCOLORATION	COMMENTS
				DENSITY (lb/ft^3)	FIBER CONTENT (%)	TEXTURE	DENSITY (lb/ft^3)	TEXTURE		
MF-2	Microquartz 108; DC-184	Fibers wet chopped-dried resin blended by hand.	100	76.4	32	Large clumps of unwetted fibers.	57.5	Edge and surface cracks	Brownish cast over all surfaces	2% shrinkage during pyro-nonuniform shrinkage.
MF-3	Astroquartz wool; DC-184	Wool dry chopped-resin and fibers placed in mold in unblended layers.	100	-	-					Binder and fibers did not mix during molding large areas of unwetted fibers - not pyrolyzed.
MF-4	Astroquartz wool; DC-184	Wool dry chopped-resin blended by hand.	100	74.3	44	Many small clumps of unwetted fibers	52.7	Very porous low strength		No shrinkage during pyro.
MF-5	Astroquartz wool; DC-184	Wool is wet-chopped-dried -dry chopped resin mixed in paddle mixer.	<10	82.8	57	Fewer and smaller clumps of unwetted fibers.	61.7	Good-some voids - strong	Dark gray and black	Not molded at pressure because fibers and binder mixed so that they were forced out of mold together when pressurized. 3% expansion in x-y during pyro. No change in Z.
MF-6	Astroquartz wool; DC-184	Wool cut into 4" squares - mixed with resin in paddle mixer.	140	80.9	55	Fibers clump as do pre-chopped.	54.5	Clumps in same pattern as molded low adherence between clumps.	Very dark	Not mixed as well as MF-5 but clumps are somewhat wetted. 3% expansion in x-y during pyro. No change in Z.
MF-7	Astroquartz wool; DC-184; hexane	Fibers are dry chopped-mixed with resin and solvent in Waring slurry is filtered wet fibers then spread out to remove solvent.	170	80.1	45	Very few fiber clumps. Clumps are resin filled.		Good-Delamination-like cracking because of expansion in Z dir. - good strength	Brown & gray discoloration not as severe as MF-5 and MF-6	Expansion during pyro. 3% in X, Y, & Z directions. Sample was pyrod without pressure in Z direction (weight on sample). This would eliminate Z direction expansion and resultant cracking.
MF-8	Astroquartz wool; DC-184; methylene chloride	Mixed in Waring blender and processed as was MF-7.	210	82.9	46	Good. Similar to MF-7	49.8	Z direction expansion cracks - otherwise good.	Brown & gray similar to MF-7	Sample was not weighted during pyro. Additional firing 16 hrs. at 1550°F does not remove all discoloration.
MF-9	Astroquartz wool; DC-184; methylene chloride	Processed as was MF-7 and MF-8	210	72.4	56	Good- All fibers wetted	66.7	Very good hard homogeneous no Z- direction expansion cracks.	Not so severe as MF-7 and MF-8 - localized areas of discoloration which may have been binder rich.	Due to furnace malfunction, Pyro. temp. was 2200°F instead of 1900°F. Sample was weighted during pyro. 7.6% shrinkage in Z direction. No change X-Y.
MF-10	Astroquartz wool; DC-184; methylene chloride	Same as MF-7, 8, and 9.	220	75.0	55	Good	58.0	Good	Discoloration more severe than MF-9	Pyrolyzed to 1550°F @ 20°F/Hr. Weighted during pyrolization. 1.6% expansion in Z direction. 3.9% in X-Y.

FIGURE 4-12
MOLDED FIBROUS, SILICONE BONDED STRUCTURES

temperature until the remaining solvent volatilized. The result was a system of resin and fibers which could be molded under pressure at 200°F. The resulting molded parts had much fewer fiber clumps than previous samples and the existing clumps were wetted with resin.

MF-7 and MF-8 were not pyrolyzed under a slight mechanical pressure (less than 1 psi) in the Z direction as were the previous samples. Some cracking occurred due to expansion in the Z direction. Other than the cracks, these pyrolyzed samples had extremely good texture and cohesive strength. MF-9 and MF 10 verified that the Z direction expansion cracks could be eliminated by placing a weight on the sample during pyrolysis of the composite. The texture of these samples was good and no cracking was observed on the surfaces or internally.

A major problem with the silicone bonded, molded fiber approach was contamination which appeared as a discoloration. This contaminant was assumed to be entrapped carbon from the DC-184 silicone binder. Unsuccessful attempts were made to solve this problem, including reducing the pyrolysis heating rate for sample MF-10 to 20°F/hour and prolonging the air heating of pyrolyzed parts in an effort to oxidize residual carbon and organic compounds. The discoloration could not be removed.

Another problem associated with this approach was that the as-pyrolized parts had a rather low density (40 to 50% of theoretical). Although this fabricated density could probably be increased, it was concluded that parts fabricated by this method would need to be reimpregnated with additional binder material of some sort in order to obtain sufficient mechanical strength. The requirement of several reimpregnations would present additional contamination and processing problems.

In view of the above considerations, this approach was deemphasized in order to concentrate on more attractive fabrication techniques. For reference, the reflectance curve for a typical molded fibrous, silicone bonded sample is shown in Figure 4-13.

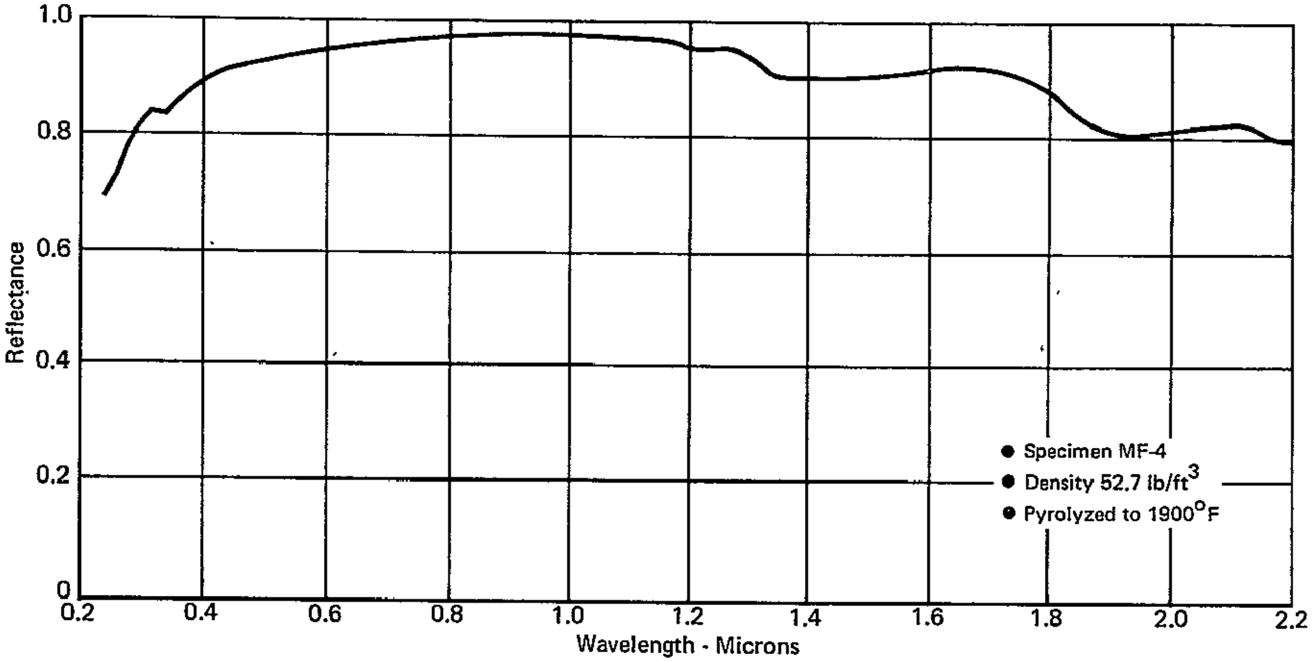

FIGURE 4-13
REFLECTANCE OF ASTROQUARTZ/SILICONE
MOLDED FIBROUS STRUCTURE

GP74-4457-11

4.5 DRY PRESSING

The dry pressing approach to the fabrication of a silica heat shield involves the use of primarily very high purity silica powders and very small amounts of a temporary organic binder and lubricant. Basically, powders of appropriate particle sizes are combined with the binder, dry pressed to a desired shape, and then sintered at high temperature.

Ultra high purity (10 ppm total metal impurities) or "hyperpure" silica powder is not available in powder form. Therefore, we developed methods for preparing and qualifying hyperpure silica grains. The starting material used for this preparation was transparent high purity silica rods purchased from two different suppliers; Dynasil Corp. of America and Amersil Inc. The hyperpure powder prepared from the material from either vendor, for our purposes, is identical. The supplier selected was Dynasil because of lower price.

The as-received rods were in various lengths of 4 inches or more and in various diameters up to 3/4 inches. The as-received rods were cut into smaller lengths and each individual piece was subjected to a cleaning process and was carefully examined. Crushing and ball milling processes were used to reduce the silica material to hyperpure powder without introducing contamination. The product from ball milling of hyperpure silica powder was separated into coarse grain for use in the next mill batch and finer grain for dry pressing. The hyperpure silica powders prepared were found to be very highly reflective. The curve in Figure 4-14 shows the reflectance of a typical hyperpure powder sample as a function of wavelength as measured on the Beckman DK2A instrument.

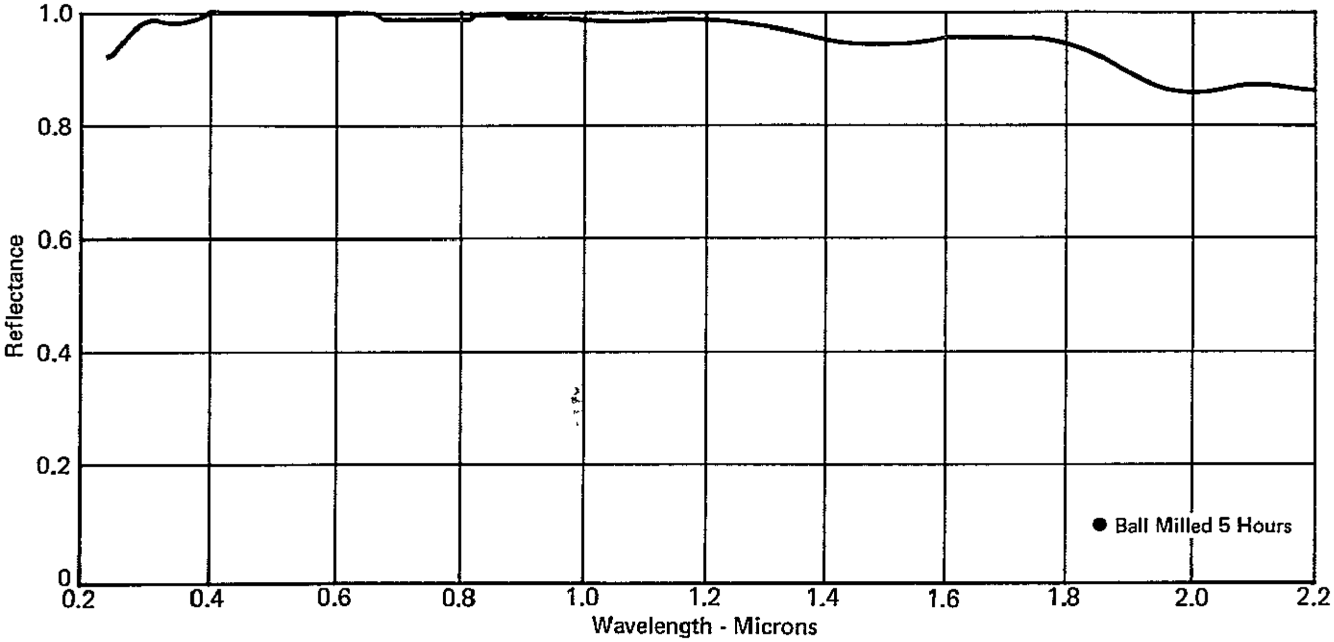

FIGURE 4-14
REFLECTANCE OF HYPERPURE SILICA POWDER
PREPARED BY BALL MILLING

GP72-4457-12

The particle size distribution of satisfactorily ground particles obtained from ball milling was determined by a sedimentation process according to ASTM Method D422-63. A weighed silica sample (slurry or powder) was dispersed in sufficient distilled water to make one liter of mixture placed inside a glass sedimentation cylinder. The liquid dispersing agent was usually pure distilled water, but a solution of sodium metaphosphate in water having a concentration in accordance with ASTM D422-63 was also tested. The specific gravity of the silica mixture was determined at periodic increments after sedimentation began, using a hydrometer designated 151H by ASTM. The temperature of the mixture and the specific gravity of a sample of the liquid dispersing agent was measured and recorded at the same time as the specific gravity of the silica mixture. The particle diameter (D) and the weight percent (P) of particles finer than D were calculated from formulas based on Stoke's law and are defined in ASTM D422-63. The values of P were plotted as a function of D on semi-logarithmic graph paper.

In order to become familiar with this test method, a non-vitreous silica powder, (S-153) which is readily available, was used. ASTM D422-63 calls for the use of sodium metaphosphate as a dispersing agent. The S-153 powder was used to verify (see Figure 4-15) that pure distilled water could be used as a substitute dispersing agent to prevent sodium contamination in the hyperpure silica material. In subsequent particle size determinations pure distilled water was used so that hyperpure powder could be recovered and used for other purposes.

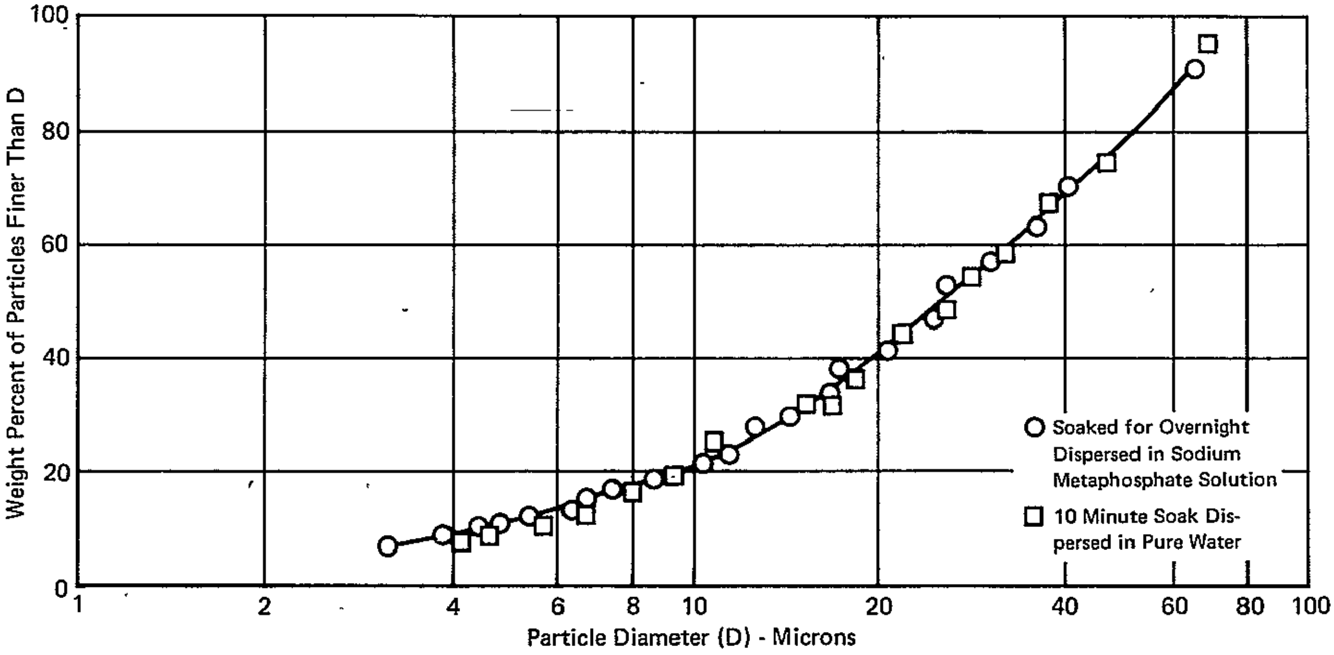

FIGURE 4-15
PARTICLE SIZE DISTRIBUTION OF UNMILLED S-153 SILICA

GP74-4457-13

The curves in Figure 4-16 show the particle size distribution of hyperpure silica powder prepared by ball milling for two different milling times.

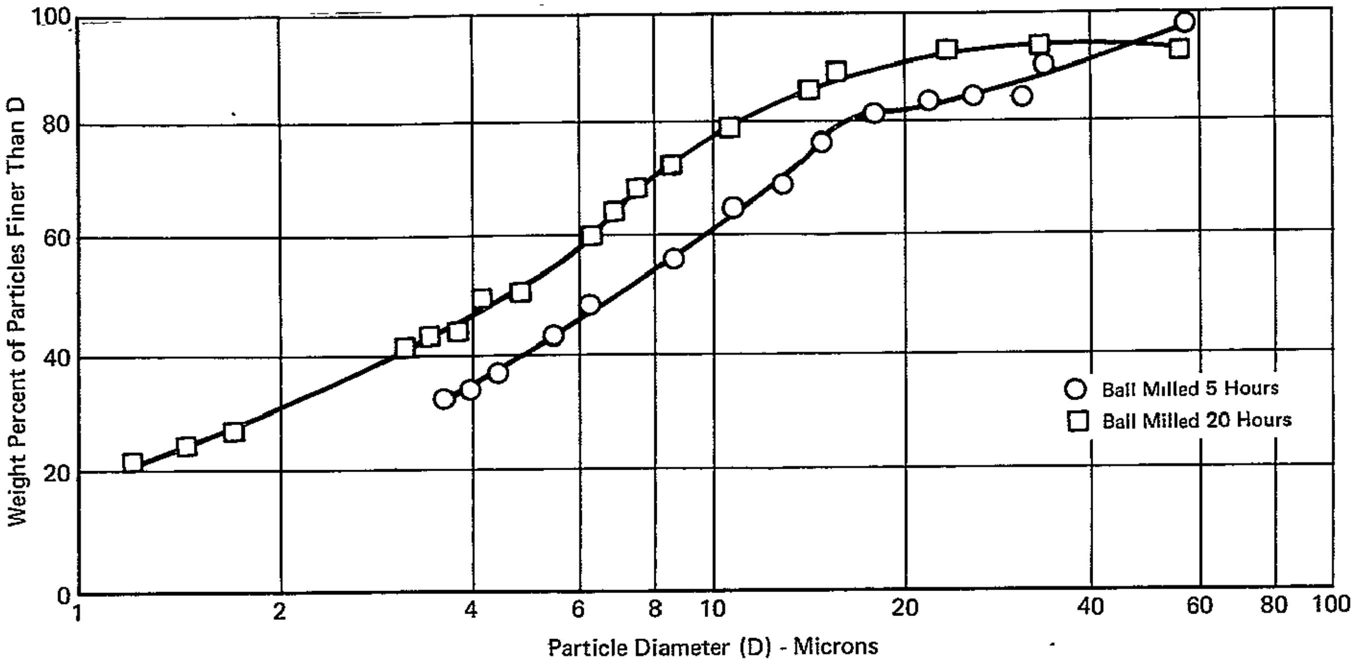

FIGURE 4-16
PARTICLE SIZE DISTRIBUTION OF HYPERPURE SILICA POWDER

GP74 4457-14

The procedure developed for the dry pressing and sintering of hyperpure silica grains is as follows:

The silica powders were mixed with an aqueous solution of polyvinyl alcohol (PVA) by ball milling. The PVA is the temporary binder which burns out during sintering. The consistency of the slurry formed was adjusted by adding PVA solution. When the slurry reached the proper consistency (thickly flowing) it was poured in a thin layer on absorbent paper which was held in a plaster mold. The slurry was dried to a cake of the proper water content and then granulated. The granules were sealed in a polypropylene bottle and stored (usually overnight) to allow the moisture content to equalize throughout the material. The material was then pressed to the desired shape using conventional molds and a hydraulic press, completely dried, and fired. The firing cycle was started at room temperature, increased to peak temperature and held at peak temperature 5 hours at which time the sample was removed from the furnace and allowed to cool rapidly.

Polyvinyl alcohol (PVA) was used exclusively as the binder for preparing material for dry pressing until a burnout test was conducted on the PVA alone showing that it has a residue of 0.67% after 5 hours at 2000°F in air. If this residue is presumed to consist entirely of oxides of metal impurities, an introduction of 67 PPM impurities into a fired dry pressed part would result from the use of 1% PVA binder. Therefore, an effort was made to find a less contaminating binder.

A sample which was pressed without binder had no green strength, showing that some binder is necessary. Burnout tests were performed on several candidate materials, the two most promising of which (from the standpoint of low residue) were sugar and hydroxypropylcellulose, a product used in the food industry having the trade name of Klucel. Samples made using these materials as binders had little or no green strength. A sample made using 3% sugar as binder exhibited barely acceptable green strength but poor fired strength.

PVA was thus established as the best binder available at this time. A study was run varying the amount of binder used and a minimum of 0.5% PVA, based on total solids, was required. This amount of binder will introduce approximately 35 PPM impurities, including oxygen, into the fired sample.

The table in Figure 4-17 shows the processing data obtained from all of the dry pressed samples made in this program, included the samples used in the binder study described above. All of the samples listed in this table were in the form of 1 1/8 inch diameter disks, and were pressed in a standard Carver cylinder in a Carver Laboratory Press.

Samples DP-1, 2, 3, and 4 were fabricated using an inexpensive, readily available, non-vitreous silica (S-153) in order to establish pressing and firing techniques. Sample DP-1 was the only sample which was not mixed by ball milling. An

SPECIMEN NUMBER	INGREDIENTS			MOLDING PRESSURE (psi)	WET DENSITY (lb/ft^3)	WATER CONTENT (%)	GREEN STATE		FIRING TEMP. (°F)	AS FIRED				COMMENTS
	MATERIAL	BATCHING %	AVG. PART SIZE				DENSITY (lb/ft^3)	BINDER CONTENT (%)		DENSITY (lb/ft^3)	SHRINKAGE (% X-Y)	SHRINKAGE (% Z)	WEIGHT LOSS (%)	
DP-1	S-153 S-153 DC184 +PVA	50 25 25	25μ 5.5μ -	10,000	87.6	2.4	85.6	22.	2,160	74.3	0.7	-3.5	11.4	PVA Content Much Too High - Fired Product is Soft - Easily Damaged - Mixture Not Ball Milled
DP-2	S-153 S-153 DC184 +PVA	50 25 25	25μ 5.5μ -	10,000	116.3	19.5	93.8	1.9	2,160	93.4	0.3	1.4	2.1	Better Texture Than DP-1
DP-3	S-153 S-153 +PVA	30 70	5.5μ 25μ	6,000	106.9	9.2	96.9	1.2	2,160	95.2	-0.4	0	0.8	Poor Texture
DP-4	S-153 S-153 +PVA	70 30	25μ 5.5μ	10,000	109.7	8.7	101.0	1.2	2,160	98.3	-0.3	-0.6	0.8	Higher Pressure Increases Green Density
DP-5	Hyperpure Hyperpure +PVA	70 30	7μ 4μ	8,000	98.4	9.4	89.1	1.0	2,050	100.5	4.1	5.6	2.0	Good Texture - Higher Shrinage Due to Use of Vitreous Silica
DP-6	Hyperpure Hyperpure +PVA	70 30	7μ 4μ	8,000	98.1	7.8	90.3	1.0	2,150	118.4	8.2	9.0	2.1	Good Texture
DP-7	Hyperpure Hyperpure DC184 +PVA	50 25 25	7μ 4μ -	8,000	89.0	10.0	79.9	2.0	2,000	99.2	7.6	7.0	2.6	Good Texture
DP-8	Hyperpure Hyperpure DC184 +PVA	50 25 25	7μ 4μ	8,000	87.8	9.5	79.5	2.0	2,050	115.9	12.6	11.5	2.6	Some Roughness On One Surface May Be Due To Large Particle of Dynasil and High Shrinkage - Otherwise Good
DP-9	Hyperpure Hyperpure DC184 +PVA	50 25 25	7μ 4μ -	8,000	87.8	9.4	79.6	2.0	2,100	131.1	15.9	14.9	2.6	Similar to DP-8

FIGURE 4-17.
DRY PRESSED HYPERPURE SILICA MATERIALS

SPECIMEN NUMBER	INGREDIENTS			MOLDING PRESSURE (psi)	WET DENSITY (lb/ft³)	WATER CONTENT (%)	GREEN STATE		FIRING TEMP. (°F)	AS FIRED				COMMENTS
	MATERIAL	BATCHING %	AVG. PART SIZE				DENSITY (lb/ft³)	BINDER CONTENT (%)		DENSITY (lb/ft³)	SHRINKAGE (% X-Y)	SHRINKAGE (% Z)	WEIGHT LOSS (%)	
DP-10	Hyperpure Hyperpure DC184 No Binder	50 25 25	7μ 4μ	8,000	- Sample Has Very Poor Green Strength Sample Not Processed Further	-	-	-	-	-	-	-	-	Binder is Required
DP-11	Hyperpure Hyperpure DC184 + Sugar	50 50 25	7μ 4μ	8,000	- Sample Has Very Poor Green Strength Sample Not Processed Further	-	-	1.4	-	-	-	-	-	Sugar is Not A Satisfactory Binder
DP-12	Hyperpure Hyperpure DC184 + Sugar	50 25 25	7μ 4μ	8,000	75.7	2.1	75.7	3.1	1,950	- Sample Has No Fired Strength	-	-	-	Sugar Is Not A Satisfactory Binder
DP-13	Hyperpure Hyperpure DC184 +PVA	50 25 25	7μ 4μ	8,000	81.3	1.1	80.4	1.8	1,950	87.5	3.5	3.4	2.8	Good Texture
DP-14	Hyperpure DC184 + Klucel	70 30	7μ	8,000	- Sample Has Very Poor Green Strength	-	-	2.3	-	-	-	-	-	Klucel Is Not A Satisfactory Binder
DP-15	Hyperpure DC184 + Klucel	70 30	7μ	10,000	- Sample Has Very Poor Green Strength	-	-	2.3	-	-	-	-	-	Klucel Is Not A Satisfactory Binder
DP-15A	Hyperpure Hyperpure DC184 +PVA	50 25 25	7μ 4μ	8,000	78.0	0.1	78.0	0.5	2,100	92.1	10.3	-4.5	0.70	
DP-16	Hyperpure Hyperpure DC184 +PVA	50 25 25	7μ 4μ	8,000	79.6	0.1	79.6	1.0	2,100	111.5	12.0	8.6	0.96	
DP-17	Hyperpure Hyperpure DC184 +PVA	50 25 25	7μ 4μ	8,000	76.3	0.3	76.0	5.6	2,100	- Edges of Sample Crumbled Off During Firing	-	-	-	Poor Fired Strength

FIGURE 4-17 (Continued)

DRY PRESSED HYPERPURE SILICA MATERIALS

	INGREDIENTS						GREEN STATE			AS FIRED				
SPECIMEN NUMBER	MATERIAL	BATCHING %	AVG. PART SIZE	MOLDING PRESSURE (psi)	WET DENSITY (lb/ft^3)	WATER CONTENT (%)	DENSITY (lb/ft^3)	BINDER CONTENT (%)	FIRING TEMP. (°F)	DENSITY (lb/ft^3)	SHRINKAGE (% X-Y)	SHRINKAGE (% Z)	WEIGHT LOSS (%)	COMMENTS
DP-18	Hyperpure Hyperpure DC184 +PVA	50 25 25	7μ 4μ	8,000	69.1	0.5	68.7	11.1	2,100	97.2	13.4	15.6	10.6	Poor Fired Strength
DP-19	Hyperpure Hyperpure DC184 +PVA	50 25 25	7μ 4μ	8,000	- Sample Delmainated During Removal From Mold	-	-	0.3	2,100	-	-	-	-	Poor Green Strength - Good Fired Strength
DP-20	Hyperpure Hyperpure Hyperpure +PVA	50 25 25	17μ 7μ 4μ	8,000	86.4	0.9	85.6	1.2	2,150	115.2	10.0	9.4	1.1	Used Trimodal Dist. with Larger Coarse Particles - Did Not Improve Green Density.
DP-21	Hyperpure Hyperpure Hyperpure +PVA	50 25 25	17μ 7μ 4μ	8,000	86.0	0.7	85.4	1.2	2,100	103.4	6.0	6.5	0.8	Discovered Metal Screen Causes Contamination
DP-22	Hyperpure Hyperpure Hyperpure +PVA	50 25 25	17μ 7μ 4μ	8,000	86.4	1.0	85.4	1.2	2,050	97.3	4.5	4.9	1.0	
DP-23	Hyperpure Hyperpure Hyperpure +PVA	25 50 25	17μ 7μ 4μ	8,000	87.9	2.5	85.7	1.2	2,000	98.8	4.9	5.1	1.1	DP23-25 Studied Properties vs Molding Pressure
DP-24	Hyperpure Hyperpure Hyperpure +PVA	25 50 25	17μ μ μ	12,000	90.3	2.7	87.8	1.2	2,000	100.4	4.6	4.9	1.1	
DP-25	Hyperpure Hyperpure Hyperpure +PVA	25 50 25	17μ 7μ 4μ	16,000	91.9	3.0	89.1	1.2	2,000	102.4	4.8	5.0	1.1	Green Density Increased Slightly by Doubling Molding Pressure

FIGURE 4-17 (Continued)

DRY PRESSED HYPERPURE SILICA MATERIALS

	INGREDIENTS					GREEN STATE				AS FIRED				
SPECIMEN NUMBER	MATERIAL	BATCHING %	AVG. PART SIZE	MOLDING PRESSURE (psi)	WET DENSITY (lb/ft^3)	WATER CONTENT (%)	DENSITY (lb/ft^3)	BINDER CONTENT (%)	FIRING TEMP. (°F)	DENSITY (lb/ft^3)	SHRINKAGE (% X-Y)	SHRINKAGE (% Z)	WEIGHT LOSS (%)	COMMENTS
DP-26	Hyperpure Hyperpure +PVA	50 50	7μ 4μ	8,000	85.2	0.3	84.9	1.4						Note Non-Optimum Packing Compared to Nos. 30, 31, 32 (See Green Density)
DP-27	Hyperpure Hyperpure +PVA	50 50	7μ 4μ	8,000	106.5	9.7	84.8	1.4						
DP-28	Hyperpure Hyperpure Hyperpure +PVA	50 25 25	10μ 7μ 4μ	8,000	92.6	5.0	88.0	1.4						Used 10-7-4u Trimodal Dist In Further Attempt to Increase Green Density
DP-29	Hyperpure Hyperpure Hyperpure +PVA	50 25 25	10μ 7μ 4μ	8,000	86.9	0.2	86.7	1.4						
DP-30	Hyperpure Hyperpure -PVA	70 30	7μ 4μ	8,000	106.9	16.9	88.9	1.4						
DP-31	Hyperpure Hyperpure +PVA	70 30	7μ 4μ	8,000	99.9	11.4	88.5	1.4						
DP-32	Hyperpure Hyperpure +PVA	70 30	7μ 4μ	8,000	100.5	12.2	88.2	0.5						
DP-33	Hyperpure Hyperpure +PVA	70 30	7μ 4μ	8,000	86.6	0.7	86.0	0.5						
DP-34	Hyperpure Hyperpure Hyperpure +PVA	50 25 25	7μ 4.5μ 4μ	8,000	91.8	6.8	85.5	0.5						Used 25% Powder Which Was Milled For Extended Time (40 Hours). Later Discovered That This Powder Was Not Finer Than 20 Hour Milled Material.

FIGURE 4-17 (Continued)

DRY PRESSED HYPERPURE SILICA MATERIALS

attempt was made to mix this sample using a rotating mechanical mixer which was not satisfactory because too large a volume of liquid was required, resulting in an excessive binder content.

The raw materials used for dry pressing high purity vitreous silica bodies included the hyperpure silica powders prepared by ball milling and the very fine (0.2 to 0.3μ) silica powder produced by the air pyrolysis of Dow Corning 184 silicone resin.

The approach taken toward the study of dry pressed bodies was to mix 2 or 3 different particle size distributions of powders, followed by pressing and sintering, while studying the processing data and the optical properties of the samples resulting from each combination of particle size distributions. A mixture of 2 or more particle size distributions produces a higher density part than a single particle size distribution due to more efficient packing of particles.

The most promising dry pressed bodies were fabricated using a bimodal and a trimodal distribution. The bimodal consisted of 70% hyperpure powder of 7μ average diameter and 30% hyperpure powder of 4μ average diameter, and the trimodal system consisted of 50% hyperpure powder of 7μ average diameter, 25% hyperpure powder of 4μ average diameter, and 25% DC184 powder of 0.2 to 0.3μ average diameter. The binder for these bodies was polyvinyl alcohol which burns out as discussed previously.

Using a molding pressure of 8000 psi, the bimodal system of powders resulted in a pressed green density of 90 lb/ft^3, while the trimodal system containing the very fine grains pressed to a green density of 80 lb/ft^3. The shrinkages resulting from the firing of these materials at various temperatures and the resulting fired densitits are shown in Figures 4-18 and 4-19 respectively.

The high fired densities obtained by firing the trimodal formulations at relatively low temperatures was originally considered to be a processing advantage.

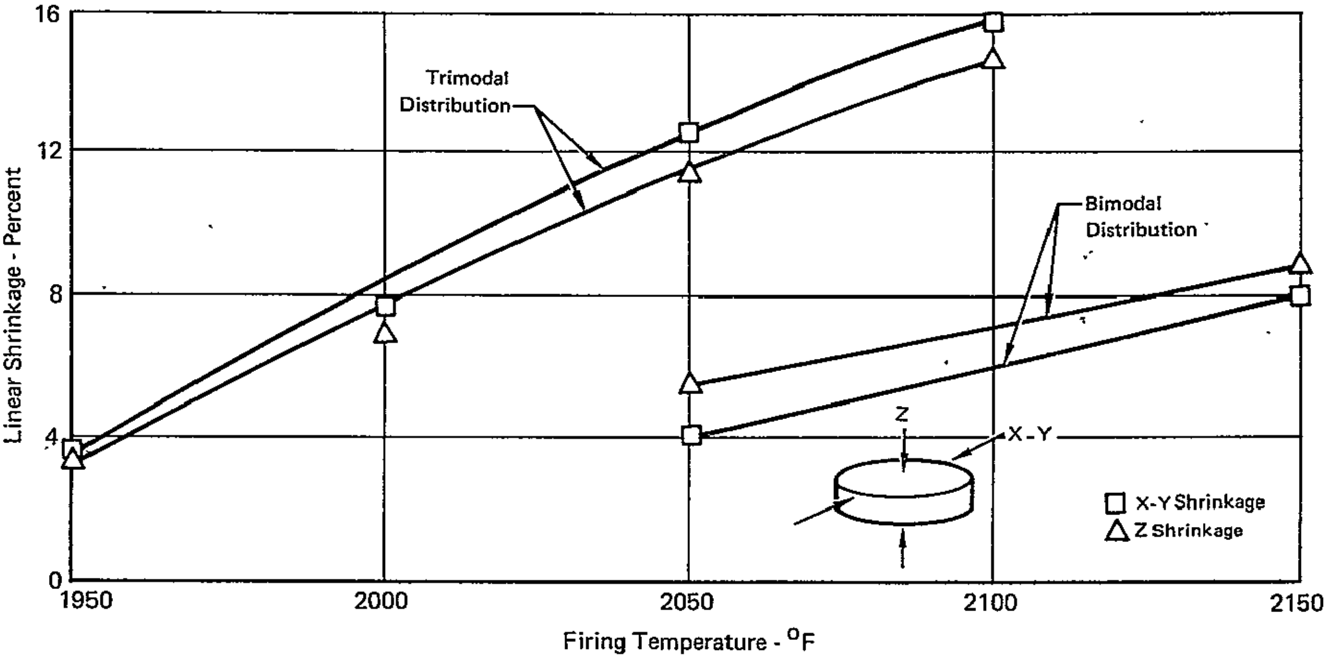

FIGURE 4-18
SHRINKAGE AS A FUNCTION OF FIRING TEMPERATURE OF DRY PRESSED BODIES

GP74 4457-15

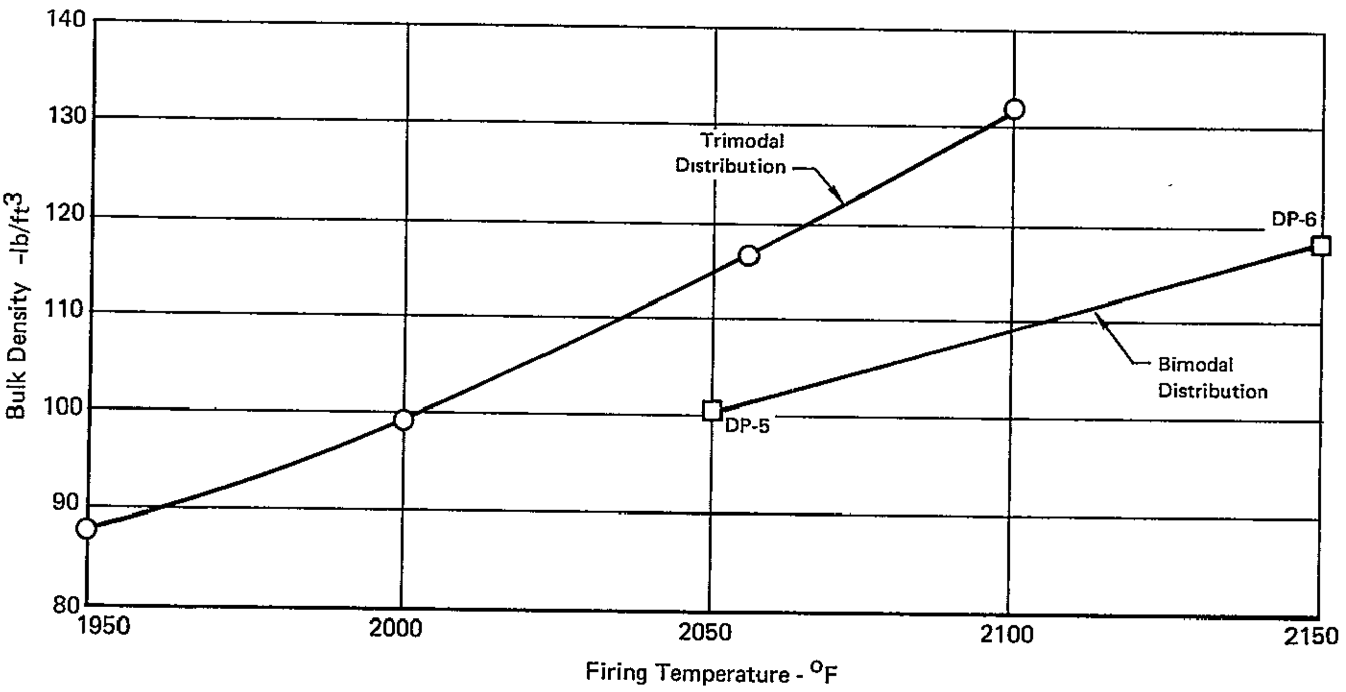

FIGURE 4-19
BULK DENSITY AS A FUNCTION OF FIRING TEMPERATURE OF DRY PRESSED BODIES

GP74-4457-16

However, as shown in Figures 4-20 and 4-21, the highest reflectance values result from lower density material in the case of both the bimodal and trimodal distributions. Therefore, the bimodal system was the most promising one of the two from a reflectance standpoint. As shown in Figure 4-21, desirable densities can be achieved by firing this material at 2050°F or lower. The lower shrinkage of the materials without the very fines is an advantage from the standpoint of processing and scale-up to full size heat shields. The optical properties of the bimodal and trimodal distributions appear to be very similar when both are fired at their optimum temperature for maximum reflectance. The reflectance as a function of wavelength for the most highly reflective sample of each formulation is shown in Figures 4-22 and 4-23.

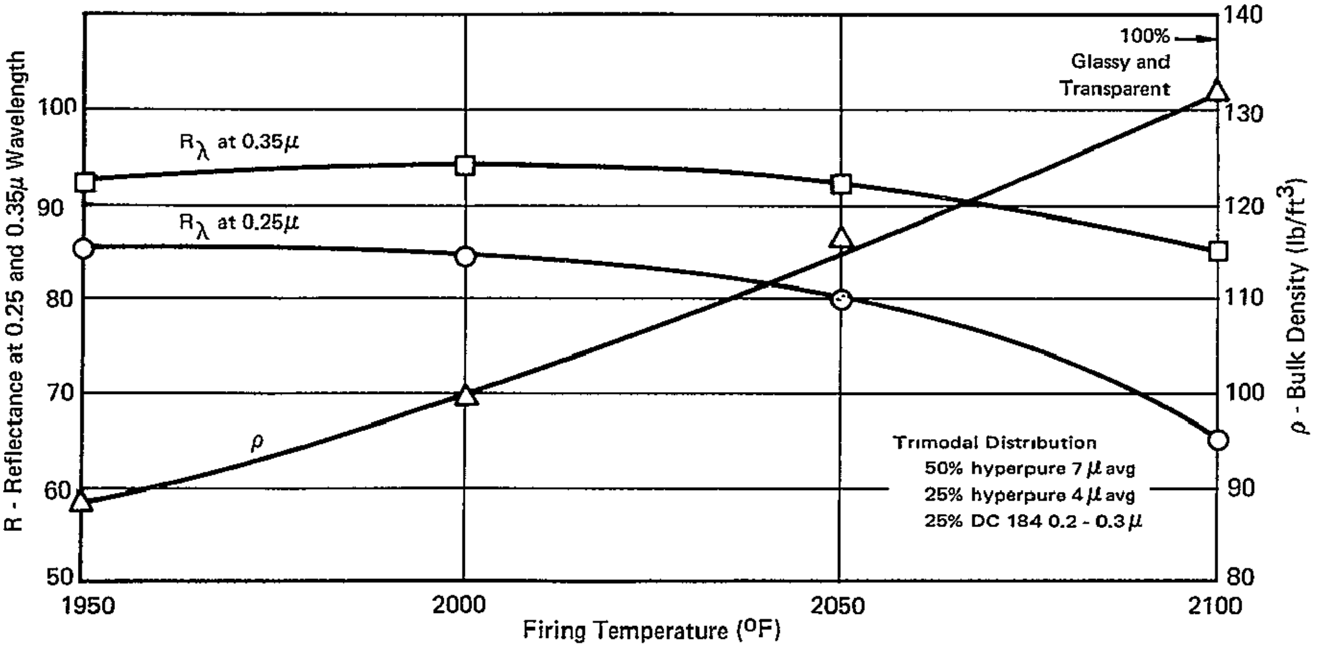

FIGURE 4-20
REFLECTANCE AND BULK DENSITY OF A TRIMODAL DISTRIBUTION OF DRY PRESSED MATERIAL AS A FUNCTION OF FIRING TEMPERATURE

GP74-4457-17

Dry pressing is considered to be a viable approach to fabricating a high purity silica reflective heat shield. It has been calculated that to fabricate a full size, 36-inch diameter heat shield, a molding force of 4,000 tons would be required. This

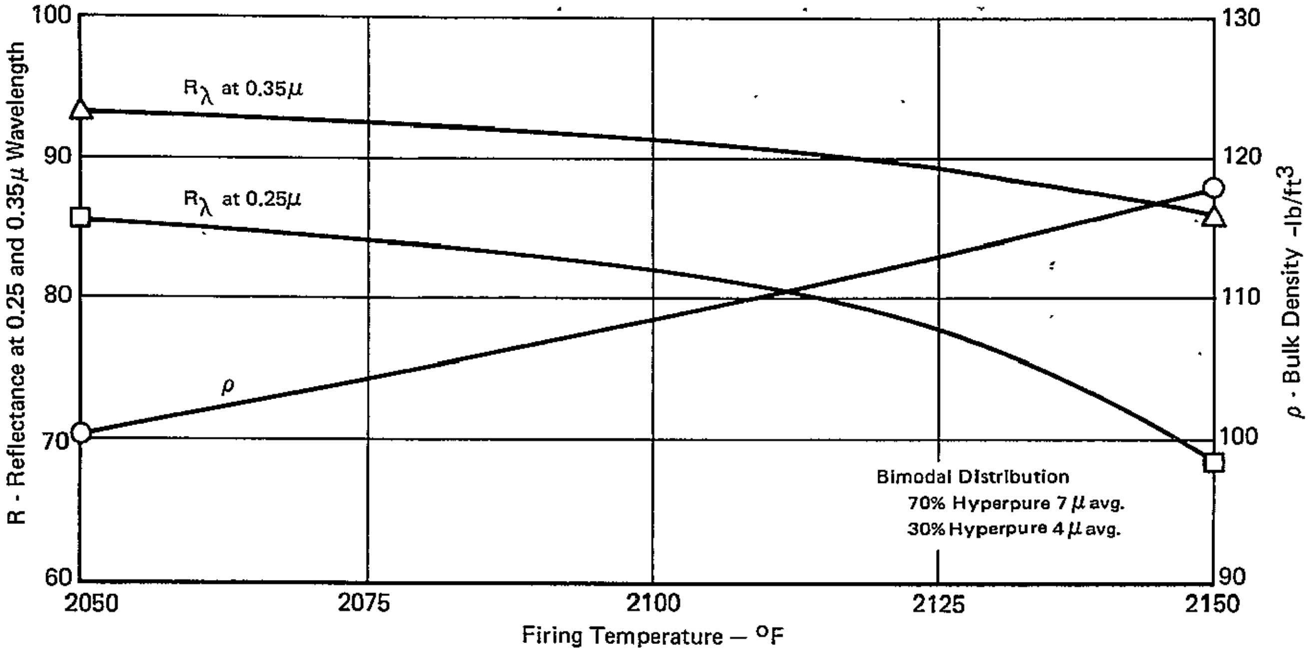

FIGURE 4-21
REFLECTANCE AND BULK DENSITY OF A BIMODAL DISTRIBUTION OF HYPERPURE DRY PRESSED MATERIAL AS A FUNCTION OF FIRING TEMPERATURE

GP74-4457-18

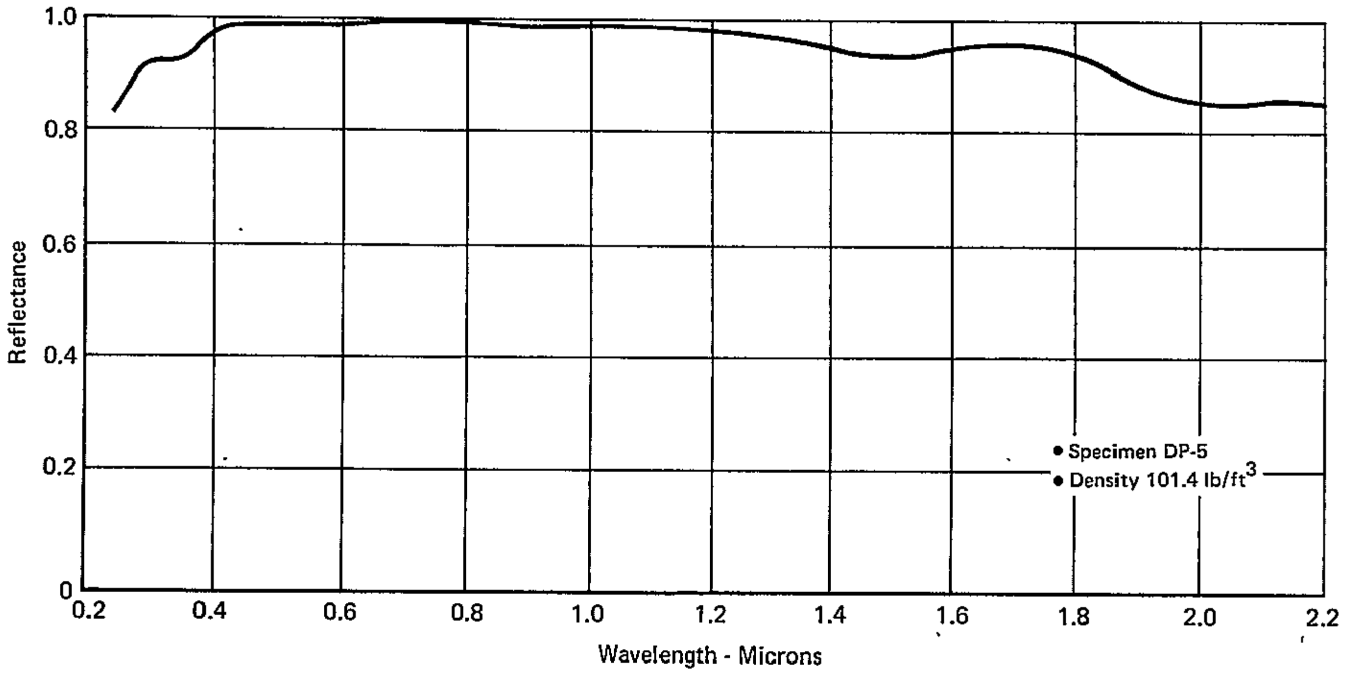

FIGURE 4-22
REFLECTANCE OF BIMODAL DISTRIBUTION OF DRY PRESSED HYPERPURE MATERIAL SINTERED AT 2050°F

GP74-4457-19

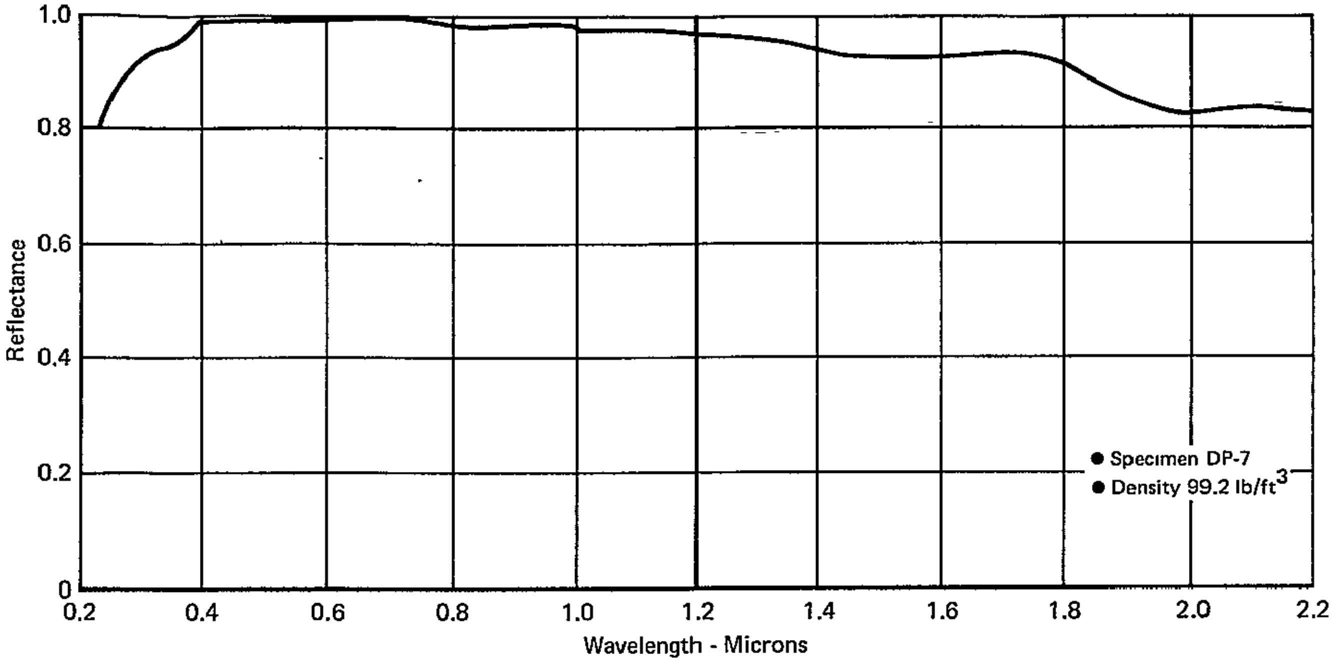

FIGURE 4-23
REFLECTANCE OF TRIMODAL DISTRIBUTION OF DRY PRESSED HYPERPURE MATERIAL SINTERED AT 2000°F

GP74-4457-20

is based on a molding pressure of 8,000 psi. Presses of this size and much larger are available.

The scope of the work on dry pressing was limited in order to concentrate on slip casting, which is now considered to be the most promising approach to silica heat shield fabrication.

4.6 SLIP CASTING

Of the various fabrication methods evaluated in this program, slip casting is the most practical and produces the most highly reflective silica heat shield. The slip casting effort performed in this program was in two major areas:

- Casting development of hyperpure silica, and,
- Slip casting of miniature heat shields.

Both of these areas are described in this section.

4.6.1 CASTING DEVELOPMENT OF HYPERPURE SILICA

The purest fused silica casting slips, commercially available, are too impure (3000 to 4000 parts per million metallic impurities) for use in making a reflective heat shield. Therefore, a method was developed for preparing hyperpure fused silica slip from optical quality, high purity fused silica. The high purity, raw material, Dynasil rod, contains approximately 10 ppm total metallic impurities. Using clean room facilities and special equipment as previously described, an impurity content of under 25 ppm can be maintained in the finished heat shield. A discussion of the relative purity of the developed hyperpure slip and commercial slip material is presented in Section 5.3.1.

The raw material used for the preparation of hyperpure silica slip was the same material, Dynasil, which was discussed in Section 4.5, as the raw material for the preparation of hyperpure powder for dry pressing. The material was received in the form of rods four inches long or longer which were cut into short lengths of one inch or less. Each individual piece of silica was then cleaned and visually examined visually. The silica was then reduced to a coarse grit by crushing.

The coarse hyperpure silica grit was next combined with high purity water (discussed in Section 3.2). The silica and water were then processed into hyperpure casting slip by ball milling.

The hyperpure slip was characterized as to solids content, viscosity, pH, and particle size distribution. All of these properties are interrelated, with the viscosity, pH and particle size distribution for slip of a given solids content being dependent on the milling time. We have determined that a casting slip of roughly 80% solids was optimum. The desired pH of typical casting slip was from 3.5 to 4.0, the pH decreasing with increasing milling time. The viscosity of slip suitable for casting was roughly 110 centipoises, as measured with a model LVT Brookfield Viscometer, and the slip was typically thixotropic.

The most important characteristic of the casting slip was the particle size distribution of the solids. The particle size distribution was measured by an ASTM method which is based on Stoke's Law and was described more fully in Section 4.5. The particle size distribution of a typical hyperpure casting slip is shown in Figure 4-24. For comparison, the particle size distribution of a commercial silica casting slip which was purchased from Glasrock Products, Inc. is shown in Figure 4-25.

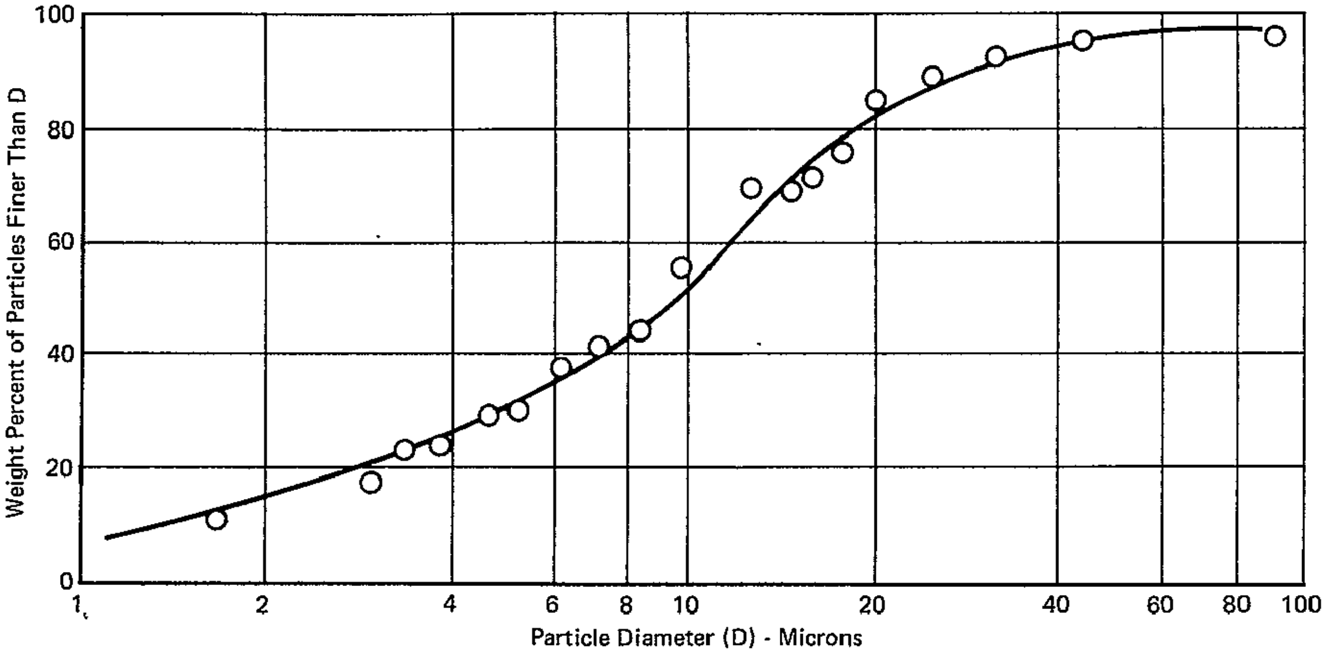

FIGURE 4-24
PARTICLE SIZE DISTRIBUTION OF A TYPICAL
HYPERPURE SILICA SLIP

GP74 4457-21

Slip cast specimens were cast in plaster of paris molds according to standard ceramic processing methods. It has been determined that vibration of the mold during testing has the desirable effect of increasing the green density of the cast parts. The vibration employed was 60 cps with an amplitude of 0.010 inch. This resulted in an increase in the green density of roughly 3.0% over parts cast without vibration.

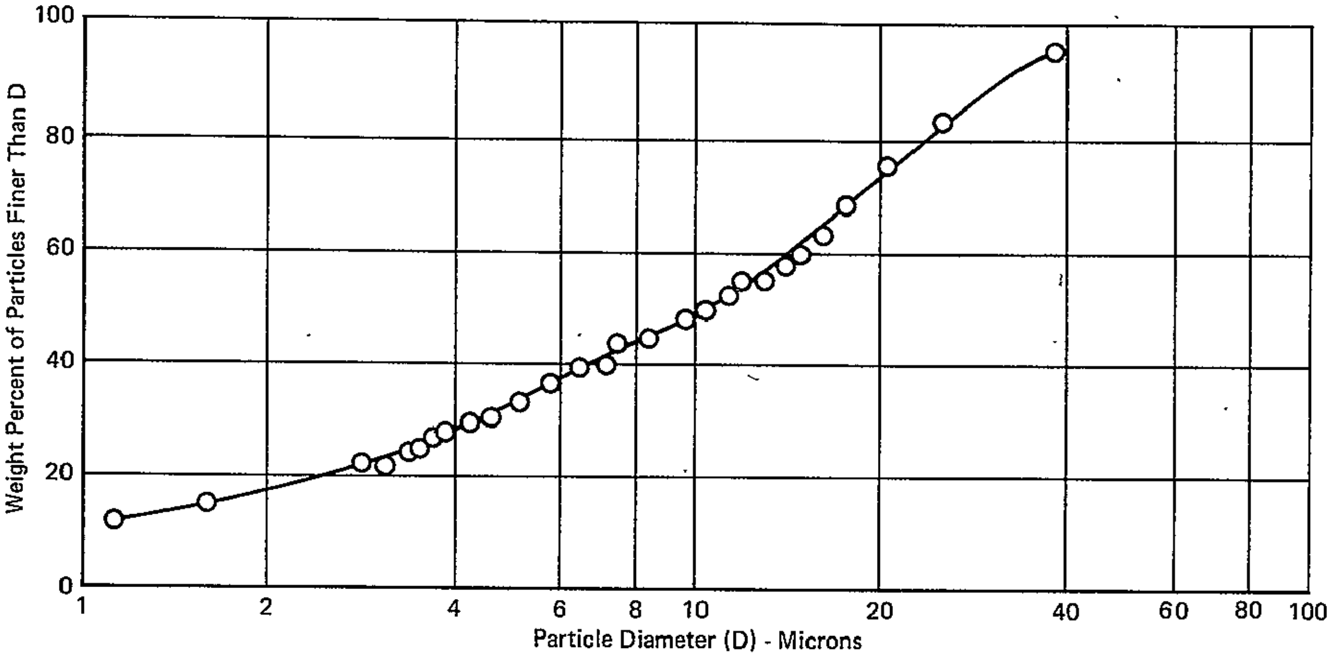

FIGURE 4-25
PARTICLE SIZE DISTRIBUTION OF "GLASROCK" SLIP

GP74-4457-22

Soon after casting, the hyperpure parts were removed from the mold. The as-cast specimens were dried very slowly to prevent cracks due to drying shrinkage, by humidity drying in a closed container. This was followed by air drying and then oven drying.

The completely dried hyperpure slip cast specimens were fired by inserting them directly into a furnace, preheated to the desired firing temperature. The furnace temperature was monitored during firing with two separate thermocouples. One was the standard furnace thermocouple which was connected to the furnace controller. A second thermocouple, which was connected to a calibrated potentiometer, was placed near the sample at the time the sample was installed in the furnace. The soak time at temperature used for firing all of the hyperpure slip cast samples prepared for this program was five hours.

A complete discussion of the physical, optical and mechanical properties of hyperpure slip cast fused silica is presented in Section 5.0. Therefore, any discussion of these properties or their variation with firing temperature or other processing variables is not presented here. For completeness, however, a table is shown in Figure 4-26 which includes processing data for each of the hyperpure slip cast fused silica samples prepared.

4.6.2 SLIP CASTING OF MINIATURE HEAT SHIELDS

In order to obtain casting experience on a shape which is representative of a reflective heat shield, it was decided to make a series of small heat shields. Commercially obtained high purity silica slip was used to fabricate the samples. These samples were approximately 6 inches in diameter x 1 inch thick having a radius of curvature of 7 inches. Commercial slip was used for this effort because of the high raw material cost and the time required to prepare hyperpure silica slip.

The casting mold was fabricated from plaster of paris using a polished wood master mold. The plaster mold, which was in four separate parts, is shown disassembled and assembled for casting in Figure 4-27. The mold had a four-inch deep riser so that excess slip could be held in position assuring a complete casting as the slip volume shrinks during casting.

A total of five miniature heat shield shapes were fabricated. The first shield was cracked in the mold because it was mistakenly allowed to dry overnight in the mold. The shield cracked longitudinally because it was not permitted to shrink by the male displacement portion of the mold.

The second miniature heat shield was removed from the mold soon after casting. It was dried overnight at room temperature, followed by drying in an air-circulating oven. The shield was then quench fired at 2100°F. After firing it was observed to have severe shrinkage cracks.

The third heat shield was cast and dried in a manner similar to shield 2. After the drying cycle was completed, this shield was observed to have severe shrinkage cracks. The cracking problem was, therefore, concluded to be associated with drying shrinkage.

SPECIMEN NUMBER	APPROXIMATE SIZE (IN)	GREEN DENSITY (LB/FT^3)	FIRING TEMP. (°F)	FIRING SHRINKAGE		FIRED DENSITY (LB/FT^3)	COMMENTS
				X-Y DIR. (%)	Z DIR. (%)		
SC-1	2.5x2.5x.4	98	2100	0.8	0.3	72.5	SC-1, 2, 3, & 4 used for study of reflectance vs. firing temperature (bulk density) including VUV measurements.
SC-2	2.5x2.5x.4	99	2200	1.8	1.2	104.5	
SC-3	2.5x2.5x.4	98	2300	5.0	3.5	113.2	
SC-4	2.5x2.5x.4	98	2250	2.9	3.8	107.5	
SC-5	2.5x2.5x.4	90	2200	2.4	1.8	96.5	Low green densities in SC-5, 7, 8 due to variations in solids content of slip; 70, 73, 80% respectively.
SC-7	2.5x2.5x.4	96	2200	1.5	1.6	100.6	
SC-8	2.5x2.5x.4	97	2300	4.1	3.3	109.9	
SC-9	5.5x5.5x3.5	100	-	-	-	-	SC-9 was damaged in green state; pieces were fired at various temperatures and eventually machined into strength bars; offal was used for x-ray diffraction studies. Higher green density (over SC-1→8) due to improved slip processing techniques.
SC-9-1			2250	3.2	2.9	110.4	
SC-9-2			2200	2.0	1.8	106.3	
SC-9-3			2300	4.0	3.7	115.6	
SC-9-4			2350	5.8	3.6	123.3	
SC-9-6			2400	6.4	9.1	130.6	
SC-9-7			2100	-	-	101.8	
SC-10	2.2x2.2x.3	100	2300	4.9	3.2	114.4	Variation in casting rate on SC-10 & 11 did not improve green density
SC-11	2.2x2.2x.3	100	2300	5.2	3.8	116.2	
SC-12	2.2x2.2x.3	103	2300	4.5	5.0	118.5	Improved green density due to vibration casting.
SC-13	7 x 7 x .35	-	2200	-	-	109.1	Green density and shrinkage not obtained for SC-13→17 due to problems in handling thin plate configuration in green state.
SC-14	7 x 7 x .35	-	2200	-	-	107.8	SC-13→17 used to obtain deliverable samples. 6"x6" from SC-13; 14 plasma arc samples from SC-14; 2 Pcs., 2.8x1.5 & 5.0x32, from SC-16.
SC-15	7 x 7 x .35	-	2350	-	-		
SC-16	7 x 7 x .35	-	2350	-	-	123.4	
SC-17	7 x 7 x .35	-	2350	-	-		A 6"x6" billet not obtained from 2350°F fired material due to warping encountered during firing.

FIGURE 4-26

PROCESSING DATA FOR HYPERPURE SLIP CAST MATERIALS

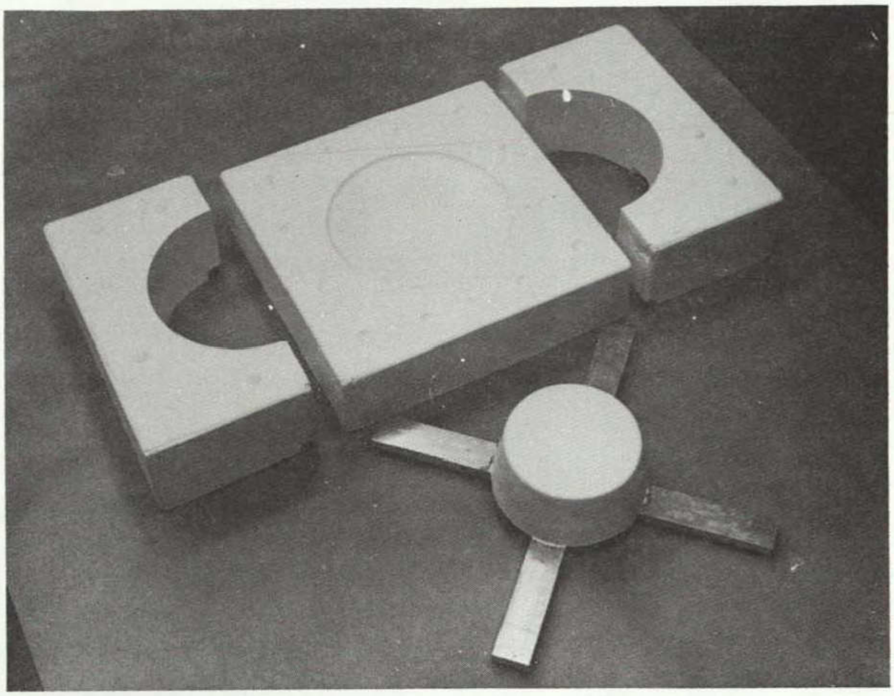

Disassembled

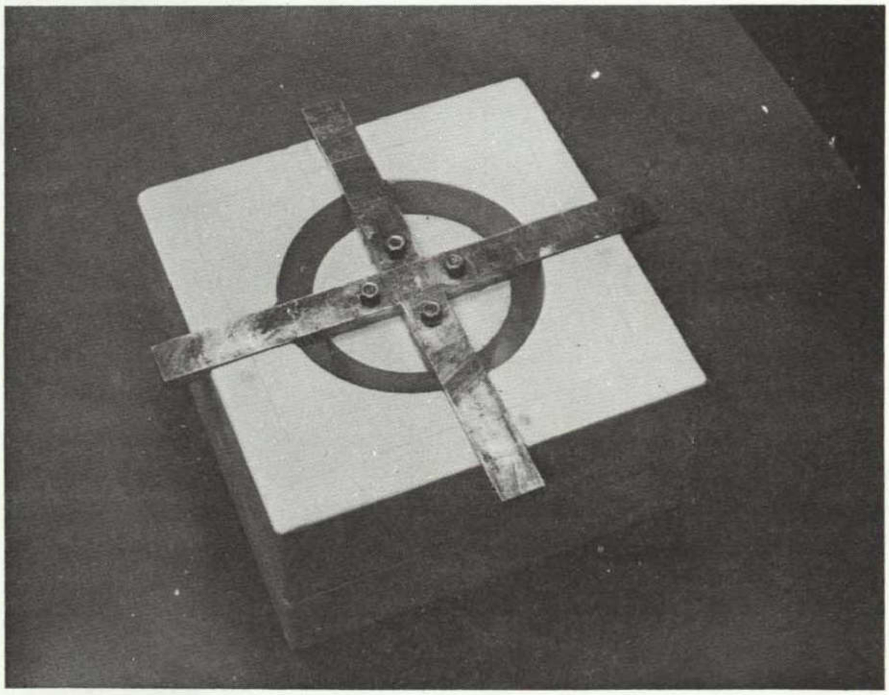

Assembled for Casting

FIGURE 4-27
PLASTER OF PARIS MOLD USED TO CAST MINIATURE
HEAT SHIELDS

GP74-4457-23

REPRODUCIBILITY OF THE
ORIGINAL PAGE IS POOR

Therefore, when heat shield sample 4 was cast, steps were taken (as described below) to insure uniform drying, which resulted in no shrinkage cracks. The shield was removed from the mold within 30 minutes of casting and placed in a plastic container with a sealed lid for a period of three days. The drying chamber lid was then unsealed, but the sample was maintained in the loosely covered container for a period of seven days, during which time it dried very slowly and uniformly. The sample was then removed from the container and allowed to dry at room temperature for one day. This was followed by an air-circulating oven dry for 4 hours at 120°F, 200°F and 350°F, respectively. The weight loss of the sample was monitored throughout the drying cycle. On a larger sample, measurements could be taken during the drying cycle to determine the point at which no further drying shrinkage takes place. This would aid in determining the optimum drying cycle.

The above drying cycle resulted in no drying shrinkage cracks of heat shield 4, as confirmed by radiographic inspection. The radiography did, however, reveal several small gas voids. These voids were in the range of 0.010" to 0.040" in diameter and all were determined to be near the interior curved surface of the shield. The voids were removed by carefully sanding this surface with coarse silicon carbide abrasive paper. The excess riser was removed with a diamond blade band saw. All of the surfaces were then cleaned and the sharp edges were removed with fine silicon carbide paper.

Shield 4 was quench fired at 2100°F. After firing, the sample was observed to have cracks which were visible on the interior curved surface. It is an accepted fact that it is virtually impossible to thermal shock slip cast fused silica in a furnace firing. The cracks resulting from firing this shield were, therefore, concluded to be shrinkage cracks resulting from non-uniform heating of the sample during the quench firing.

Accordingly, a fifth 6-inch diameter heat shield was cast, dried, and prepared for firing in a manner similar to that described above for shield 4. Radiographic inspection revealed the shield to be crack free before firing. The shield was fired by installing it in a cold furnace and heating slowly to 2100°F. Upon completion of firing, the shield had no visible cracks.

This subscale heat shield sample has been delivered to NASA-Ames as one of the deliverable samples for this contract. A photograph of a typical heat shield sample as it is removed from the mold, as well as photographs of heat shield sample 5, are shown in Figure 4-28.

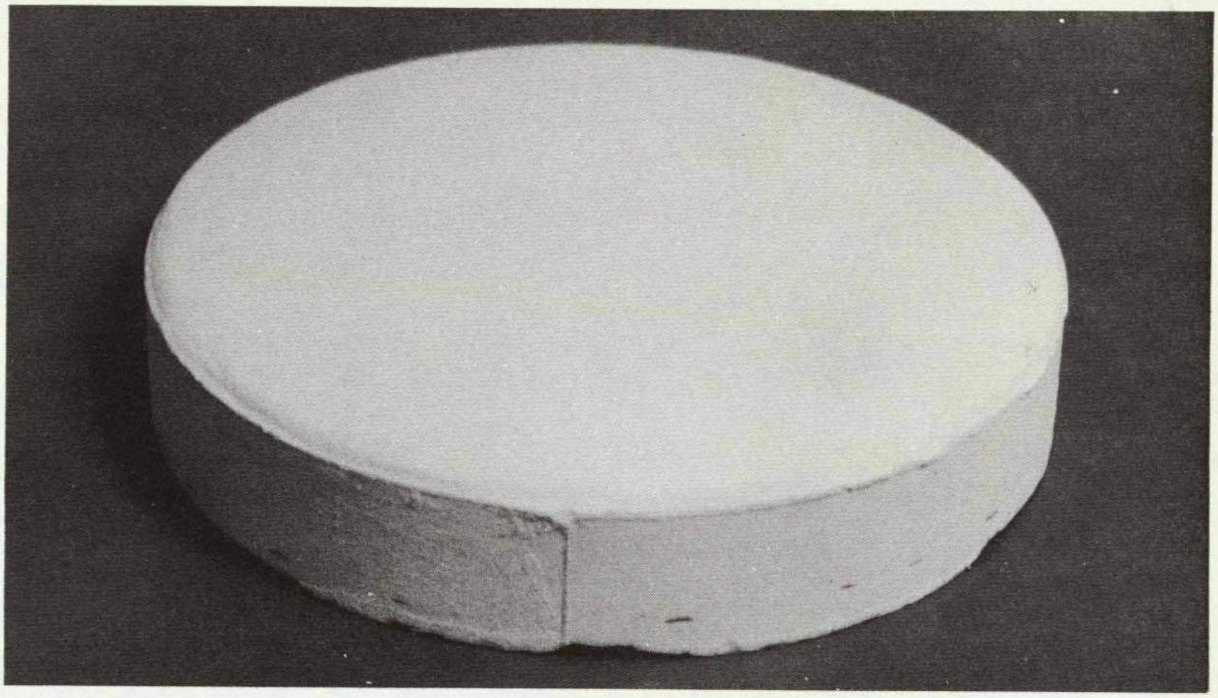

Typical Heat Shield as Removed from Mold

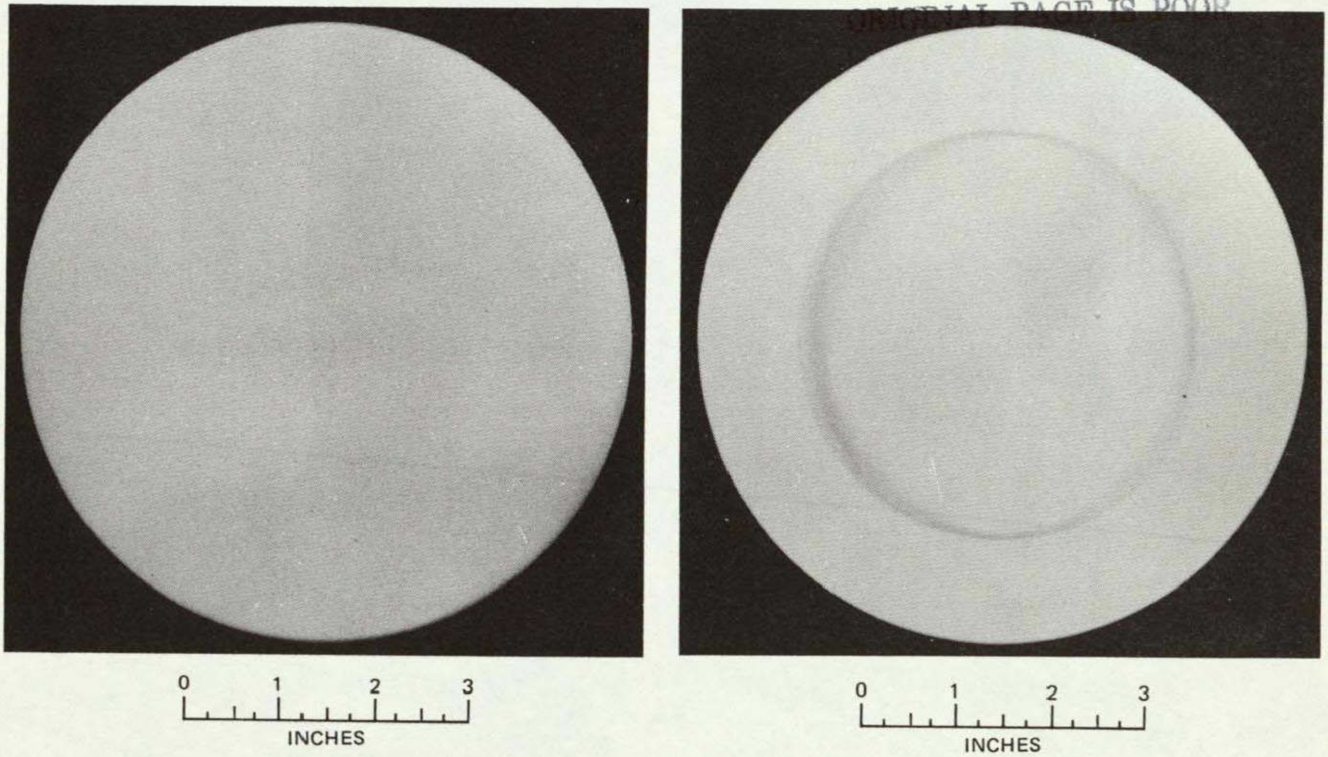

Heat Shield Number 5 After Firing

FIGURE 4-28
MINIATURE SLIP CAST FUSED SILICA HEAT SHIELD

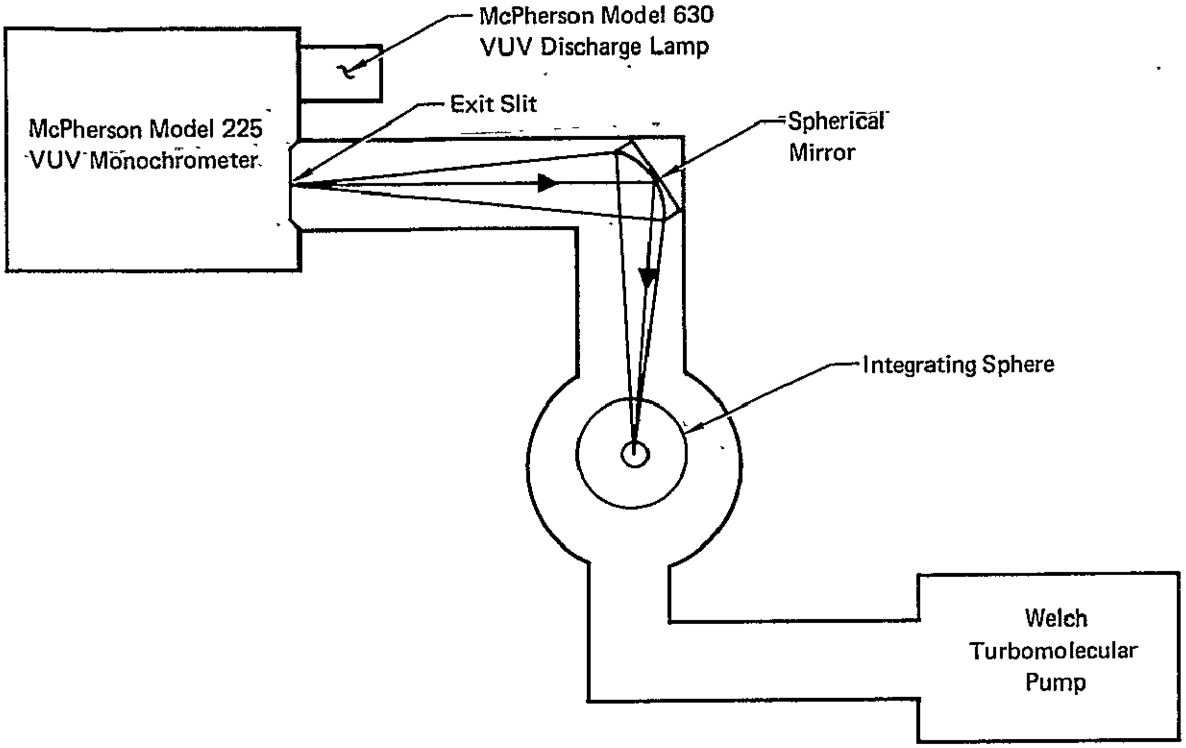

FIGURE 5-1
VUV REFLECTOMETER (TOP VIEW)

GP74-4457-25

absorption by atmospheric oxygen below 0.18 microns. The entrance and exit slits were set at 2mm wide x 10mm high for all measurements herein, providing a bandpass of 0.0066 microns.

A specially designed vacuum attachment to the monochrometer exit slit assembly housed the VUV reflectometer (see Figure 5-2). A spherical mirror imaged the exit slit onto the sample which was located at the center of the integrating sphere. The 500 l/sec Welch Turbomolecular Pump reduced the pressure in the reflectometer to 10^{-6} torr. A glass plate covered the top of the reflectometer vacuum system and provided an unobstructed view of the integrating sphere/sample holder assembly. The sample was positioned at the center of a 4-inch diameter integrating sphere. The sphere wall was coated first with a 1mm thick layer of Kodak Barium Sulphate White Reflectance Paint and then with a thin layer of sodium salicylate. The VUV flux within the sphere causes the salicylate coating to fluoresce at wavelengths

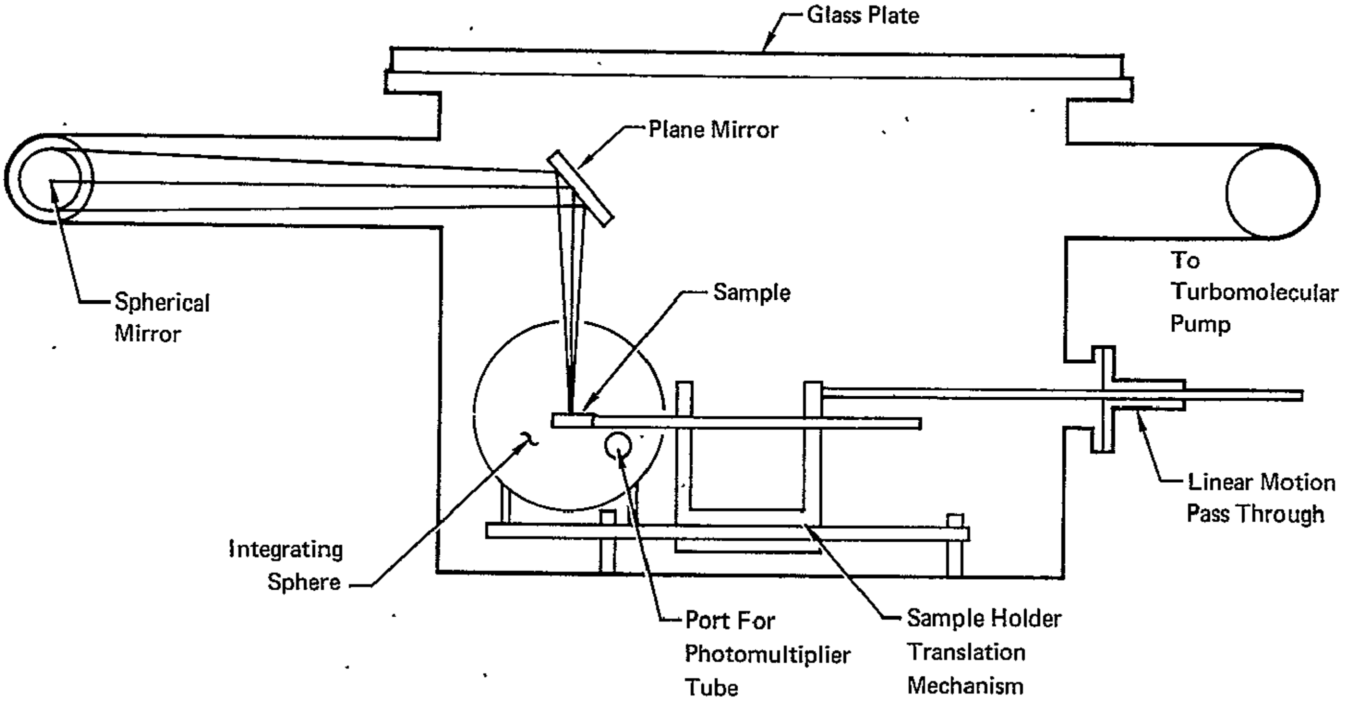

FIGURE 5-2
VUV REFLECTOMETER (SIDE VIEW)

GP74-4457-26

from 0.38 to 0.48 microns. The thin salicylate coating transmits the fluorescent flux sufficiently such that the sphere wall appears white and highly reflecting to the fluorescent light, which was detected by an EMI 9601 photomultiplier tube (PMT) mounted on the sphere wall.

During the initial phase of evaluation, the VUV reflectometer was found to contain a source of contamination which caused severe degradation of the slip cast silica reflectance at wavelengths less than 0.3 microns. The source of contamination was determined to be a combination of remanent silicone pump oil on the walls of the VUV vacuum chamber, a leaking seal in the Turbomolecular Pump and mechanical pump oil contamination from the exit slit assembly of the grating monochrometer. When repeated chemical cleaning and bakeout cycles failed to clean the VUV vacuum chamber, an Ultek ion-pumped chamber was substituted for the original chamber. Using sorption rough pumping, the Ultek chamber was found to be free of contamination. A calcium fluoride window was installed in the elbow connection between the grating monochrometer and the Ultek vacuum chamber to eliminate any contamination from the exit slit assembly. The VUV reflectance is computed from Equation (1):

$$R = \frac{V_s - V_B}{V_o - V_B} \qquad (1)$$

where V_s = PMT output with VUV flux incident on the sample located at the center of the sphere

V_o = PMT output with VUV flux incident on the sphere wall (sample removed from Sphere)

V_B = PMT output with the source blocked (background measurement).

It should be noted that the VUV sphere is an absolute reflectometer, i.e., the measured reflectance of the sample is given directly by the voltage ratio, Equation (1), without reference to the reflectance of a standard material. In contrast, the sample reflectance as determined by the DK-2A reflectometer is measured relative to Kodak Barium Sulfate White Reflectance Standard. Published values (Reference 4) of the absolute reflectance of the Kodak material were used to obtain absolute values of sample reflectance.

5.1.2 EFFECT OF FIRING TEMPERATURE ON MORPHOLOGY/REFLECTANCE

A series of hyperpure silica slip cast samples, prepared from the same batch of raw material and fired at different temperatures, were evaluated with the VUV Reflectometer (Figure 5-3). It is apparent that firing temperature is an important parameter. The optimum firing temperature for maximum UV reflectance appears to be about 2200°F. Each of these samples was refired to 2000°F after completion of the wet machining process in order to remove water and hydroxyl ions (see Figure 5-4).

Figures 5-5 thru 5-8 show the reflectance curves for the four samples of Figure 5-3 from 0.23 to 2.3 microns. There is little difference in the reflectances of these four samples at wavelengths greater than 0.3 microns. The effects of process

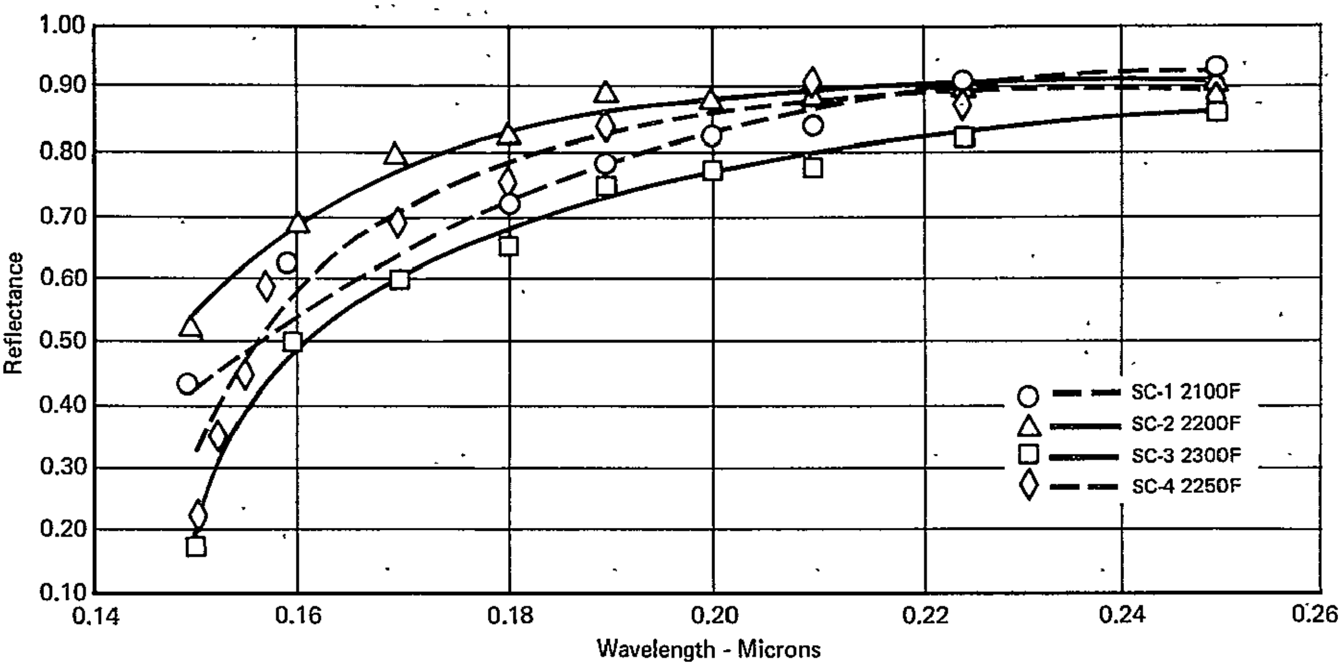

FIGURE 5-3
VUV REFLECTANCE OF HYPERPURE SLIP CAST MATERIALS

GP74-4457-28

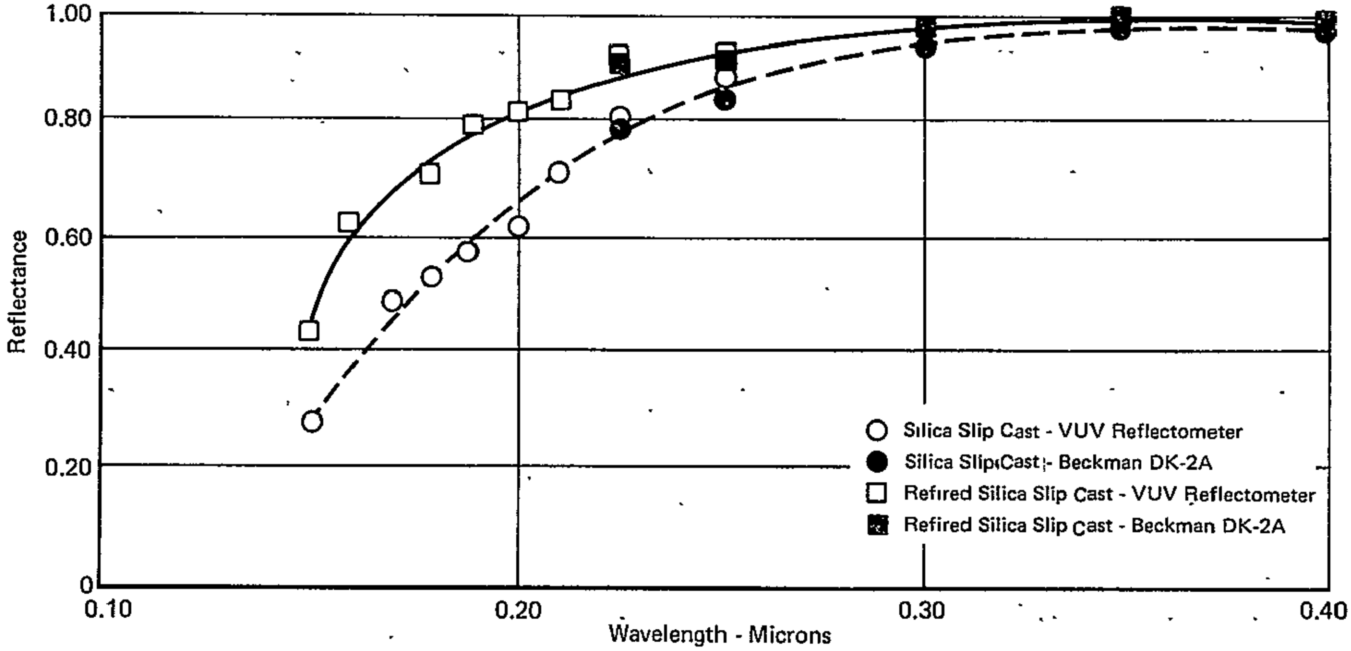

FIGURE 5-4
DK-2A AND VUV REFLECTOMETER
DATA FOR HYPERPURE SILICA SLIP CAST MATERIAL

GP74-4457-27

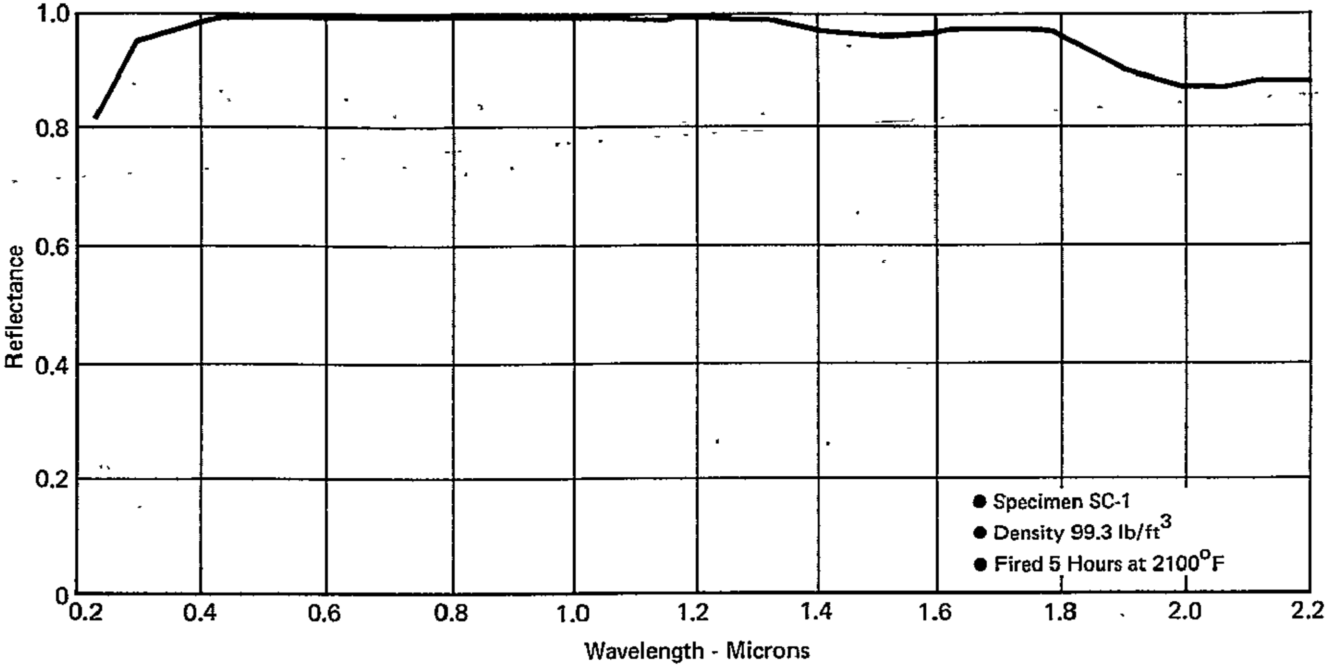

FIGURE 5-5
REFLECTANCE FOR HYPERPURE SLIP CAST SILICA

GP74 4457-29

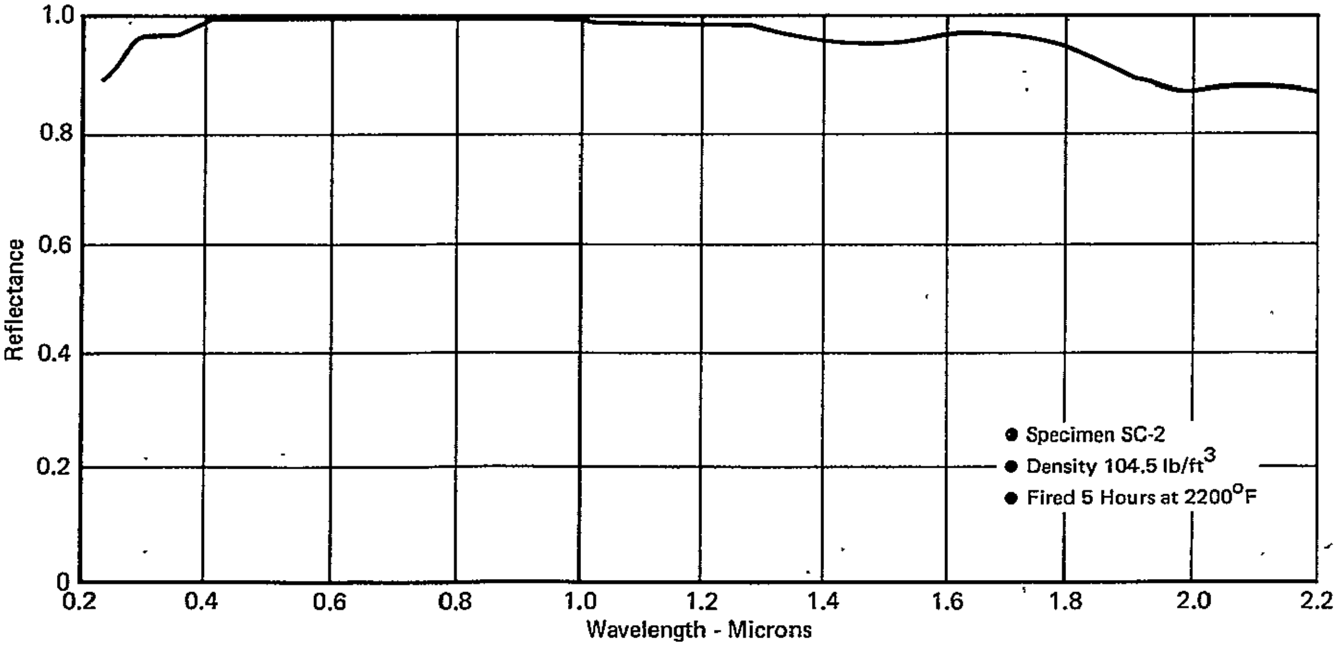

FIGURE 5-6
REFLECTANCE FOR HYPERPURE SLIP CAST SILICA

GP74-4457-30

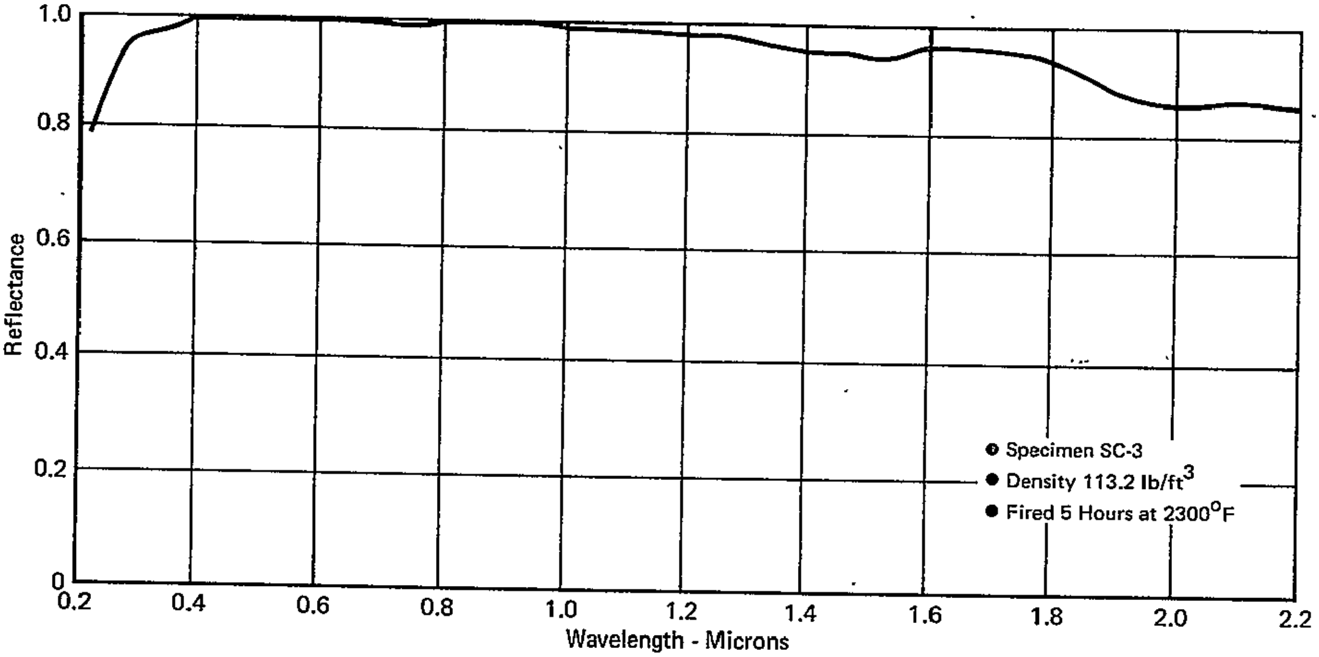

FIGURE 5-7
REFLECTANCE FOR HYPERPURE SLIP CAST SILICA

GP74-4457-31

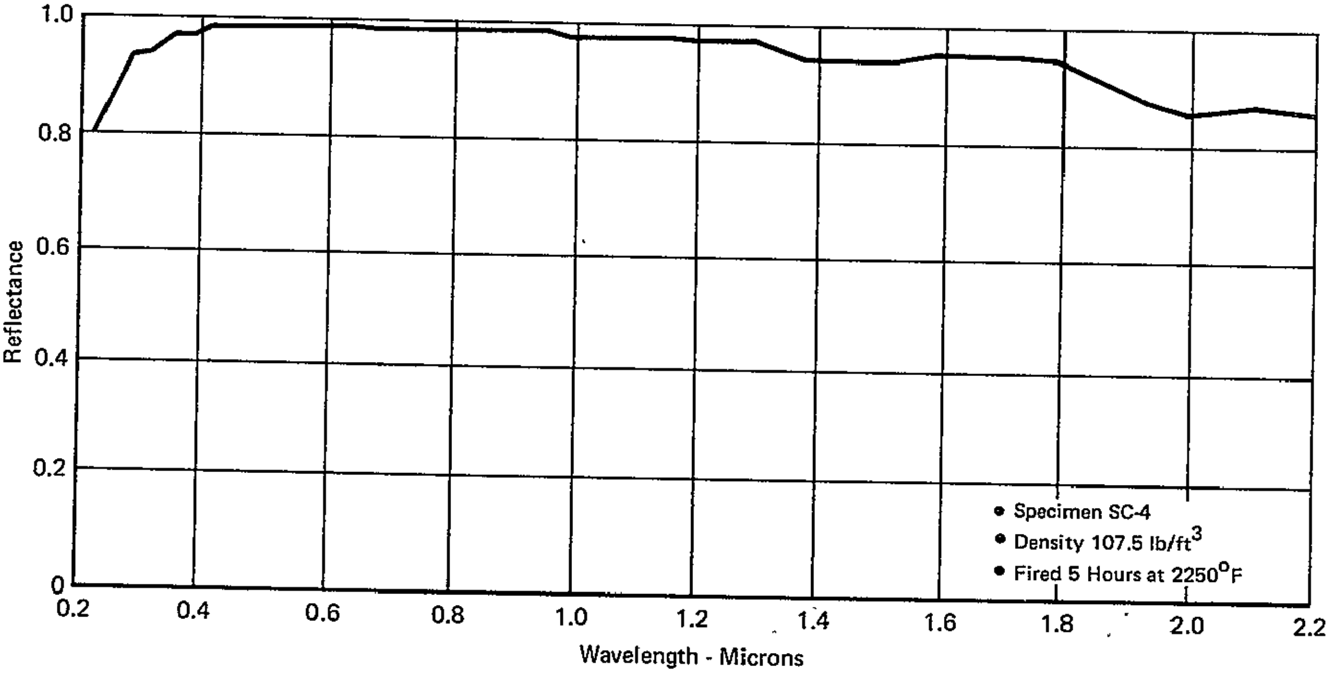

FIGURE 5-8
REFLECTANCE FOR HYPERPURE SLIP CAST SILICA

GP74-4457-32

temperature appear mainly at wavelengths less than 0.3 microns.

In addition to optimizing the silica slip cast material for highest possible reflectance, it is desirable that the fired density be as close as possible to the theoretical density (137 lb/ft^3) since the reflective heat shield must also function as a high efficiency ablator, and should be as strong as possible. The four samples previously discussed in Figures 5-4 thru 5-8 showed different fired densities as a result of the different firing temperatures. Figure 5-9 shows the relation between fired density and reflectance at two wavelengths, 0.25 and 0.35 microns. Sample SC-2 (104.5 lb/ft^3 fired density), which was fired at 2200°F, has the highest reflectance of the four samples at 0.25 microns, but does not have the highest fired density. Evidently, a tradeoff can be made between UV reflectance and fired density as evidenced by Figure 5-9 and also by Figure 2-3 in Section 2.1. The exact trade which one effects is mission-dependent because the required reflective performance of the heat shield depends on the intensity and wavelength of the radiative heating.

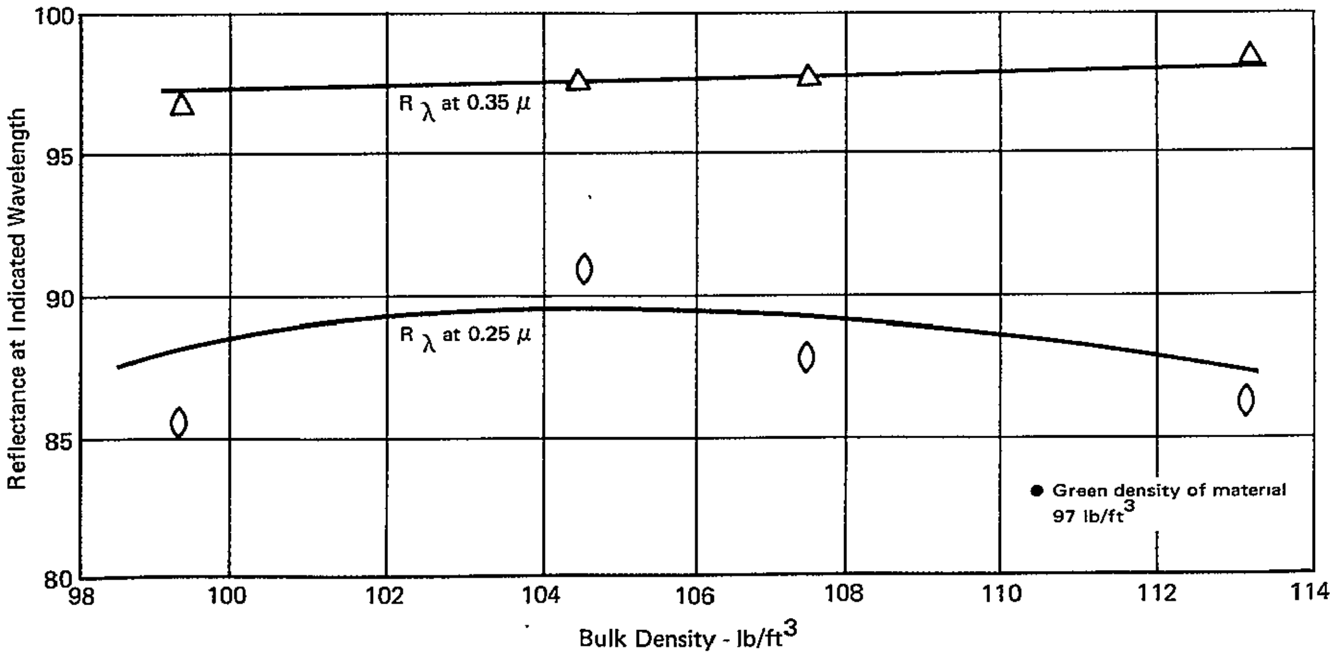

FIGURE 5-9
REFLECTANCE AS A FUNCTION OF BULK DENSITY
OF CASTINGS OF HYPERPURE SILICA SLIP

GP74-4457-33

Scanning electron photomicrographs (SEM's) of samples SC-1, SC-2, and SC-3, shown in Figure 5-10 reveal the morphological changes accompanying increases in the process temperature. The 500X photographs show a higher degree of densification as the firing temperature is increased which is in agreement with the bulk density measurements. The 10,000X magnification SEM's show a great deal more about the ultimate particles that make up the reflective materials. The SEM of the specimen fired at the lowest firing temperature (SC-1) shows very angular, sharp silica particles. As the temperature is increased, a rounding of edges can be noted along with some sintering of particles (SC-2). At the highest firing temperature, relatively large areas of sintering can be noted. These areas are clear, vitreous silica and are highly transparent over the entire 0.2 to 2.3 micron waveband. Incident light which penetrates deep into samples SC-3, is more effectively trapped within this sample than it is by the other two samples, resulting in the reduced reflectance of sample SC-3 at wavelengths less than 0.3 microns.

5.1.3 PURITY VARIABLES

The purity of the raw material from which the silica slip is made also has a pronounced effect on the reflectance of the finished product. Figure 5-11 compares the reflectances of hyperpure silica slip cast silica to Glasrock slip cast silica. Both castings were fired at 2200°F and both batches of slip were found to have similar particle size distributions. The lower reflectance of Glasrock is due largely to the difference in metallic ion impurity levels of the two materials. The hyperpure silica material has a total metallic ion impurity concentration of approximately 24 ppm while the Glasrock level is over 3000 ppm.

A more complete discussion on purity variables is found in Section 2.0.

5.1.4 SCATTERING AND ABSORPTION COEFFICIENTS

In addition to the reflectance measurements made on numerous effectively

GP74-4457-34

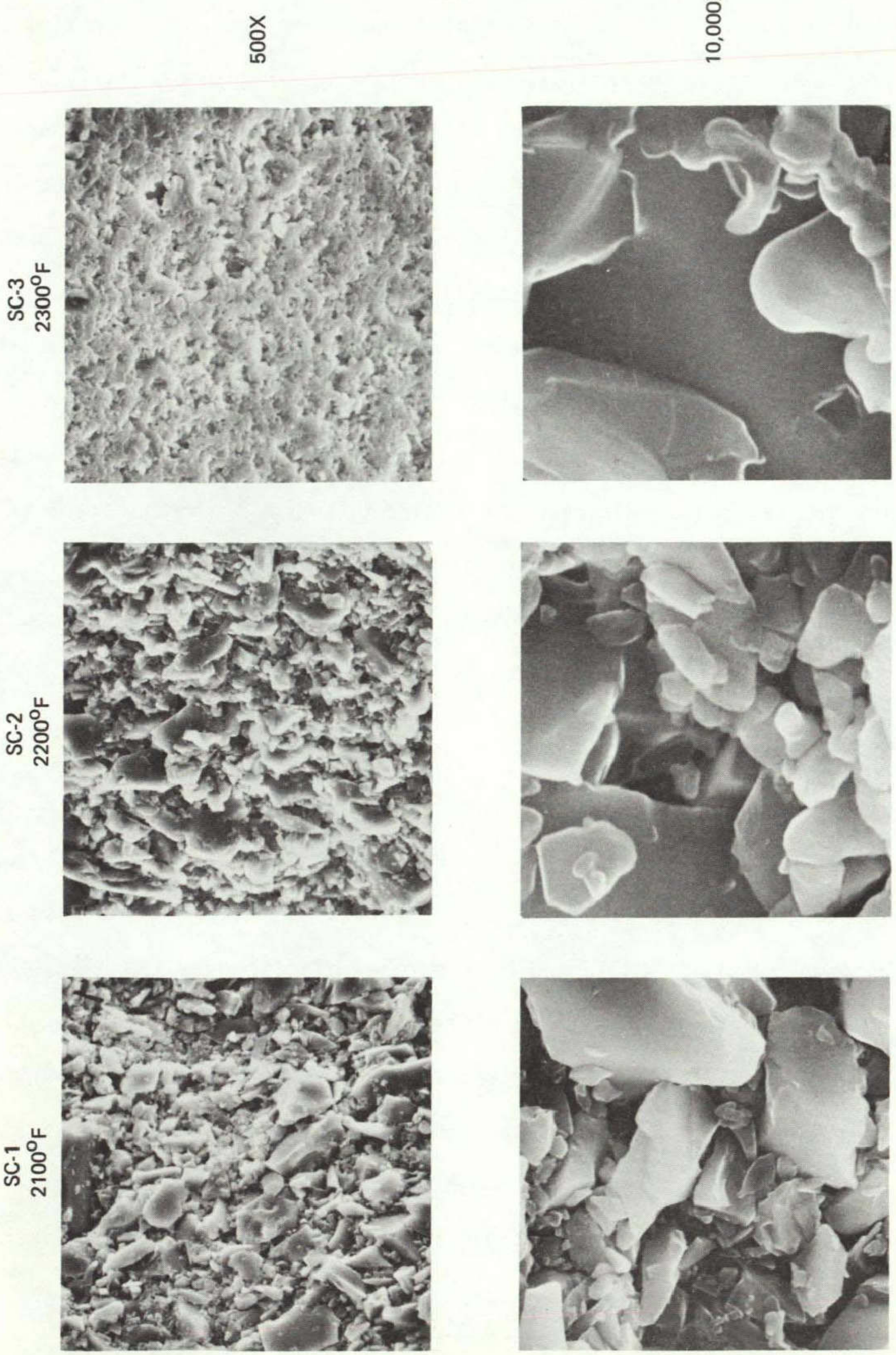

FIGURE 5-10
MICROSTRUCTURE OF HYPERPURE SLIP CAST SILICA

$$R = \left(\frac{\omega}{2}\right) \frac{3R_\infty - (1-R_\infty^{\ 2})e^{-(1+\alpha)\tau} - 1 - R_\infty\,(3-R_\infty)\,e^{-2\alpha\tau}}{(4\omega - 3)\,(1-R_\infty^{\ 2}\,e^{-2\alpha\tau})} \tag{2}$$

$$T = \left(\frac{\omega}{2}\right) \frac{3(1-R_\infty^{\ 2})e^{-\alpha\tau} - (3-R_\infty)e^{-\tau} + R_\infty\,(3R_\infty - 1)e^{-(\tau+2\alpha\tau)}}{(4\omega-3)\,(1-R_\infty^{\ 2}e^{-2\alpha\tau})} + e^{-\tau} \tag{3}$$

$\alpha = 2\ \sqrt{1-\omega}$

$$R_\infty = \frac{2}{\omega} - 1 - \frac{2}{\omega}\ \sqrt{1-\omega} \tag{4}$$

$$\tau = (\kappa+\sigma)\delta \tag{5}$$

δ = sample thickness (cm)

κ = Reichman absorption coefficient (cm^{-1})

σ = Reichman scattering coefficient (cm^{-1})

R_∞ = infinite thickness reflectance

$$\omega = \sigma/(\sigma + \kappa) \tag{6}$$

The Reichman coefficients are related to the usual K-M coefficients K and S:

$K = 2\kappa$

$S = \sigma$(for isotropic scattering)

A pair of R and T measurements on a sample yields a corresponding pair (τ,ω) from which κ and σ (given δ) can be calculated.

Equations (2) and (3) apply to the case where the light incident on the sample is confined to a narrow solid angle normal to the surface of the sample and where the reflected light is hemispherically collected (e.g., via an integrating sphere). Equation (3) also includes the contribution to T of that part of the incident flux which passes through the sample without undergoing scattering processes.

As it is impossible to solve Equations (2) and (3) explicitly for τ and ω in terms of R and T, a computer-generated plot of R vs T for nunerous values of the parameters τ and ω was obtained (Figure 5-12). Measured values of R and T for a sample at a given wavelength defines a point in the R-T plane which falls on a

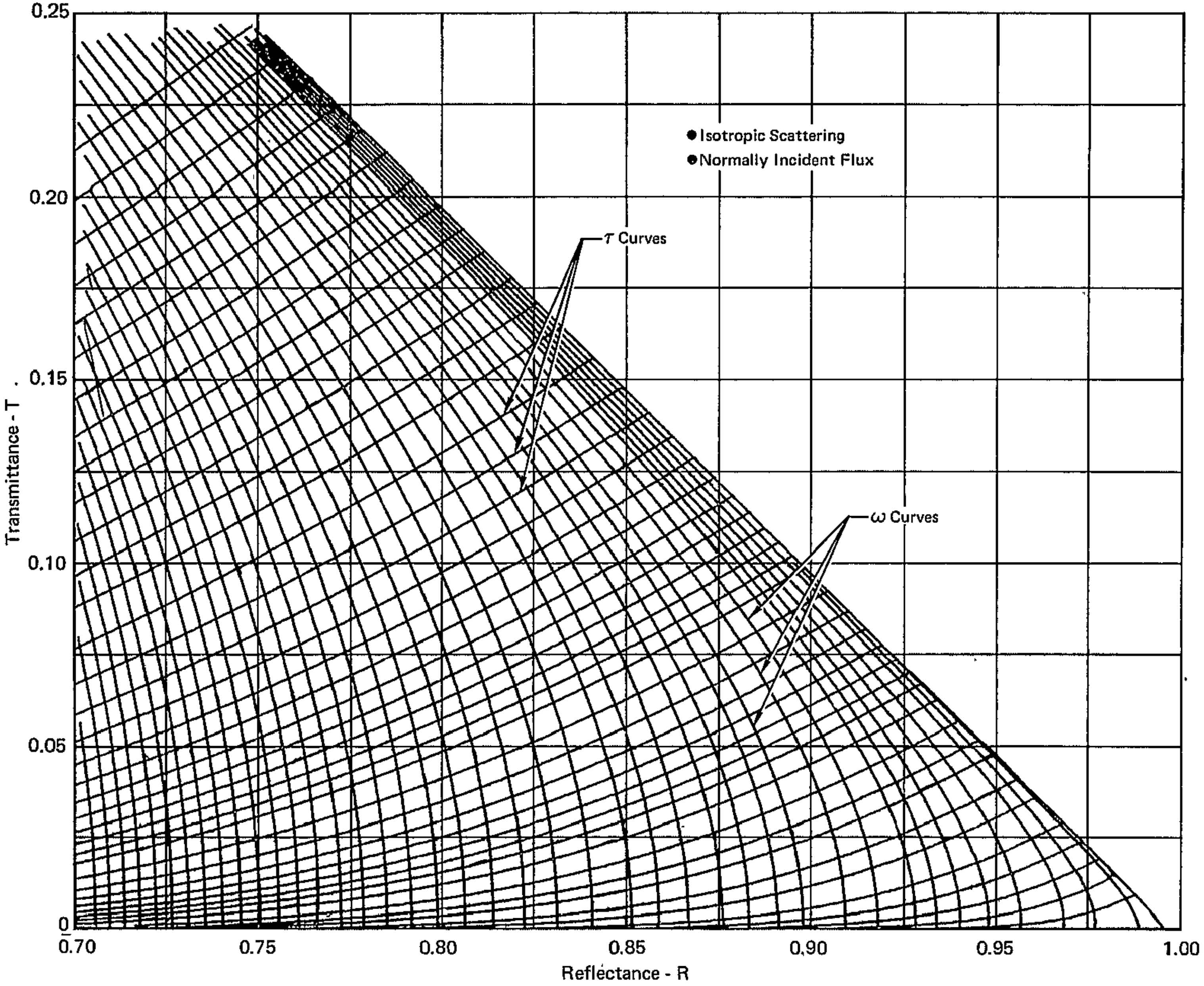

FIGURE 5-12
REICHMAN SCATTERING THEORY - τ AND ω CURVES

GP74 4457 48

single τ-curve and on a single ω-curve. The values of τ and ω thus determined are used together with the sample thickness in Equations (5) and (6) to obtain the coefficients K and S.

Reflectance and transmittance data typical of the hyperpure slip cast fused silica is shown in Figure 5-13 for several sample thicknesses. The diamond machining facility was used to produce the thin samples which were dried and refired at 2000°F. Using Figure 5-12, the absorption (K) and scattering (S) coefficients of Figure 5-14 were determined. If the samples are homogeneous, (i.e., have the same density, porosity, particle size distribution, etc.), we expect that identical K and S curves should result. While the S curves track fairly well, the K curves show greater deviations. This is not unexpected since it is extremely difficult to measure small absorption coefficients in the presence of large backscattering (high S). However, it appears that a representative average curve can be drawn through the K data of Figure 5-14. An estimate of the accuracy of these K and S coefficients can be obtained as follows. For the silica samples of Figure 5-14, $S = 650\ \text{cm}^{-1}$ and $K = 0.9\ \text{cm}^{-1}$ at $\lambda = 0.6\mu$. The slope of Equation (2) for R evaluated at $S = 650\ \text{cm}^{-1}$ for $0.1 \leq K \leq 2$ is approximately $-0.027/\text{cm}^{-1}$, while for T in Equation (3), the slope is $-0.018/\text{cm}^{-1}$. The boundary conditions of the Reichman scattering model require that, for both R and T measurements, a collimated or nearly-collimated flux be incident on the sample and that the reflected or transmitted flux be gathered by a 2π steradian (hemispherical) collator, such as the Beckman DK-2A Integrating Sphere Reflectometer. The accuracy of reflectance measurements on diffusely reflecting samples is typically $\Delta R/R = \pm 0.01$ for this type of integrating sphere (a comparison sphere) and to a large degree is due to the inaccuracy in the reflectance of the standard material (e.g., barium sulfate). The corresponding error in K due to the inaccuracy in the measurement of R is $(\pm 0.01/0.027)\ \text{cm}^{-1} = \pm 0.4\text{cm}^{-1}$. Then, the

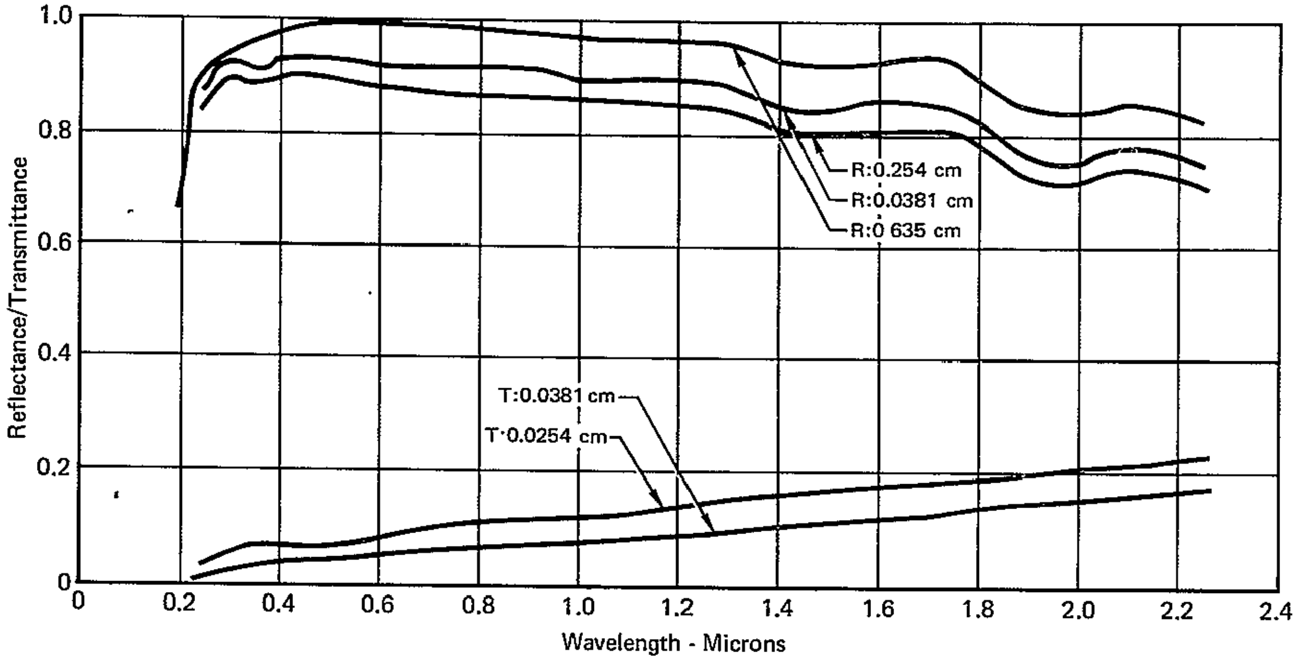

FIGURE 5-13
REFLECTANCE AND TRANSMITTANCE OF HYPERPURE SLIP CAST SILICA

GP74-4457-36

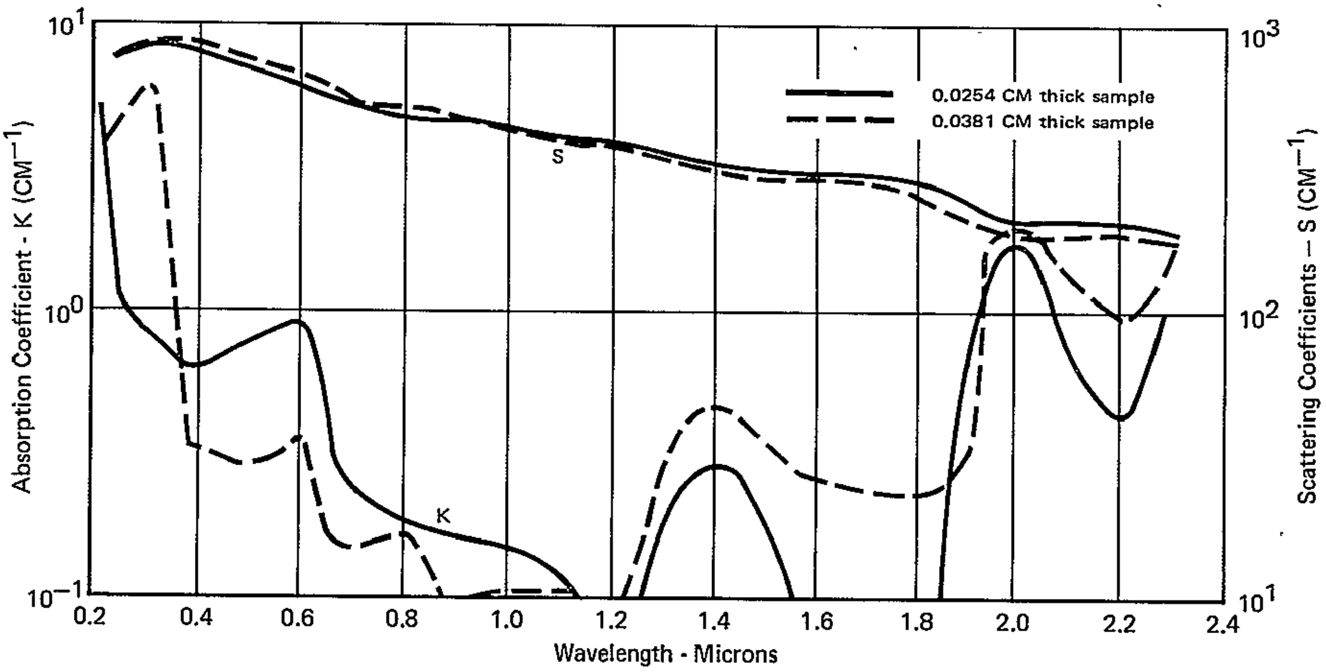

FIGURE 5-14
SCATTERING AND ABSORPTION COEFFICIENTS HYPERPURE SLIP CAST SILICA

GP74-4457-37

percentage error in K at $\lambda = 0.6\mu$ is approximately ±44%. This result is not unexpected and points out the considerable difficulty involved in measuring absorption coefficients by reflectance techniques for these highly reflecting slip cast silica materials. In fact, these silica materials generally have reflectances equal to or greater than the reflectance of the reference material, barium sulfate, which is ordinarily assumed to be a nonabsorbing scatterer.

The scattering coefficient, S, is more accurately determined by reflectance techniques than the absorption coefficient, K. Using the slope of the R_σ vs σ curve, Equation (2), in the vicinity of $S = 650\ \text{cm}^{-1}$ and $K = 0.9\ \text{cm}^{-1}$, we find the percent error in S due to the ± 0.01 inaccuracy in the measurement of R, is about ± 11%.

5.1.5 MELT LAYER EFFECTS

Another issue involved in the optical characterization of the silica materials centers around the effects of a surface melt layer on the reflectance of the silica. During at least part of an entry trajectory, we expect a very thin surface melt layer to be present on the windward side of the silica heat shield. The question arises as to what effect a glassy melt layer has on the radiant flux which is backscattered by the unmelted silica. The worst possible condition occurs if the interface between the melt layer and the virgin material is optically smooth because the reflectance of the interface could approach 0.60 since the refractive index is 1.5.

A check on the effects of the melt layer was made by fire polishing slip cast sample SC-8 (0.207 inch thick) with an oxy-hydrogen torch. Figure 5-15 shows reflectance and transmittance of the sample with a 0.020 inch thick melt layer. There is several percent difference in reflectance between the glazed and the unglazed sides of the sample. The transmittance curve (Figure 5-15) for the 0.02 inch glaze sample is identical to that of the sample prior to the fire-polishing operation.

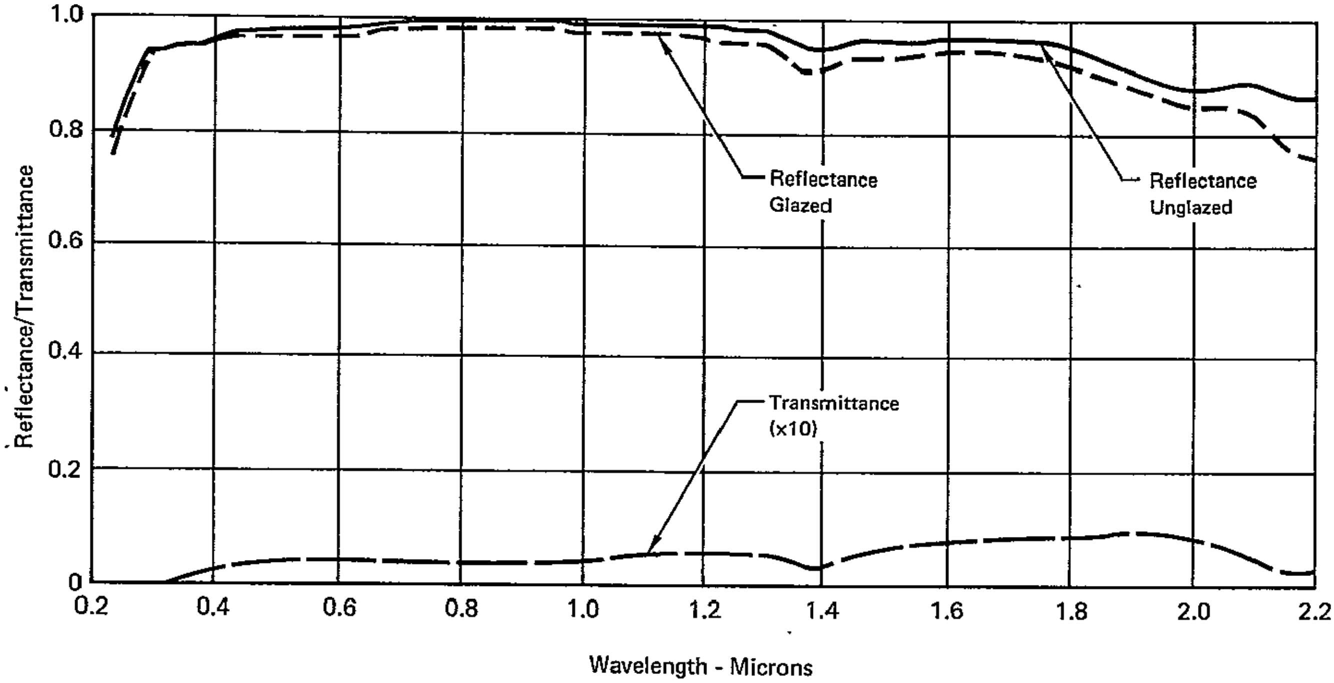

FIGURE 5-15
FIRE-POLISHED HYPERPURE SLIP CAST SILICA - 0.02 IN. MELT LAYER

GP74-4457-38

The fire-polishing was continued until a melt layer thickness of approximately 0.040 inch was achieved. Figure 5-16 shows a degradation of about 20 percent in reflectance, while the transmittance increased by a factor of two compared to the unglazed sample. Note that the transmittance of the sample is less than 2 percent at all wavelengths from 0.225 to 2.3μ and that the reflectance of the unglazed side is nearly identical in Figures 5-15 and 5-16. Figure 5-17 contains photographic enlargements of the sample cross-section with different glaze thicknesses. Evidently the glazed samples are exhibiting a light trapping phenomenon.

An estimate of the internal reflectance r_i can be obtained from the data of Figure 5-16. The interface between the melt layer and the virgin material was assumed to be rough instead of smooth, and multiple transmission and reflection processes in the melt layer were neglected. Under these conditions the measured

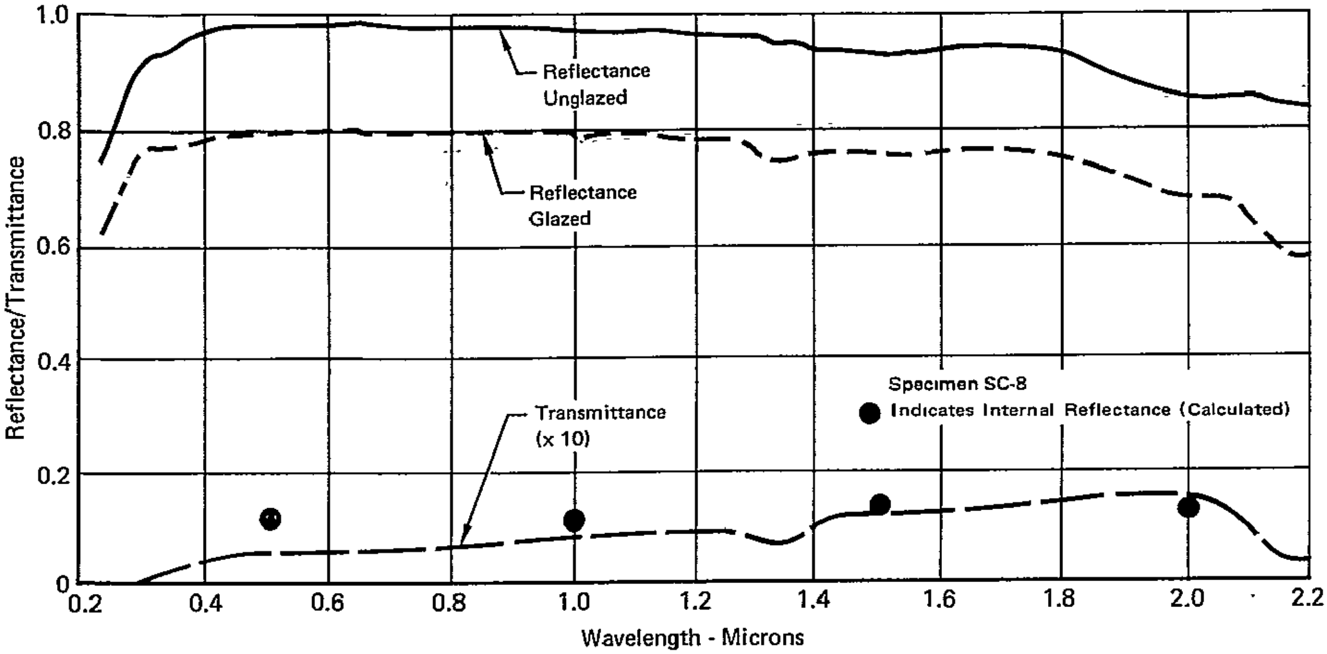

FIGURE 5-16
FIRE POLISHED HYPERPURE SLIP CAST SILICA
0.04 IN. MELT LAYER

GP74 4457-39

effective reflectance of an infinitely thick sample with a thin melt layer on the surface is given by Equation (7):

$$R_1 = r_e + \frac{(1-r_i)(1-r_e)R_c}{1-r_iR_d} \tag{7}$$

where:

R_1 = measured effective reflectance for collimated incident flux

$r_e = \left(\frac{n-1}{n+1}\right)^2$ = Fresnel reflectance of the melt

n = melt layer refractive index (∿1.50)

r_i = internal reflectance of the interface between melt layer and the slip cast material

R_d = reflectance of the slip cast material for diffuse incident flux

R_c = reflectance of the slip cast material for collimated incident flux.

Assuming that $R_c = R_d$ for the slip cast material, the data of Figure 5-16 can be used to compute the values of r_i indicated by the solid circles. It is seen that r_i is about 0.12 for most wavelengths.

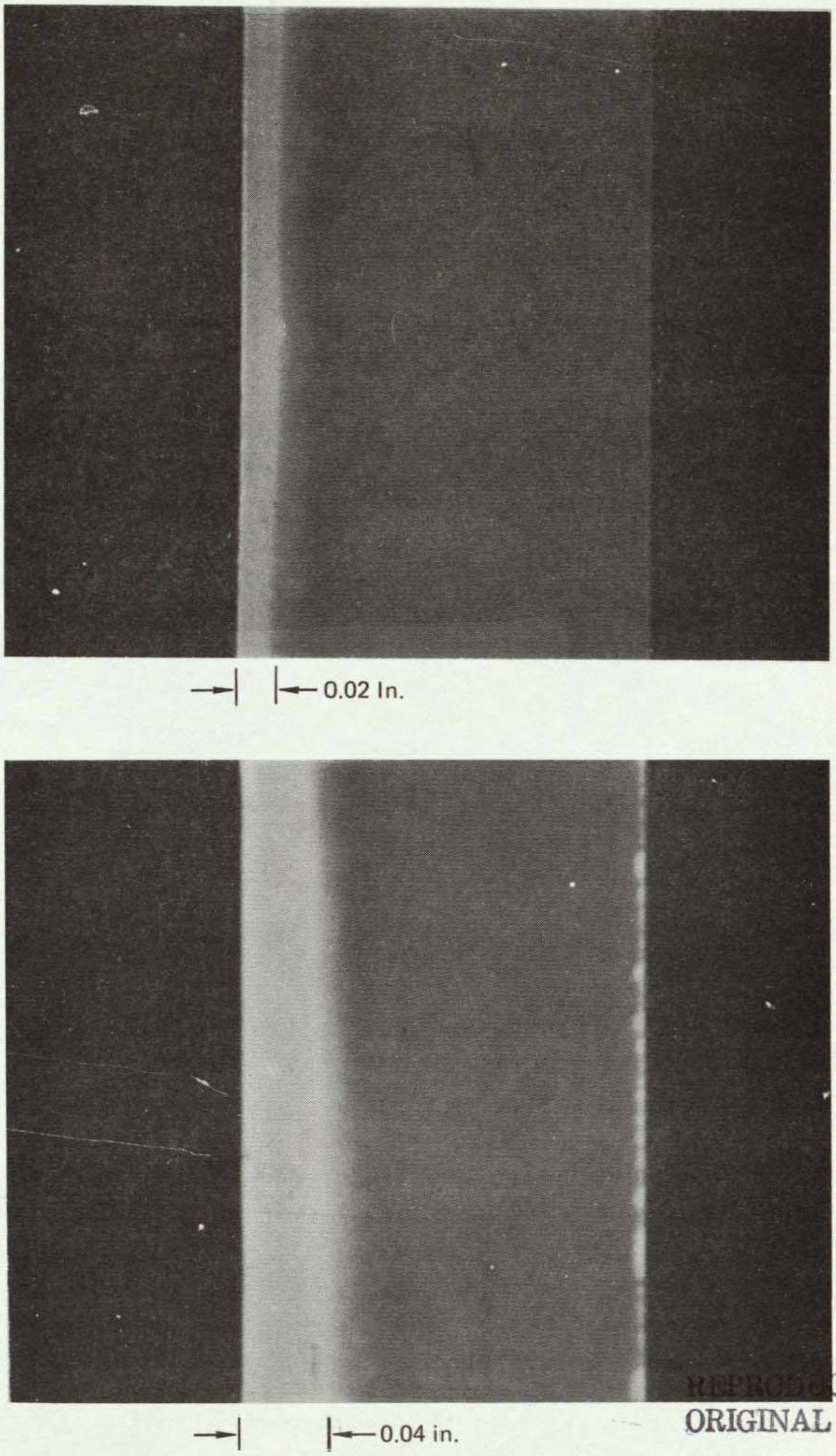

FIGURE 5-17
MELT LAYERS ON SILICA SAMPLE SC-8

GP 74-4457-40

The results shown in Figures 5-15 and 5-16 indicate that the magnitude of the trapped radiation phenomenon due to the presence of the melt layer is somewhat dependent on the melt layer thickness and, therefore, is a mission-dependent variable. Aero-thermochemical analysis will be required to fully determine the importance of this phenomenon for a given mission.

5.2 PHYSICAL CHARACTERIZATION

This section contains a discussion of various physical and chemical properties, including the purity level of hyperpure slip cast fused silica. The variation of properties, such as bulk density, porosity and water absorption, with firing temperature is discussed. Also, the resistance of the hyperpure material to devitrification, as verified by x-ray diffraction, is described.

5.2.1 PURITY VERIFICATION

Various methods of chemical analysis of silica materials were investigated. With all of the commonly accepted methods of analysis, problems were encountered when attempting to analyze materials having a few parts per million (ppm) metallic impurities. These problems included the use of suitable standards as well as the impurity level of reagents required to dissolve unknowns. There are some rather recently developed methods of chemical analysis, neutron activation for example, which are purported to be reliable for detecting small amounts of impurities. These methods are, however, relatively expensive and adapting them was outside the scope of this program.

A purity-reflectance relationship was developed based on the reflectance of silica materials as measured of the Beckman DK-2A spectral reflectometer, which gives a relative indication of the level of metallic impurities present. This curve, shown in Figure 5-18, is the shortest wavelength at which the reflectance of the material is measured to be 0.90 ploted as a function of the total metallic

The differences in physical structure, in turn, have an important effect on the reflectance of the material as discussed in Section 5.1. For purposes of this program various sintering temperatures were studied while using a standard sintering time of five hours for all temperatures. In order to completely characterize the material with respect to firing temperature, it will be desirable to study the effect of varying the sintering time at each temperature.

Since it is virtually impossible to thermal shock fused silica due to its very low thermal expansion coefficient, all of the hyperpure slip cast samples were quench fired; placed directly into a furnace preheated to the firing temperature and then directly removed from the furnace after the soak time of 5 hours. As expected, this resulted in no thermal shock or cracking due to differential shrinkage/thermal stresses.

A typical bulk density of hyperpure slip cast fused silica after a five hour soak at various sintering temperatures is shown in Figure 5-19. The curve in Figure 5-19 is for material which had a green density of ~ 103 lb/ft^3. This is the green density routinely achieved using vibration casting, as discussed in Section 4.6.

Figure 5-20 shows the bulk density and water absorption for samples from hyperpure casting SC-9 (See Figure 4-26) which were sintered at various temperatures for five hours. The density curve in this figure is shifted slightly downward as compared to Figure 5-19, because SC-9 was not vibration cast and had a green density of ~ 100 lb/ft^3. The water absorption figures for this curve were obtained by a technique involving immersion of the samples in boiling water and measuring the resultant weight change. This method is described in Reference 6 as follows:

$$\%\ \text{Absorption} = \frac{\text{Saturated Wt. (gm)} - \text{Fired Wt. (gm)}}{\text{Fired Wt. (gm)}} \times (100) \qquad (8)$$

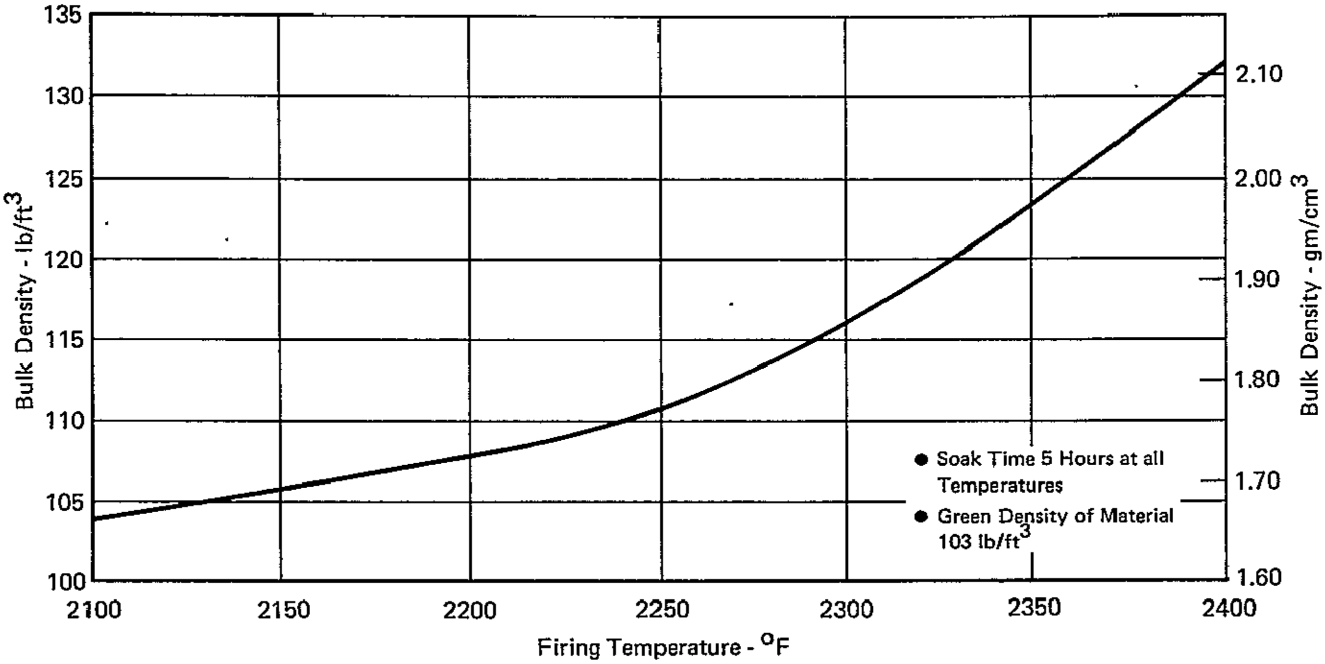

GP74-4457-42

FIGURE 5-19
BULK DENSITY AS A FUNCTION OF SINTERING TEMPERATURE FOR HYPERPURE SLIP CAST FUSED SILICA

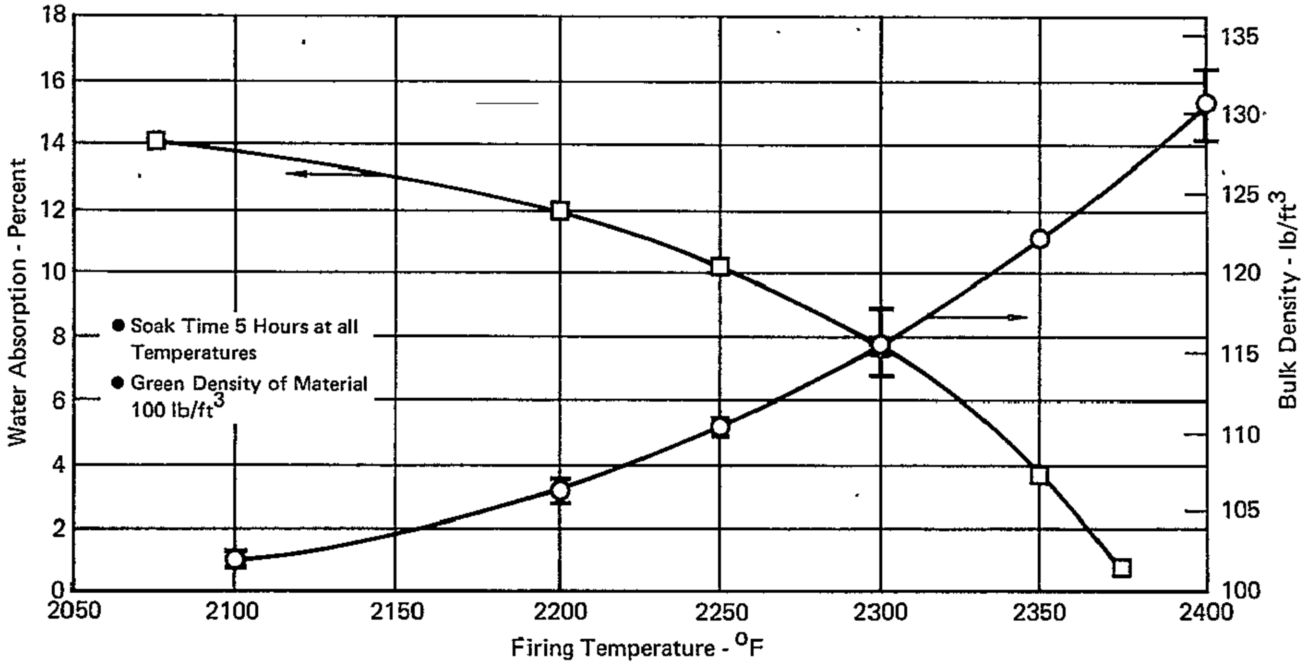

FIGURE 5-20
WATER ABSORPTION AND BULK DENSITY OF HYPERPURE SLIP CAST FUSED SILICA AS A FUNCTION OF SINTERING TEMPERATURE

GP74-4457-43

Figure 5-21 shows the bulk density and porosity as a function of firing temperature for hyperpure samples from casting SC-9. The total porosity is determined simply from the measured bulk density and using 137.3 lb/ft^3 as the maximum theoretical density of fused silica. The open porosity is determined from the weight change from immersion in boiling water as follows (Reference 6):

$$\%\ \text{Open Porosity} = \frac{\text{Saturated Wt. (gm)} - \text{Fired Wt. (gm)}}{\text{Volume (cm}^3\text{)}} \times (100) \qquad (9)$$

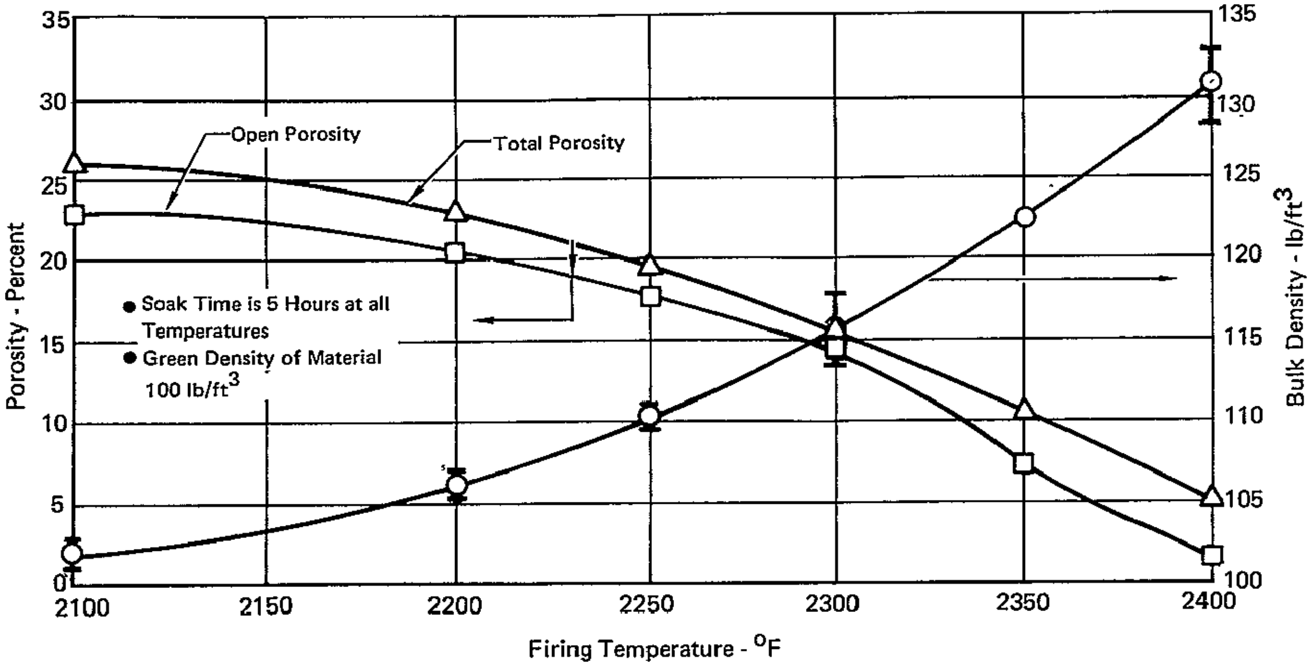

FIGURE 5-21
POROSITY AND BULK DENSITY OF HYPERPURE SLIP CAST FUSED SILICA AS A FUNCTION OF SINTERING TEMPERATURES

GP74 4457-44

5.2.3 DEVITRIFICATION

Most firing temperatures on commercial high purity fused silica are limited to about 2100°F due to minor impurity contents which cause devitrification, a change from the vitreous (or glassy) state to the crystalline state. The crystal phase which is usually first detected in fused silica on devitrification is alpha cristobalite. The calibration curve for x-ray diffraction analysis of silica is shown in Figure 5-22. Figure 5-23 shows some of the traces used to generate the

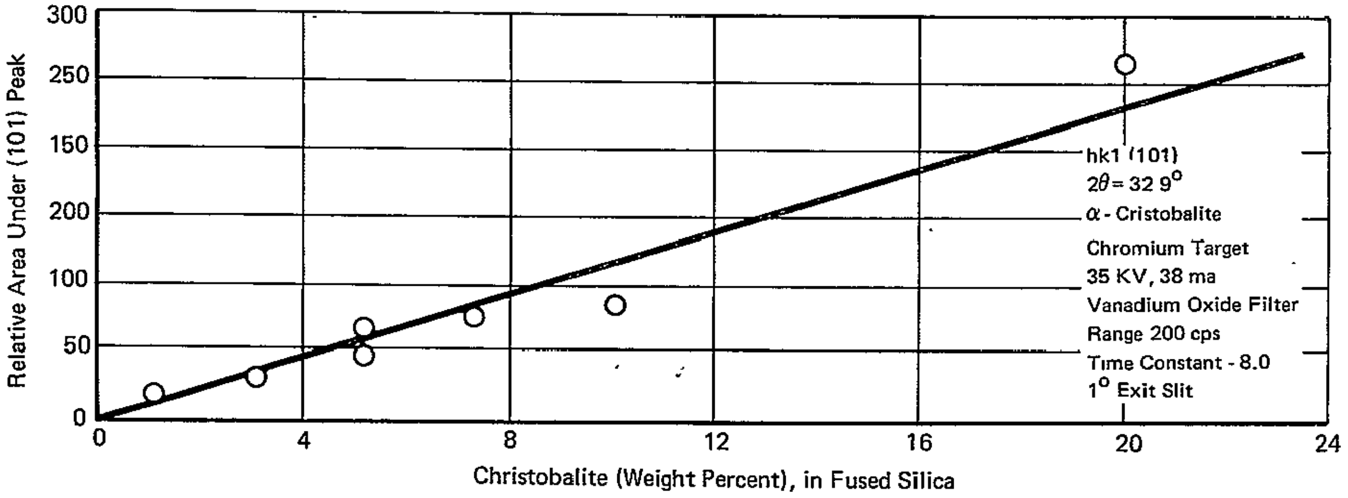

FIGURE 5-22
CALIBRATION CURVE FOR X-RAY DIFFRACTION ANALYSIS
FOR CRISTOBALITE FORMATION IN FUSED SILICA

GP74-4457-45

calibration curve. Cristobalite reference material was made in our laboratory by heating silicic acid to 2560°F for two hours. The fused silica reference used to produce the curve was the hyperpure powdered material.

Samples of the hyperpure slip cast material taken from the same casting (SC-9) were sintered at various temperatures ranging from 2100°F through 2800°F for the standard firing time of five hours. These samples were then powdered and examined for devitrification using x-ray diffraction techniques. The actual x-ray diffraction traces of these samples are shown in Figure 5-24.

As shown in Figure 5-24 no devitrification was found in the specimen which was fired at 2400°F for 5 hours. This amount of resistance to devitrification is very unusual and makes the hyperpure slip cast silica a unique material compared to other slip cast materials. The sample which was fired at 2600°F is estimated (from the x-ray diffraction trace) to have 2.3% cristobalite. The 2800°F fired sample exhibited considerable devitrification, the cristobalite content being greater than 20%.

Although no crystal formation was observed at 2400°F, we have established that this is too high a sintering temperature for a material to have optimum reflectance (See Section 5.1).

100% Fused Silica - 0% Cristobalite

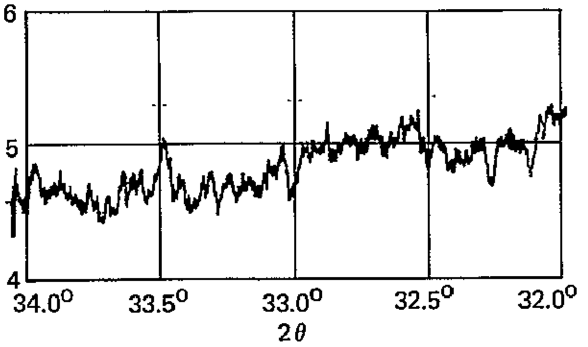

99% Fused Silica - 1% Cristobalite

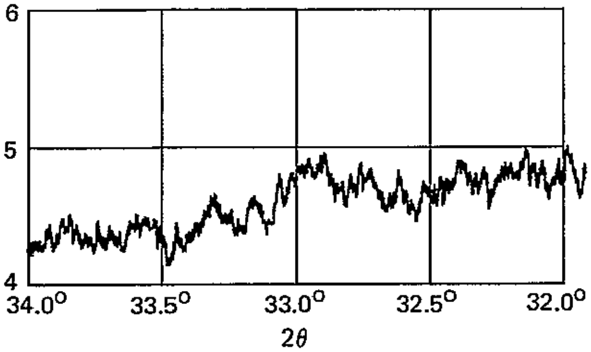

97% Fused Silica - 3% Cristobalite

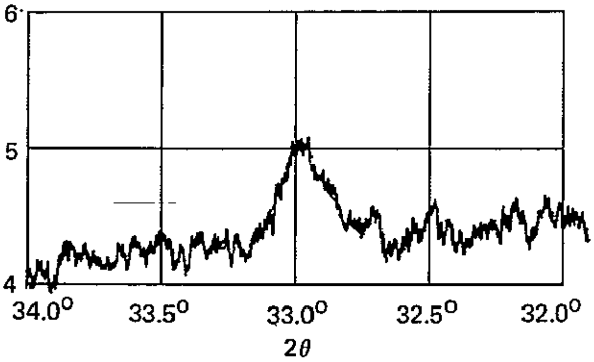

95% Fused Silica - 5% Cristobalite

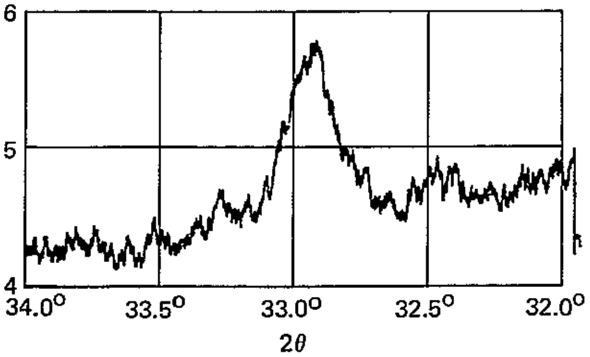

FIGURE 5-23
X-RAY DIFFRACTION TRACES OF FUSED SILICA WITH KNOWN AMOUNTS OF CRISTOBALITE ADDED

GP74-4457-46

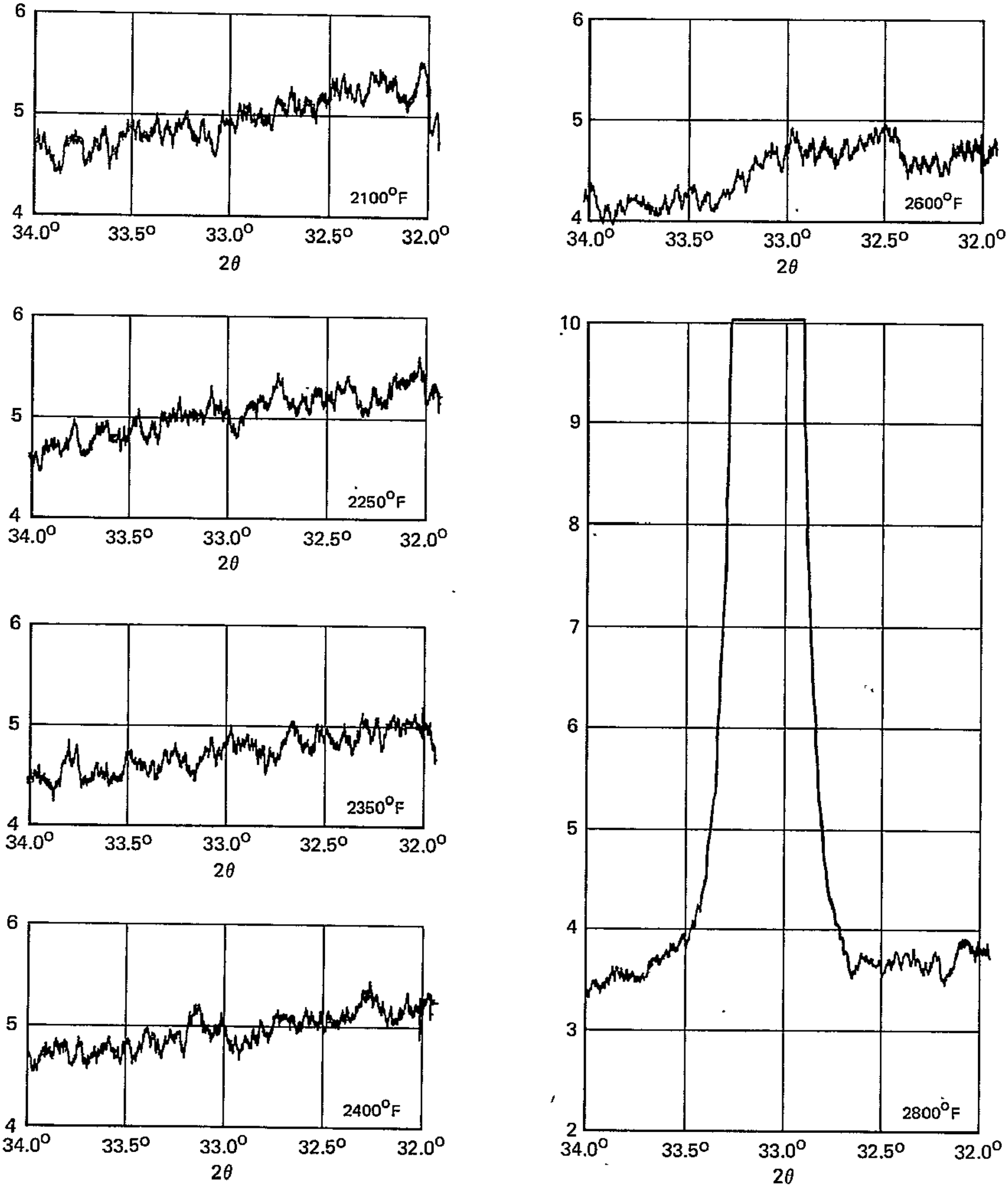

FIGURE 5-24
X-RAY DIFFRACTION TRACES OF HYPERPURE SLIP CAST SILICA
FIRED AT VARIOUS TEMPERATURES FOR 5 HOURS

GP74-4457-47

5.3 MECHANICAL CHARACTERIZATION

Mechanical properties were determined on the hyperpure slip cast material which had been fired to various processing temperatures. All tests were conducted at room temperature on small rectangular bars. This section of the report discusses sample preparation, measurements and analysis of data.

5.3.1 SPECIMEN PREPARATION

Hyperpure slip cast silica samples were taken from casting number SC-9 and were fired at various temperatures in order to determine flexural strength and modulus of elasticity as a function of firing temperature. A total of twelve test bars (2 x 0.3 x 0.1 inches) were wet machined using a diamond impregnated machine tool. These twelve test bars were taken from five samples which had been fired at different temperatures, ranging from 2100 to 2400°F. A standard firing soak time of five hours, at the indicated temperature, was used for all the firings. All sides of each bar were machined flat and parallel, and the bars were then measured to the nearest one thousandth of an inch.

5.3.2 STRENGTH AND MODULUS MEASUREMENTS

Flexural testing was performed using four point loading while the specimens were at room temperature. Four point loading was used so that a uniform maximum bending moment was developed over a large area of the sample such that the fracture was most likely to occur in the area of maximum moment. The specimens did fracture as predicted.

Since bending tests were used to develop the required tensile stresses to fracture the material, it was important to minimize shear stresses for accurate results. This was accomplished by making the length of the strength bar long relative to its thickness. The length used was approximately 20 times the thickness which produced a shear stress in the specimen of less than 2 percent of the tensile stress.

Deflection measurements were made at the midpoint of the bar using a continuous read-out, electromagnetic plunger device. The small load developed by the plunger was subtracted from the total load.

5.3.3 ANALYSIS OF DATA

The data obtained from the measurements described above are shown in Figure 5-25. Flexural strength increased as firing temperature increased, as was expected since more sintering (increased densification) resulted from a higher firing temperature. The four specimens which were fired at 2200°F had an average flexural strength of 2,192 psi, while the two samples fired at 2400°F developed an average strength of 6,917 psi. It is realized that these are only a very limited number of data points, but it can be seen in Figure 5-26 that the flexural strength clearly increases with increased firing temperature.

Two strength tests were conducted on specimens which were fired at 2100°F and very low strength values resulted. This low strength for a 2100°F firing is interesting in that 2100°F is the upper firing temperature normally used for commercial fused silica due to devitrification limitations. Cristobalite, the crystalline phase which normally first forms upon devitrification, when present in fused silica in amounts above 5 percent can cause abrupt strength reduction and loss of thermal shock resistance. The strength results obtained here illustrate the effect of relatively small amounts of impurities on sintering.

While the strength results are quite high for the material fired to 2400°F, the reflectance data on this same material is not nearly as desirable as for the material fired to only 2200°F. For example, data in Figure 2-4 shows that for the material fired at 2200°F, the reflectance is 53 percent (at 0.15μ) compared to only

FIGURE 5-25. MECHANICAL PROPERTIES DATA FOR HYPERPURE FUSED SILICA

Sample No.	Firing Temperature (°F)	Length (In)	Width (In)	Thickness (In)	Weight (Gm)	Density (Lb/Ft^3)	Load (Lbs.)	Flexural Strength (Lb/In^2)	Midpoint Deflection at Fracture (In)	Flexural Modulus of Elasticity (Lb/In^2)
SC-9-1-1	2250	2.010	0.340	0.101	2.0130	111.0	0.20	-	-	-
SC-9-1-2	2250	2.012	0.340	0.100	1.9744	109.8	7.10	4400	.01075	5,340,000
SC-9-2-1	2200	2.032	0.340	0.100	1.9284	106.2	3.40	2100	.00825	3,320,000
SC-9-2-2	2200	2.035	0.340	0.101	1.9559	106.5	3.55	2150	.00675	4,120,000
SC-9-2-3	2200	2.023	0.339	0.101	1.9448	106.9	4.55	2760	.00861	4,150,000
SC-9-2-4	2200	2.021	0.339	0.101	1.9188	105.5	2.90	1760	.00700	3,260,000
SC-9-3-1	2300	1.994	0.340	0.100	2.0997	117.8	9.50	5860	.00837	9,150,000
SC-9-3-2	2300	2.000	0.340	0.101	2.0457	113.4	8.65	5240	.00750	9,050,000
SC-9-6-1	2400	2.007	0.340	0.094	2.2408	132.9	8.75	6120	.00600	14,210,000
SC-9-6-2	2400	2.007	0.340	0.100	2.3010	128.3	12.50	7715	.00713	14,160,000
SC-9-7-1	2100	1.996	0.339	0.101	1.8201	101.4	0.70	425	-	-
SC-9-7-2	2100	1.994	0.340	0.100	1.8214	102.2	0.90	555	-	-

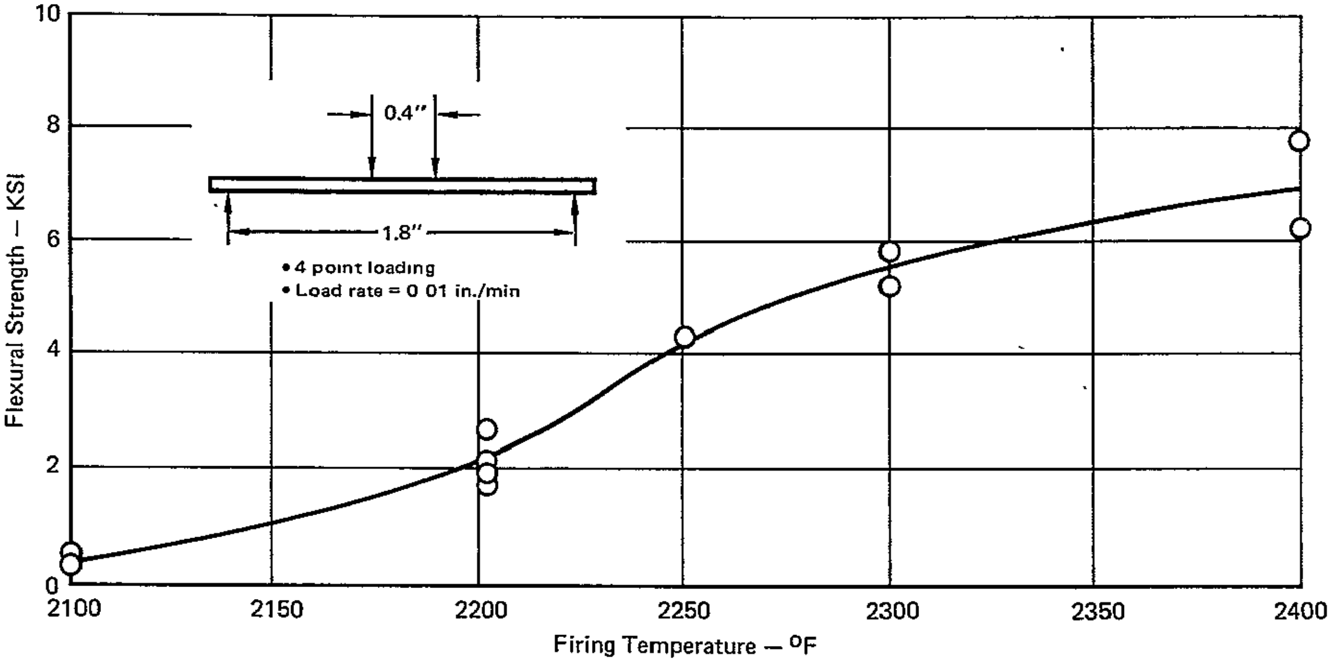

FIGURE 5-26
FLEXURAL STRENGTH OF SLIP CAST HYPERPURE FUSED SILICA AS A FUNCTION OF FIRING TEMPERATURE

GP74-4457-49

16 percent for the material fired at 2350°F. Even with this limited quantity of data, it is clear that there will be some compromise between strength properties and reflectance. The mission requirements must be considered in arriving at an optimum compromise.

The flexural modulus of elasticity was also determined for the hyperpure material, and, as expected, it also increased with firing temperature. A graphical presentation of this data is shown in Figure 5-27. A calculation was made to determine the relative strain at failure for the hyperpure material fired at different temperatures. The strain was determined by dividing the ultimate flexural strength by the flexural modulus of elasticity. The highest value obtained was a strain of 0.00082 in/in, which was for a specimen fired to 2250°F and the lowest value obtained was 0.00043 in/in, for a specimen fired at 2400°F. These values compare favorably with the relative strain at failure for common plate glass of 0.00080 in/in, calculated in the same manner.

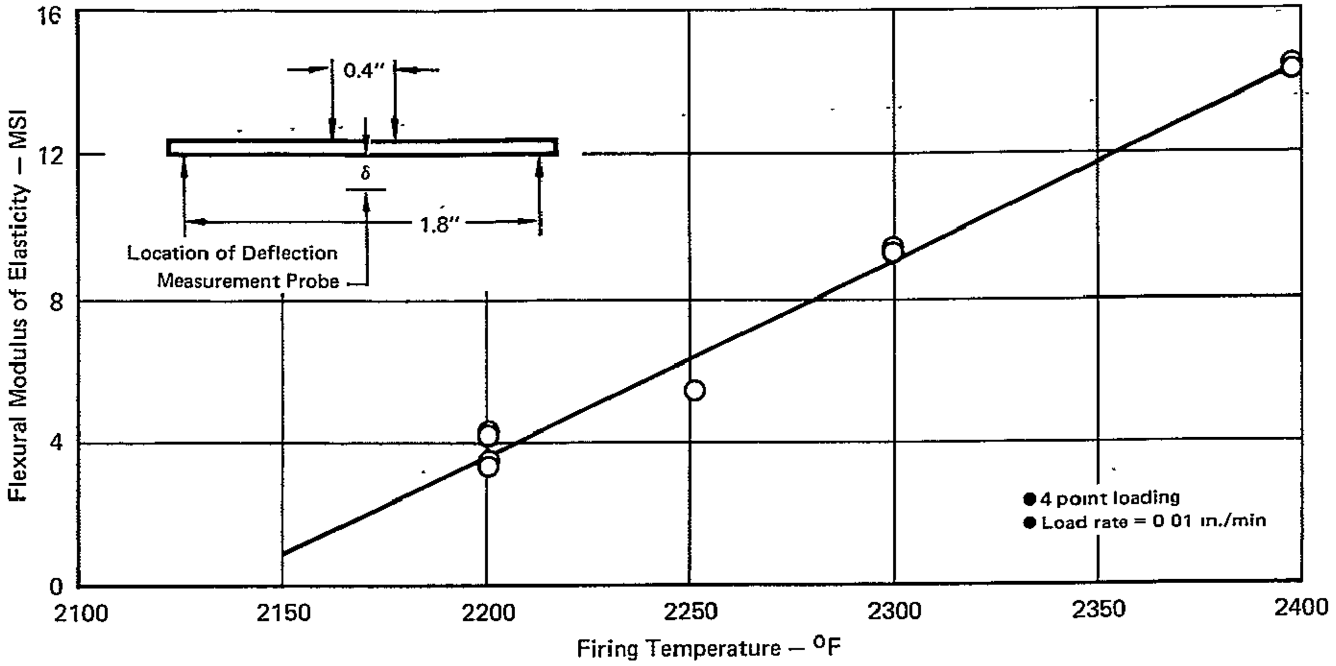

FIGURE 5-27
FLEXURAL MODULUS OF ELASTICITY OF SLIP CAST HYPERPURE FUSED SILICA AS A FUNCTION OF FIRING TEMPERATURE

GP74-4457-50

5.4 COST CHARACTERIZATION

Slip casting is the process selected for producing the silica reflective heat shields, based on the results of this program. By using the slip casting process, very little material is wasted, since the heat shield can be cast to nearly the exact shape required. This is important since the raw material cost (in rod form) is $155 per pound.

It is difficult to estimate the cost of a production heat shield based on the laboratory experience to date. The estimate given below assumed that a scale-up program had been completed, while in reality this program has not yet been started. It was also anticipated that final machining would be performed only on selected areas of the heat shield, such as on attachment surfaces.

The manhours required to perform the major processing steps, as described in Section 4.0, for an 18-inch diameter, one inch thick, curved heat shield is estimated as follows:

° Raw material size reduction	190 manhours
° Slip preparation and milling	70 manhours
° Mold fabrication	70 manhours
° Casting and drying	50 manhours
° Firing	46 manhours
° Machining	46 manhours
° Inspection (visual and x-ray)	33 manhours
	505 manhours
10% Contingencies	51 manhours
	556 manhours

The material required to produce this heat shield is 20 pounds. These estimates assume a reasonable production run of 5 to 10 heat shield units.

Comparing these cost estimates with a carbon-phenolic heat shield, using the same basis, it is estimated that the silica heat shield would be approximately 35 percent more costly.

6.0 CONCLUSIONS AND RECOMMENDATIONS FOR FUTURE WORK

This section contains the major conclusions of this program and suggestions for future work in the silica reflective heat shield area.

6.1 CONCLUSIONS

The following conclusions have been reached based on the results of this program:

- Purity and internal morphology are the two most important factors for obtaining maximum reflectance of a fused silica heat shield.
- Very high purity silica raw materials (<1 ppm total metallic impurities) are available from at least two domestic suppliers.
- The required purity (<50 ppm) and morphology can be maintained in the heat shield material using reasonable care in production and in handling, such as is available in a "clean room" manufacturing area.
- The selected baseline material produced in this program has higher reflectance values than any other materials available at the time of this writing. Reflectance values of 0.99 have been measured from 0.4 to 1.2 microns, and above 0.90 from 0.25 to 0.4 microns.
- The selected slip cast material when fired at 2200°F has a 108 lb/ft^3 density, 2200 psi flexural strength and 3,500,000 psi elastic modulus. Higher strength and modulus results from a higher firing temperature.
- All processing steps for slip casting are now defined and can be controlled to produce a 7 x 7 x 1 inch part. These steps can be readily scaled up to do large parts.
- The next logical step in the development of a silica reflective heat shield is a scale-up effort where full sized heat shields would be fabricated.

- Enough preliminary data has been generated in this program to justify characterizing the hyperpure material. This would include more testing at room temperature and testing at elevated temperature.
- The costs of hyperpure silica heat shields are competitive with other candidate materials, such as carbon-phenolic.

6.2 RECOMMENDATIONS FOR FUTURE WORK

This section contains recommendations for future work which are based on the observations and findings of this program. The recommendations which are detailed below are described in three parts:

- Further materials improvements,
- Scale up,
- and properties as a function of temperature.

6.2.1 FURTHER MATERIALS IMPROVEMENTS

Further materials development is suggested in the areas of green and fired strength improvement, and in thermal conductivity reduction.

Vibration and pressure casting appear to be processing methods which would increase density during casting and this would therefore increase the strength of the material. These methods would also increase the number of scattering sites per unit volume which would probably increase reflectance. It is also suggested that firing times be varied as a part of such studies as they were in this program.

It is desirable to reduce the thermal conductivity of the silica to reduce heat shield weight. Advanced design studies indicate that this is especially true when a shallow entry is made into one of the outer planets and the resulting entry time is relatively long. A dual density silica material (high density on the outside, low density on the inside) having a lower thermal conductivity compared to the entirely dense material is suggested for study as a solution to this problem. A dual density material of this type has been successfully made, on a small scale, in the MDAC-East Facility.

6.2.2 SCALE UP OF HYPERPURE HEAT SHIELD MATERIAL

To date slip cast hyperpure silica has been fabricated into flat shapes in sizes up to 7 x 7 inches. Also, using commercial high purity slips, sub-scale heat shields having curvature and a simulated attachment ring have been successfully fabricated. In fabricating these parts, certain processing steps have been found to be very critical, such as drying and firing cycles. These steps have been successfully controlled in producing the sub-scale heat shields.

It seems very logical that these same critical processing steps and others will have to be considered and controlled in scaling up the processing to produce full scale, hyperpure silica heat shields. Therefore, this scale-up effort is suggested as an important item for near term future work.

6.2.3 PROPERTIES AS A FUNCTION OF TEMPERATURE

It has been shown in this program that hyperpure silica is a promising candidate for a planetary entry reflective heat shield because it has a high reflectance to the incident radiation, is a good ablator, has excellent resistance to thermal stress and is available in various forms.

What is needed is quantitative, thermophysical and mechanical data as a function of temperature in order to support the design of a silica heat shield.

The published data obtained from Project Fire shows that the optical properties of silica change with temperature. Published data from Corning Glass Works indicate that the mechanical properties of pure, dense silica also change with temperature. However, no quantitative data is available at elevated temperatures on the hyperpure, reflective material that is now available.

Data is available from the Georgia Institute of Technology on commercial high purity material. However, the hyperpure silica material is quite different from the commercial product, not only in being more pure and more reflective, but different also in mechanical properties.

Further, it is recognized that silica materials exhibit enhanced chemical activity at elevated temperatures and properties may be altered by chemical reaction with the surrounding atmosphere. In actual use, the silica heat shield will experience heating in predominantly hydrogen atmospheres for outer planet entry missions. It is not immediately evident what the chemical reactions of silica heat shields will be in the reducing environments of the outer planets and at the reentry temperatures expected.

7.0 REFERENCES

1. Nachtsheim, P. R., Peterson, D. L., and Howe, J. T., "Reflecting Ablative Heat Shields for Radiative Environments", American Astronautical Society, the 17th Annual Meeting, 28-30 June 1971.

2. Harris, J. N., and Welsh, E. A., Fused Silica Design Manual, Volumes I and II, Georgia Institute of Technology, Atlanta, Georgia, May 1973.

3. "Mechanical and Electrical Properties of Glasrock Technical Ceramics", Data Sheet from Glasrock Products, Inc., Atlanta, Georgia.

4. Grum, F., and Luckey, G. W., "Optical Sphere Paint and A Working Standard of Reflectance", Applied Optics 7, #11 (1968) pp. 2289-2294.

5. Reichman, J. C., "Determination of Absorption and Scattering Coefficients for Nonhomogeneous Media", Applied Optics, 12, #8 1973), 1811-1823.

6. Andrews, A. I., Ceramic Tests and Calculations, John Wiley and Sons, Inc., New York, 1928.